Supporting information

Determining the Inherent Selectivity for Carbon Radical Hydroxylation Versus Halogenation with $Fe^{III}(OH)(X)$ Complexes: Relevance to the Rebound Step in Nonheme Iron Halogenases

Vishal Yadav, Rodolfo J. Rodriguez,

Maxime A. Siegler, David P. Goldberg*

Department of Chemistry, The Johns Hopkins University, Baltimore, Maryland 21218, United States

Table of contents

A. Materials and instrumentation.

Materials. All syntheses and manipulations were conducted in an N_2-filled drybox (Vacuum Atmospheres, O_2 < 0.2 ppm, H_2O < 0.5 ppm) or using standard Schlenk techniques under an atmosphere of Ar unless otherwise noted. $Fe(OTf)_2$•2MeCN and $^{57}Fe(OTf)_2$•2MeCN were prepared according to a literature procedure.[1] Powdered ^{57}Fe metal (95.93%) was purchased from Cambridge Isotope Laboratories. Anhydrous $FeCl_2$, $FeBr_2$, $FeCl_3$, tetrabutylammonium chloride and tetrabutylammonium bromide were purchased from Sigma-Aldrich and dried over P_2O_5 under vacuum before use. The isotopically labelled $^{18}O_2$ (98 atom %) was purchased from ICON Isotopes (Summit, N.J.). Acetonitrile and acetonitrile-d_3 were distilled from CaH_2. Tetrahydrofuran, tetrahydrofuran-d_8, toluene and toluene-d_8 were dried over Na/benzophenone and subsequently distilled. All other non-deuterated solvents were obtained from a Pure-solv solvent purification system from Innovative Technologies, Inc. Anhydrous 2-methyltetrahydrofuran and pentane (sure seal) were purchased from Sigma-Aldrich, and distilled over Na/benzophenone. All solvents were degassed by a minimum of three freeze−pump−thaw cycles and stored over freshly activated 3 Å molecular sieves in the drybox following distillation. All other reagents were purchased from commercial vendors and used without further purification. The ligand $BNPA^{Ph2}OH$ was prepared by a literature procedure[2] and was dried over P_2O_5 for 12 h under vacuum before metalation. The compounds tris(*p*-methoxyphenyl)methyl radical,[3] tris(*p*-chlorophenyl)methyl radical,[3] $Fe^{II}(BNPA^{Ph2}O)(OTf)$,[2] $^{57}Fe^{II}(BNPA^{Ph2}O)(OTf)$,[2] $Fe^{II}(BNPA^{Ph2}O)(OH)(OTf)$,[2] $^{57}Fe^{II}(BNPA^{Ph2}O)(OH)(OTf)$[2] and Gomberg's dimer[4] ($(Ph_3C)_2$) were synthesized following literature procedures.

Instrumentation. The ^1H NMR spectra were measured on a Bruker 300 MHz or a Bruker 400 MHz NMR spectrometer. Chemical shifts were referenced to reported solvent resonances.[5] UV−vis experiments were carried out on a Cary 60 UV−vis spectrophotometer equipped with a Unisoku USP-203A cryostat using a 1 cm modified Schlenk cuvette. Midwest Microlab LLC (Indianapolis, IN) conducted elemental analyses on samples prepared and shipped in ampules sealed under vacuum. Mössbauer spectra were recorded on a

spectrometer from SEE Co. (Edina, MN) operating in the constant acceleration mode in a transmission geometry. The sample was kept in an SVT-400 cryostat from Janis Research Co. (Wilmington, MA), using liquid N_2 as a cryogen for 80 K measurements. Isomer shifts were determined relative to the centroid of the spectrum of a metallic foil of α-Fe collected at room temperature. Data analysis was performed using version F of the program WMOSS (www.wmoss.org), and quadrupole doublets were fit to Lorentzian lineshapes. Electron paramagnetic resonance (EPR) spectra were recorded with a Bruker EMX spectrometer equipped with a Bruker ER 041 X G microwave bridge and a continuous-flow liquid helium cryostat (ESR900) coupled to an Oxford Instruments TC503 temperature controller for low temperature data collection.

DFT computational study.

All calculations were performed with the ORCA-4.0.1.2 program package.[6] Initial geometries were obtained from X-ray crystallographic models. Optimized geometries were calculated using the B3LYP functional. The 6-311g* basis set was used for all Fe, N, O, Cl and Br atoms and the 6-31g* basis set was used for all C and H atoms. Frequency calculations at the same level of theory confirmed that all optimizations had converged to true minima on the potential energy surface (i.e., no imaginary frequencies).

B. Synthesis of metal complexes.

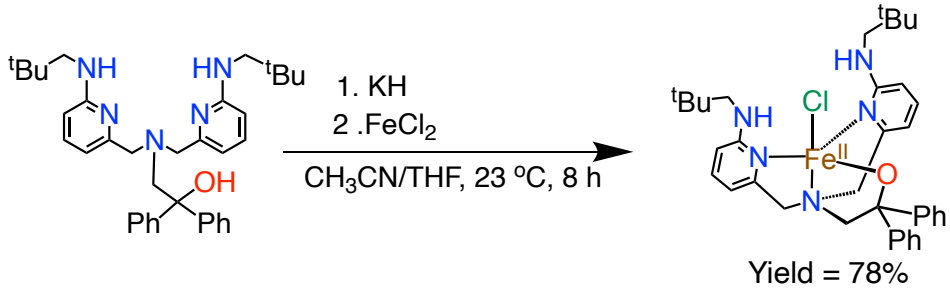

Yield = 78%

$Fe^{II}(BNPA^{Ph2}O)(Cl)$ (1). The ligand $BNPA^{Ph2}OH$ (58.7 mg, 0.11 mmol) was dissolved in THF (2 mL) and a suspension of KH (4.0 mg, 0.11 mmol) in THF (1 mL) was added. The solution was stirred for 1 h at 23 °C. An amount of anhydrous $FeCl_2$ (13.0 mg, 0.11 mmol) was dissolved in acetonitrile (2 mL) and added dropwise to the $BNPA^{Ph2}OH$/KH mixture. An immediate color change from colorless to dark yellow was noted, and the reaction mixture was stirred for 8 h. The resulting dark yellow reaction mixture was evaporated to dryness under vacuum giving a dark yellow solid. The yellow solid was dissolved in THF and filtered through Celite and the solution was left to stand with slow vapor diffusion of pentane. Yellow crystals (blocks, 53 mg (78%)) suitable for X-ray diffraction were obtained after 3 d. UV-vis (THF) λ_{max} (ε, M^{-1} cm^{-1}) = 330 nm (10965), 425 nm (276). Anal. Calcd for $C_{36}H_{46}ClFeN_5O$: C, 65.90; H, 7.25; N, 10.67. Found: C, 65.35; H, 7.52; N, 9.76. ^1H NMR (CD_3CN, 400 MHz): δ 73.31, 70.15, 56.41, 25.28, 23.80, 11.47, 9.05, 5.48, 3.67, 0.24, -11.30 ppm.

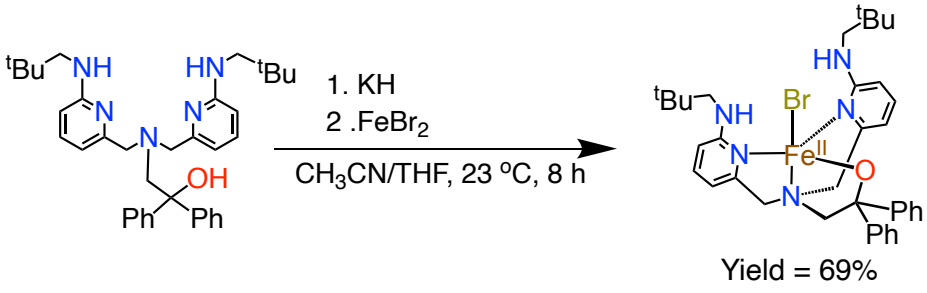

Yield = 69%

$Fe^{II}(BNPA^{Ph2}O)(Br)$ (2). The ligand $BNPA^{Ph2}OH$ (56 mg, 0.10 mmol) was dissolved in THF (2 mL) and a suspension of KH (4 mg, 0.10 mmol) in THF (1 mL) was added. The solution was stirred for 1 h at 23 °C. An amount of anhydrous $FeBr_2$ (22 mg, 0.10 mmol) was dissolved in acetonitrile (2 mL) and added

dropwise to the BNPA^{Ph2}OH/KH mixture. An immediate color change from colorless to dark yellow was noted, and the reaction mixture was stirred for 8 h. The resulting dark yellow reaction mixture was evaporated to dryness under vacuum giving a dark yellow solid. The yellow solid was dissolved in THF and filtered through Celite and the solution was left to stand with slow vapor diffusion of pentane. Yellow crystals (blocks, 48 mg (69%)) suitable for X-ray diffraction were obtained after 3 d. UV-vis (THF) λ_{max} (ε, M^{-1} cm^{-1}) = 330 nm (11500), 420 nm (368). Anal. Calcd for $C_{36}H_{46}BrFeN_5O$: C, 61.72; H, 6.62; N, 10.00. Found: C, 61.28; H, 6.74; N, 9.96. ^{1}H NMR (CD_3CN, 400 MHz): δ 79.56, 71.56, 56.86, 25.94, 23.21, 11.07, 8.66, 5.74, 3.45, 1.15, 0.02, -0.54, -11.70 ppm.

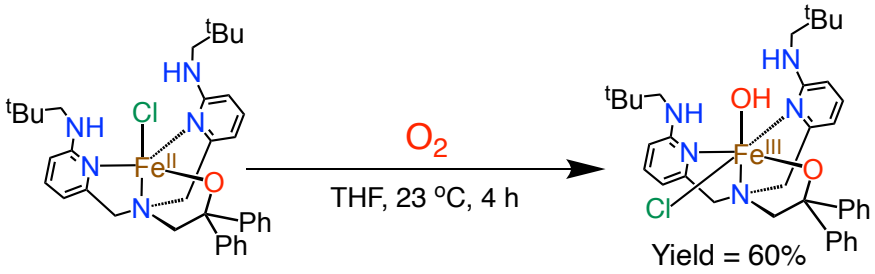

Fe^{III}(BNPA^{Ph2}O)(OH)(Cl) (3). Crystalline **1** (30.0 mg, 0.045 mmol) was dissolved in THF (5 – 10 mL), and this solution was bubbled with excess, dry O_2 for 15 min, causing a color change from yellow to bright orange. The reaction was stirred for 4 h at 23 °C, and the final dark red solution was evaporated to dryness under vacuum to give a dark orange solid. This solid was dissolved in THF and filtered through a Celite bed to remove insoluble material. The resulting dark red filtrate was evaporated to dryness under vacuum and washed with Et_2O and pentane to give a dark orange powder, which was dissolved in THF and the solution was left to stand with slow vapor diffusion of pentane. Bright orange crystals (blocks, 18.4 mg (60%)), suitable for X-ray diffraction were obtained after 2 d. UV-vis (THF) λ_{max} (ε, M^{-1} cm^{-1}) = 325 nm (12000), 425 nm (1615). Anal. Calcd for $C_{36}H_{47}ClFeN_5O_2$: C, 64.24; H, 7.04; N, 10.40. Found: C, 64.04; H, 6.99; N, 10.29. ^{1}H NMR (CD_3CN, 400 MHz): δ 74.41, 15.43, 10.65, 7.79, 7.14, 3.67 ppm.

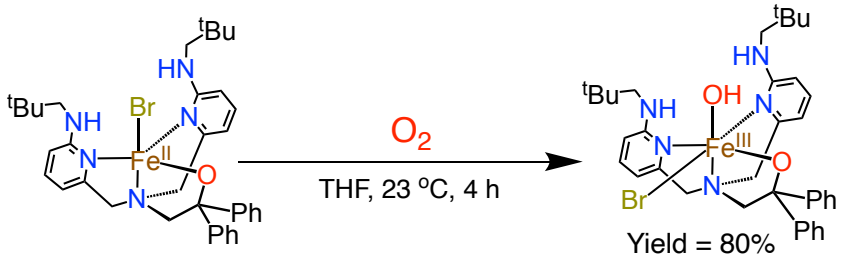

$Fe^{III}(BNPA^{Ph2}O)(OH)(Br)$ (4). Crystalline **2** (30.0 mg, 0.042 mmol) was dissolved in THF (5 – 10 mL), and this solution was bubbled with excess, dry O_2 for 15 min, causing a color change from yellow to dark orange. The reaction was stirred for 4 h at 23 °C, and the final dark red solution was evaporated to dryness under vacuum to give a dark orange solid. This solid was dissolved in THF and filtered through a Celite bed to remove insoluble material. The resulting dark red filtrate was evaporated to dryness under vacuum and washed with Et_2O and pentane to give a dark orange powder, which was dissolved in THF and the solution was left to stand with slow vapor diffusion of pentane. Bright orange crystals (blocks, 24.6 mg (80%)), suitable for X-ray diffraction were obtained after 2 d. UV-vis (THF) λ_{max} (ε, M^{-1} cm^{-1}) = 325 nm (11500), 415 nm (1360), 440 nm (880). Anal. Calcd for $C_{36}H_{47}BrFeN_5O_2$: C, 60.26; H, 6.60; N, 9.76. Found: C, 59.72; H, 6.45; N, 9.22. ^{1}H NMR (CD_3CN, 400 MHz): δ 74.91, 15.43, 10.66, 7.09, 3.68 ppm.

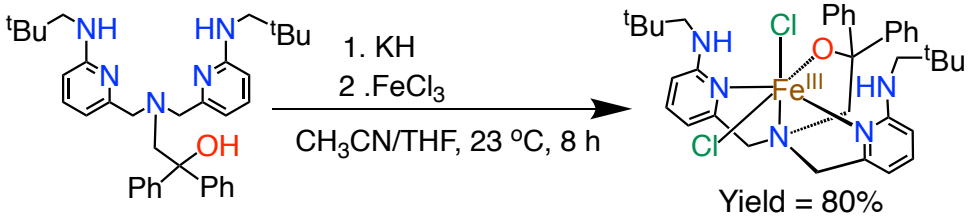

$Fe^{III}(BNPA^{Ph2}O)(Cl)_2$ (5). The ligand $BNPA^{Ph2}OH$ (70.8 mg, 0.125 mmol) was dissolved in THF (2 mL) and a suspension of KH (5.0 mg, 0.125 mmol) in THF (1 mL) was added. The solution was stirred for 1 h at 23 °C. An amount of anhydrous $FeCl_3$ (20.6 mg, 0.125 mmol) was dissolved in acetonitrile (2 mL) and added dropwise to the $BNPA^{Ph2}OH$/KH mixture. An immediate color change from colorless to dark red was noted, and the reaction mixture was stirred for 8 h. The resulting dark red reaction mixture was evaporated to dryness under vacuum giving a dark red solid. The red solid was dissolved in THF and filtered through Celite and the solution was left to stand with slow vapor diffusion of pentane. Red crystals (blocks, 70 mg (80%)) suitable for X-ray diffraction were obtained after 3 d. UV-vis (CH_3CN) λ_{max} (ε, M^{-1} cm^{-1}) =

320 nm (10090), 375 nm (2800), 425 nm (1120). Anal. Calcd for $C_{36}H_{47}Cl_2FeN_5O$: C, 60.53; H, 6.71; N, 10.13. Found: C, 59.72; H, 6.45; N, 9.76. ^{1}H NMR (CD_3CN, 400 MHz): δ 65.67, 17.47, 15.29, 8.54, 7.79, 3.67, 0.92, -1.61, -2.89 ppm.

C. Experimental Procedure

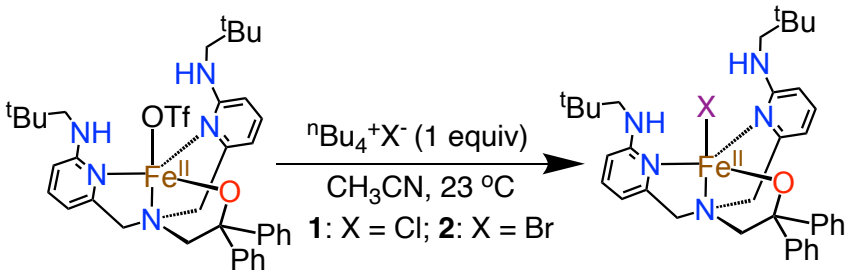

Preparation of ^{57}Fe-enriched 1 and 2 for Mössbauer spectroscopy. Crystalline $^{57}Fe^{II}(BNPA^{Ph2}O)(OTf)$ (3 mg) was dissolved in CH_3CN (500 µL, 8 mM) and $^nBu_4NX$ (X = Cl, Br) (1 equiv) was added causing a color change from colorless to dark yellow. The completion of the reaction was verified by ^{1}H NMR spectroscopy which showed the disappearance of the peaks corresponding to the $^{57}Fe^{II}(BNPA^{Ph2}O)(OTf)$ and formation of new peaks corresponding to $Fe^{II}(X)$ complexes. The solvent was removed, the solid was dissolved in 2-MeTHF (300 µL, 11 mM) and transferred into a Mössbauer cup. The sample was then frozen in liquid nitrogen, and Mössbauer spectra were collected at 80 K in the absence of any external magnetic field.

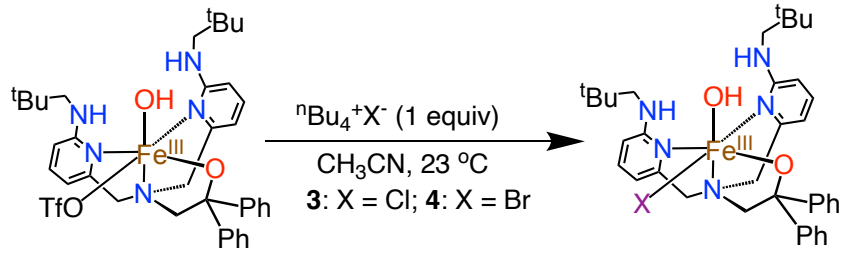

Preparation of ^{57}Fe enriched 3 and 4 for Mössbauer spectroscopy. Crystalline $^{57}Fe^{III}(BNPA^{Ph2}O)(OH)(OTf)$ (3 mg) was dissolved in CH_3CN (500 µL, 7.6 mM) and $^nBu_4NX$ (X = Cl, Br) (1 equiv) was added causing a color change from colorless to dark yellow. The completion of the reaction

was verified by ^{1}H NMR spectroscopy which showed the disappearance of the peaks corresponding to the $^{57}Fe^{III}$(BNPA^{Ph2}O)(OH)(OTf) and formation of new peaks corresponding to Fe^{III}(OH)(X) complexes. The solvent was removed, a solid film was made in the Mössbauer cup, and Mössbauer spectra were collected at 80 K in the absence of any external magnetic field.

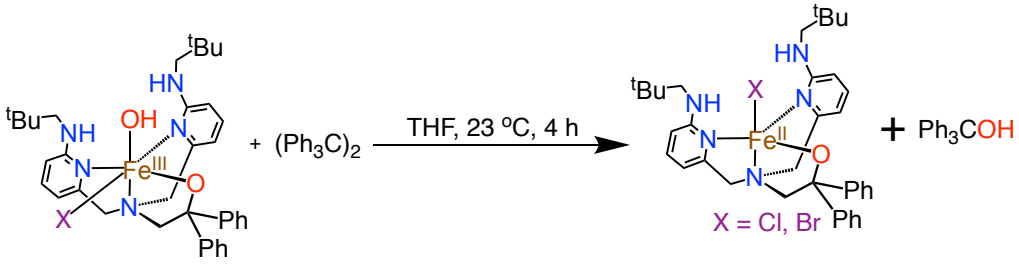

Reaction of 3 - 4 with triphenylmethyl radical (Ph_3C•). Crystalline **3** (5.0 mg, 0.006 mmol) was dissolved in a THF-toluene mixture (4/1 v/v) and excess $(Ph_3C)_2$ (30 mg, 0.064 mmol, 10 equiv) was added. The reaction mixture was stirred in the dark for 4 h at 23 °C. The reaction mixture turned from bright orange to dark yellow, and then was dried under vacuum to give a dark yellow solid. The residue was dissolved in CD_3CN and analyzed by ^{1}H NMR spectroscopy. The ^{1}H NMR spectrum showed complete disappearance of the broad, paramagnetically shifted peaks for **3**, and appearance of the relatively sharp, paramagnetically shifted peaks corresponding to the **1**. For analysis by Mössbauer spectroscopy, complex **3** was enriched in ^{57}Fe (95.93%) and 2-MeTHF was employed in place of CD_3CN because 2-MeTHF gives a better resolved, sharp doublet for the Mössbauer spectrum of **1**. The Mössbauer spectrum (80 K) of the final reaction mixture showed a sharp quadrupole doublet ($\delta = 1.02$, $|\Delta E_Q| = 2.69$ mm s^{-1}, 91% of the fit) corresponding to **1**. The analogous reaction was performed with **4** (5.0 mg, 0.006 mmol) under identical reaction conditions, yielding **2** as seen by ^{1}H NMR and ^{57}Fe Mössbauer spectroscopy.

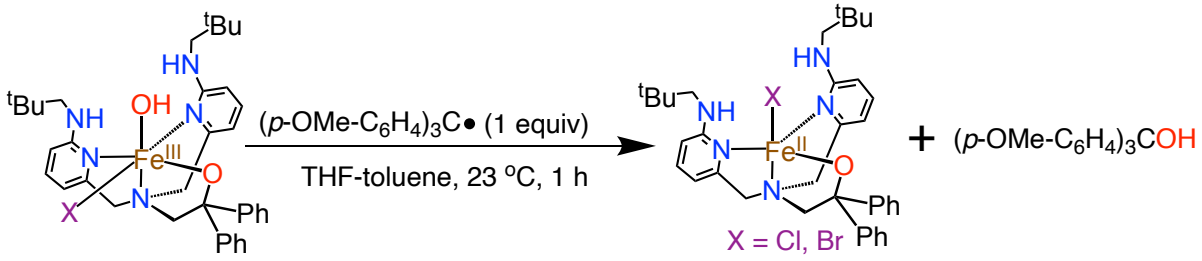

Reaction between 3 - 4 and (p-OMe-C_6H_4)$_3$C•. Crystalline **3** (3.0 mg, 0.004 mmol) was dissolved in THF (600 µL). The radical (p-OMe-C_6H_4)$_3$C• was freshly prepared according to a literature procedure,[3] as follows: an amount of (p-OMe-C_6H_4)$_3$CCl (21 mg, 0.057 mmol) was dissolved in toluene-d_8 (1 mL), excess Cu powder was added, and the heterogenous mixture was heated in the dark for 1 h at 75 ºC. The resulting dark red solution was cooled to 23 °C, filtered through Celite, and an aliquot of this solution (120 µL, 1 equiv) was added to **3**. The reaction was stirred for 1 h, and then the solvent was removed under vacuum to give an orange residue, which was dissolved in CD_3CN and analyzed by ^{1}H NMR spectroscopy. The ^{1}H NMR spectrum showed complete disappearance of the broad, paramagnetically shifted peaks for **3**, and appearance of the relatively sharp, paramagnetically shifted peaks corresponding to **1**. For analysis by Mössbauer spectroscopy, complex **3** was enriched in ^{57}Fe (95.93%) and 2-MeTHF was employed in place of CD_3CN because it gives a better resolved, sharp doublet for the Mössbauer spectrum of **1**. The Mössbauer spectrum (80 K) of the final reaction mixture showed a sharp quadrupole doublet (δ = 1.02, $|\Delta E_Q|$ = 2.69 mm s^{-1}, 92 % of the fit) corresponding to **1**. The analogous reaction was performed with **4** (3.0 mg, 0.004 mmol) under identical reaction conditions, yielding **2** as seen by ^{1}H NMR and ^{57}Fe Mössbauer spectroscopy.

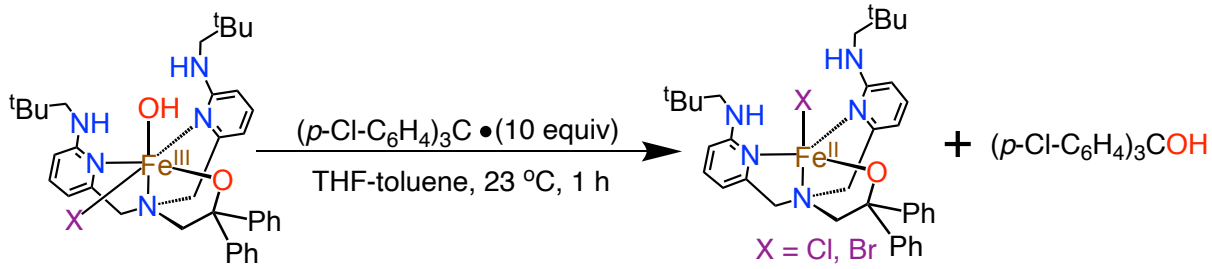

Reaction between 3 - 4 and (p-Cl-C_6H_4)$_3$C•. Crystalline **3** (3.0 mg, 0.004 mmol) was dissolved in THF (1 mL). The radical (p-Cl-C_6H_4)$_3$C• was freshly prepared according to a literature procedure,[3] as follows: an amount of (p-Cl-C_6H_4)$_3$CBr (35.5 mg, 0.083 mmol) was dissolved in toluene-d_8 (1 mL), excess Cu powder was added, and the heterogenous mixture was heated in the dark for 1 h at 75 ºC. The resulting dark red solution was cooled to 23 °C, filtered through Celite, and an aliquot of this solution (500 µL, 10 equiv) was added to **3**. The reaction was stirred for 1 h, and then the solvent was removed under vacuum to give an orange residue, which was dissolved in CD_3CN and analyzed by ^{1}H NMR spectroscopy. The ^{1}H NMR

spectrum showed complete disappearance of the broad, paramagnetically shifted peaks for **3**, and appearance of the relatively sharp, paramagnetically shifted peaks corresponding to **1**. For analysis by Mössbauer spectroscopy, **3** was enriched in ^{57}Fe (95.93%) and 2-MeTHF was employed in place of CD_3CN because it gives a better resolved, sharp doublet for the Mössbauer spectrum of **1**. The Mössbauer spectrum (80 K) showed of the final reaction mixture a sharp quadrupole doublet (δ = 1.02, $|\Delta E_Q|$ = 2.69 mm s^{-1}, 94 % of the fit) corresponding to **1.** The analogous reaction was performed with **4** (3.0 mg, 0.004 mmol) under identical reaction conditions, yielding **2** as seen by ^{1}H NMR and ^{57}Fe Mössbauer spectroscopy.

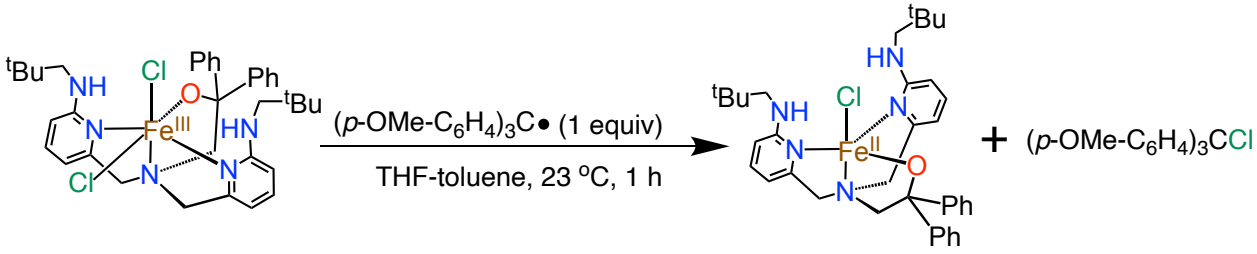

Reaction between 5 and (*p*-OMe-C$_6$H$_4$)$_3$C•. Crystalline **5** (3.0 mg, 0.004 mmol) was dissolved in THF (600 µL). The radical (*p*-OMe-C$_6$H$_4$)$_3$C• was freshly prepared according to a literature procedure,[3] as follows: an amount of (*p*-OMe-C$_6$H$_4$)$_3$CCl (21 mg, 0.057 mmol) was dissolved in toluene-d_8 (1 mL), excess Cu powder was added, and the heterogenous mixture was heated in the dark for 1 h at 75 °C. The resulting dark red solution was cooled to 23 °C, filtered through Celite, and an aliquot of this solution (100 µL, 1 equiv) was added to **5**. The reaction was stirred for 2 h, and then the solvent was removed under vacuum to give an orange residue, which was dissolved in CD_3CN and analyzed by ^{1}H NMR spectroscopy. The ^{1}H NMR spectrum showed complete disappearance of the broad, paramagnetically shifted peaks for **5**, and appearance of the relatively sharp, paramagnetically shifted peaks corresponding to **1**.

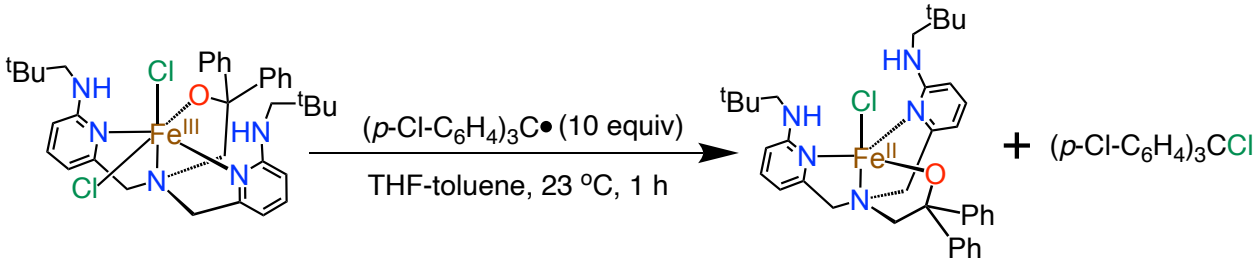

Reaction between 5 and (p-Cl-C_6H_4)$_3$C•. Crystalline **5** (3.0 mg, 0.004 mmol) was dissolved in THF (1 mL). The radical (p-Cl-C_6H_4)$_3$C• was freshly prepared according to a literature procedure,[3] as follows: an amount of (p-Cl-C_6H_4)$_3$CBr (35.5 mg, 0.056 mmol) was dissolved in toluene-d_8 (1 mL), excess Cu powder was added, and the heterogenous mixture was heated in the dark for 1 h at 75 ºC. The resulting dark red solution was cooled to 23 °C, filtered through Celite, and an aliquot of this solution (500 µL, 10 equiv) was added to **5**. The reaction was stirred for 1 h, and then the solvent was removed under vacuum to give an orange residue, which was dissolved in CD_3CN and analyzed by ^{1}H NMR spectroscopy. The ^{1}H NMR spectrum showed complete disappearance of the broad, paramagnetically shifted peaks for the $Fe^{III}(Cl)_2$ complex **5**, and appearance of the relatively sharp, paramagnetically shifted peaks corresponding to the Fe^{II}(Cl) complex **1**.

Quantification of Ph_3COH. A stock solution was prepared by dissolving crystalline **3** (5 mg, 0.007 mmol) in THF-d_8 (1.5 mL, 4.96 mM). Solid (Ph_3C)$_2$ (11.4 mg, 0.0235 mmol, 10 equiv) was added to the stock solution of **3** in THF-d_8/toluene- d_8 (500 µL, 4.96 mM) and stirred in the dark for 4 h. An amount of trimethylphenylsilane (TMPS) (10 µL, 7 mM) was added as an internal standard, and the mixture was analyzed by ^{1}H NMR spectroscopy. A well-separated singlet at 5.50 ppm was observed, which was assigned to the OH proton of Ph_3COH based on comparison with an authentic sample. Integration of this peak and comparison with the TMPS standard gave an average yield (3 runs) for Ph_3COH of 91 ± 3%. The same procedure was employed for **4**, giving an average yield (3 runs) for Ph_3COH of 88 ± 3%.

Quantification of (p-OMe-C_6H_4)$_3$COH. The same procedure as described for Ph_3COH was employed to quantify (p-OMe-C_6H_4)$_3$COH**,** except in this case, the starting radical was freshly prepared following a literature procedure,[3] as follows: An amount of (p-OMe-C_6H_4)$_3$CCl (20.8 mg, 0.056 mmol) was dissolved in toluene-d_8 (1 mL) and excess Cu powder was added, and the heterogenous mixture was heated in the dark for 1 h at 75 ºC. The resulting dark red solution was cooled to 23 °C, filtered through Celite, and an aliquot of this solution was then added to a solution of **3** or **4** in a 1:1 molar ratio. Integration of the singlet at 5.24 ppm, corresponding to the OH proton of (p-OMe-C_6H_4)$_3$COH, gave an average yield (3 runs) for (p-OMe-C_6H_4)$_3$COH of 88 ± 3% for **3** and 84 ± 3% for **4**.

Quantification of (p-Cl-C_6H_4)$_3$COH. The same procedure as described for (p-OMe-C_6H_4)$_3$COH was employed to quantify (p-Cl-C_6H_4)$_3$COH**.** The starting radical was freshly prepared following a literature procedure,[3] as follows: An amount of (p-Cl-C_6H_4)$_3$CBr (35 mg, 0.082 mmol) was dissolved in toluene-d_8 (1 mL) and excess Cu powder was added, and the heterogenous mixture was heated in the dark for 1 h at 75 ^{o}C. The resulting pink solution was cooled to 23 °C, filtered through Celite, and an aliquot of this solution was then added to a solution of **3** or **4** in a 1:10 molar ratio. Integration of the singlet at 5.91 ppm corresponding to the OH proton of (p-Cl-C_6H_4)$_3$COH, gave an average yield (3 runs) for (p-Cl-C_6H_4)$_3$COH of 87 ± 3% for **3** and 84 ± 3% for **4**.

Quantification of (p-OMe-C_6H_4)$_3$CCl. Crystalline **5** (20 mg, 0.029 mmol) was dissolved in THF (5 mL, 5.78 mM). The radical (p-OMe-C_6H_4)$_3$C• was freshly prepared according to a literature procedure,[3] as follows: an amount of (p-OMe-C_6H_4)$_3$CCl (20.5 mg, 0.056 mmol) was dissolved in toluene (5 mL) and excess Cu powder was added, and the heterogenous mixture was heated in the dark for 1 h at 75 ^{o}C. The resulting dark red solution was cooled to 23 °C, filtered through Celite, and an aliquot of this solution (2 mL, 1 equiv) was added to the solution of **5**. The reaction was stirred for 4 h at 23 ^{o}C and then dried under vacuum, and the resulting solids were dissolved in ethyl acetate and filtered through a small plug of silica gel to remove impurities. The ethyl acetate was then removed under vacuum, and the crude solid was purified by silica gel column chromatography (9:1 hexane:EtOAc v/v) to give (p-OMe-C_6H_4)$_3$CCl as an orange solid (9.5 mg, 90%) . ^{1}H NMR (CD_2Cl_2, 400MHz) δ 7.24 (d, 6H), 6.93 (d, 6H), 3.90 (s, 9H).

Quantification of (p-Cl-C_6H_4)$_3$CCl. The same procedure as described for (p-OMe-C_6H_4)$_3$CCl was employed to quantify (p-Cl-C_6H_4)$_3$CCl**.** Purification by silica gel column chromatography (9:1 hexane:EtOAc v/v) gave (p-Cl-C_6H_4)$_3$CCl as an orange solid (8.6 mg, 80%) . ^{1}H NMR (CD_2Cl_2, 400MHz) δ 7.30 – 7.17 (m, 12H).

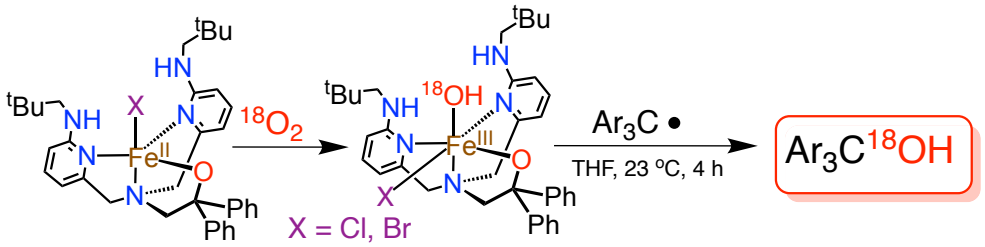

^{18}O labeling studies. Crystalline **1** (5 mg, 0.007 mmol) was dissolved in THF (1 mL). Dry $^{18}O_2$ (2 mL) was added via a gas-tight three way syringe, leading to a color change from yellow to orange that was consistent with the formation of **3**. The volatiles were removed under vacuum, the residue was dissolved in THF (1 mL) and $(Ph_3C)_2$ (34 mg, 0.07 mmol) was added. The reaction was stirred for 4 h under light limiting conditions. A color change from orange to dark yellow was noted. The volatiles were removed under vacuum, and the crude reaction mixture was analyzed by electron ionization mass spectrometry (EI-MS). A peak at *m/z* 262.2 was observed, corresponding to $Ph_3C^{18}OH$. A control reaction with $^{16}O_2$ carried out in an identical manner gave a peak at *m/z* 260.2, two mass units below the ^{18}O-labeled product. The same reaction was carried out between **4** and $(p\text{-Cl-}C_6H_4)_3C\bullet$. A peak at *m/z* 364 was observed, corresponding to $(p\text{-Cl-}C_6H_4)_3C^{18}OH$. A control reaction with $^{16}O_2$ carried out in an identical manner gave a peak at *m/z* 362, two mass units below the ^{18}O-labeled product.

Single Crystal X-ray Crystallography.

All reflection intensities were measured at 110(2) K using a SuperNova diffractometer (equipped with Atlas detector) with Mo *K*α radiation (λ = 0.71073 Å) under the program CrysAlisPro (Version CrysAlisPro 1.171.39.29c, Rigaku OD, 2017). The same program was used to refine the cell dimensions and for data reduction. The structures were solved with the program SHELXS-2018/3 (Sheldrick, 2018) and were refined on F^2 with SHELXL-2018/3 (Sheldrick, 2018). Numerical absorption correction based on gaussian integration over a multifaceted crystal model was applied using CrysAlisPro. The temperature of the data collection was controlled using the system Cryojet (manufactured by Oxford Instruments). The H atoms were placed at calculated positions (unless otherwise specified) using the instructions AFIX 23, AFIX 43 or AFIX 137 with isotropic displacement parameters having values 1.2 or 1.5 *U*eq of the attached C atoms.

Refinement of 1. The H atoms attached to N1 and N5 were found from difference Fourier maps, and their coordinates were refined pseudofreely using the DFIX instruction in order to keep the N–H bond distances within an acceptable range. The absolute configuration has been established by anomalous-dispersion effects in diffraction measurements on the crystal. The Flack and Hooft parameters refine to -0.014(4) and -0.012(1), respectively.

Refinement of 2. The H atoms attached to N1 and N5 were found from difference Fourier maps, and their coordinates were refined pseudofreely using the DFIX instruction in order to keep the N–H bond distances within acceptable ranges. The absolute configuration has been established by anomalous-dispersion effects in diffraction measurements on the crystal. The Flack and Hooft parameters refine to -0.008(2) and -0.001(4), respectively.

Refinement of 3. The H atoms attached to N1, N5 and O2 were found from difference Fourier maps, and their coordinates were refined pseudofreely using the DFIX instruction in order to keep the N–H and O–H bond distances within acceptable ranges. The C18 → C22 moiety is found to be disordered over two orientations, and the occupancy factor of the major component of the disorder refines to 0.730(4). There is also some small amount of substitutional disorder at the site O2–H/Cl2. The occupancy factor of the hydroxide (major component) refines to 0.942(3).

Refinement of 4. The H atoms attached to NI, N5 and O1 were found from difference Fourier maps, and their coordinates were refined pseudofreely using the DFIX instruction in order to keep the N–H and O–H bond distances within acceptable ranges. At the same coordination site occupied mostly by $-OH^-$, a small Br^- impurity is found, and its occupancy factor refines to 0.0114(8).

Refinement of 5. The H atoms attached to N1 and N5 were found from difference Fourier maps, and their coordinates were refined pseudofreely using the DFIX instruction in order to keep the N–H distance within an acceptable range. One of the two crystallographically independent THF solvent molecule is found to be disordered over two orientations, and the occupancy factor of the major component of the disorder refines to 0.585(16). The crystal was found to be pseudo-merohedrally twinned as the true *C* monoclinic unit cell

has a beta angle very close to 90° and emulates a *C* orthorhombic unit cell. The twinning was handled using the TWIN 1 0 0 0 -1 0 0 0 -1 instruction. Once the twinning was taken into account, the refinement had no further problems.

A. **Supporting Tables.** **Table S1**. Comparison of metrical parameters obtained from X-ray crystallography and DFT calculations for **1** and **2.**

	Complex **1** (X =Cl)		Complex **2** (X =Br)	
Bond lengths	Bond lengths (Å) and bond angles (º) by XRD	Bond lengths (Å) and bond angles (º) by DFT	Bond lengths (Å) and bond angles (º) by XRD	Bond lengths (Å) and bond angles (º) by DFT
Fe1–N2	2.2268(16)	2.226	2.2392(19)	2.229
Fe1–N3	2.2039(17)	2.243	2.197(2)	2.158
Fe1–N4	2.1783(16)	2.152	2.186(2)	2.244
Fe1–O1	1.9221(14)	1.888	1.9175(16)	1.891
Fe1–X1	2.3972(5)	2.392	2.5570(4)	2.505
N1–X1	3.2064(18)	3.157	3.360(2)	3.353
N5–X1	3.2395(19)	3.378	3.366(2)	3.581
Bond Angles				
N2–Fe1–N3	75.67(6)	75.69	75.85(7)	75.46
N2–Fe1–N4	106.75(6)	101.9	108.02(7)	101.61
N3–Fe1–N4	77.65(6)	77.92	77.17(7)	77.46
N2–Fe1–O1	135.74(6)	140.97	135.01(7)	141.78
N3–Fe1–O1	82.14(6)	80.53	82.18(7)	80.35
N4–Fe1–O1	105.15(6)	102.81	104.56(7)	101.46
O1–Fe1–X1	96.82(4)	99.11	95.64(5)	97.82
X1–Fe1–N2	100.91(4)	97.82	101.54(5)	97.69
X1–Fe1–N3	173.30(5)	167.63	173.12(5)	164.34
X1–Fe1–N4	108.96(4)	114.02	109.72(5)	118.01
N1–H1–X1	176(3)	167	166(3)	160
N5–H5–X1	167(2)	162	166(3)	165

Table S2. Comparison of metrical parameters obtained from X-ray crystallography and DFT calculations for **3** and **4**.

	Complex **3** (X =Cl)		Complex **4** (X =Br)	
Bond lengths	Bond lengths (Å) and bond angles (°) by XRD	Bond lengths (Å) and bond angles (°) by DFT	Bond lengths (Å) and bond angles (°) by XRD	Bond lengths (Å) and bond angles (°) by DFT
Fe1–N2	2.2674(17)	2.299	2.248(2)	2.295
Fe1–N3	2.2649(17)	2.307	2.174(2)	2.235
Fe1–N4	2.1757(17)	2.233	2.2581(19)	2.315
Fe1–O1	1.9128(13)	1.877	1.9026(19)	1.876
Fe1–X1	2.3945(6)	2.394	2.5835(4)	2.56
Fe1–O2	1.903(2)	1.917	1.9008(16)	1.916
N1–O2	2.703(3)	2.691	2.693(3)	2.695
N5–O2	2.867(2)	2.822	2.861(3)	2.819
Bond angles				
N2–Fe1–N3	78.77(6)	73.97	79.50(7)	78.19
N2–Fe1–N4	88.52(6)	89.08	88.87(7)	89.1
N3–Fe1–N4	73.63(6)	78.29	73.59(7)	73.98
N2–Fe1–O1	88.91(6)	87.26	91.32(8)	87.49
N3–Fe1–O1	81.41(6)	80.13	166.90(8)	153.9
N4–Fe1–O1	153.93(6)	154.04	97.09(7)	79.99
O1–Fe1–X1	93.32(4)	96.25	91.04(6)	96.14
X1–Fe1–N4	97.19(7)	96.37	87.38(5)	85.6
X1–Fe1–N2	175.38(5)	173.48	175.79(5)	174.1
X1–Fe1–N3	97.55(5)	96.85	97.59(5)	97.83
O2–Fe1–N4	87.74(4)	85.37	154.89(7)	165.51
O2–Fe1–N2	91.03(8)	90.96	89.47(7)	90.94
O2–Fe1–N3	166.28(7)	165.48	81.47(7)	96.53
O2–Fe1–X1	92.15(6)	93.04	93.12(5)	92.23
O2–Fe1–O1	107.79(7)	109.38	108.00(7)	109.38

N1–H1–O2	161(3)	163	156(3)	164
N5–H5–O2	162(3)	163	162(3)	163

Table S3. Comparison of metrical parameters obtained from X-ray crystallography and DFT calculations for **5**.

	Bond lengths (Å) and bond angles (°) by XRD	Bond lengths (Å) and bond angle (°) by DFT
Bond lengths		
Fe1–N2	2.2582(16)	2.302
Fe1–N3	2.1518(17)	2.229
Fe1–N4	2.2152(16)	2.335
Fe1–O1	1.8659(14)	1.864
Fe1–Cl2	2.3665(5)	2.349
Fe1–Cl1	2.3360(5)	2.351
N1–Cl1	3.2012(19)	3.274
N5–Cl1	3.1582(19)	3.298
Bond angles		
N2–Fe1–N3	74.10(6)	75.36
N2–Fe1–N4	152.77(6)	152.44
N3–Fe1–N4	78.74(6)	77.26
N2–Fe1–O1	90.30(6)	89.94
N3–Fe1–O1	83.11(6)	79.94
N4–Fe1–O1	84.54(6)	88.32
O1–Fe1–Cl2	170.87(5)	169.79
Cl2–Fe1–N4	88.93(6)	87.77
Cl2–Fe1–N2	92.76(5)	89.17
Cl2–Fe1–N3	89.46(5)	90.00

Cl1–Fe1–N4	106.85(6)	104.84
Cl1–Fe1–N2	100.62(4)	102.72
Cl1–Fe1–N3	174.72(5)	173.56
Cl1–Fe1–Cl2	91.14(2)	96.14
O2–Fe1–O1	96.75(5)	93.98
N1–H1–Cl1	154(2)	169
N5–H5–Cl1	174(3)	169

Table S4. DFT optimized coordinates for **1**.

Fe	4.88220013651211	0.82037094245890	4.43625132917522
C	8.20349398774879	3.75999998173240	6.79044710942307
H	7.80446052528327	4.76709115866820	6.57126058392618
H	7.90789016929889	3.08406004151019	5.97023102048449

H	9.30633435786916	3.82224289070050	6.78254502747175
C	8.25827363048332	1.83360835719877	8.43711595506970
H	9.36304527304828	1.84804490086792	8.46169424745281
H	7.95536049028402	1.12168128736922	7.65032302850874
H	7.90227116630679	1.45322413829648	9.41253331147951
C	8.21272408137677	4.21088134934404	9.27069810112009
H	7.88704310037428	3.87834805812404	10.27376664806182
H	7.84047357083742	5.24002477836924	9.11513804363693
H	9.31663534945395	4.25038557371412	9.27158231229073
C	7.71296085840541	3.25287212557849	8.16565178099279
C	6.16552441369125	3.26839050045200	8.23541179958057
H	5.85440714165851	2.94611756923056	9.25150851376560
H	5.81861242723959	4.31588775332415	8.10778975243905
C	4.16268154329241	2.41620327902451	7.05354311364197
C	3.28201721730479	3.12053233186772	7.92828963057904
C	1.91994809490457	3.12084900082646	7.65951263034888
C	1.42788207212268	2.43121920440256	6.53557107129220
H	0.36390243257596	2.43270010822228	6.28339575689967
C	2.34008035350933	1.73472511549037	5.74032554832607
C	1.86280908811602	0.92065123691517	4.54965719818217
H	1.70913138468772	-0.12512172538692	4.87432433326211
H	0.87710066695134	1.29582242631302	4.20198222643032
C	2.82361684056173	-0.32588857744839	2.66608520775703
H	3.55510230419011	-0.20690920247069	1.84711147294060
H	1.82857086653258	-0.49394143513796	2.19822323020152
C	3.20232453532013	-1.51824651339447	3.52034448729916
C	2.58368916597294	-2.75441264142976	3.33476896528859
H	1.80323291117823	-2.86931416552844	2.57753714621889
C	2.98901214680889	-3.82916694883229	4.14857695763328
C	3.96684288563027	-3.62776704757594	5.11321130590753
C	4.56122392284496	-2.33946828249130	5.25214479466340
C	6.24268847126359	-3.04229904065831	6.99167324006387
H	7.31348274343213	-2.77074179430712	6.93507471431738
H	6.15195937696556	-4.04771813918286	6.54008102794474
C	5.82283670677672	-3.09623051622690	8.49089551339497
C	6.02919774805895	-1.70868602958057	9.13328670733118
H	7.08833575518669	-1.39685942568784	9.08157314560919
H	5.73314383590845	-1.72281913071856	10.19737334724977
H	5.42475536737757	-0.93980435395076	8.62094150699760
C	6.72584417527195	-4.13551776716439	9.18850441984402
H	6.60526636173169	-5.14050548302170	8.74267580032641
H	6.47453675333096	-4.21469674108859	10.26136046438583
H	7.79317625463629	-3.85721030664574	9.11340596614206
C	4.34550912215544	-3.51696336901649	8.62477157434543
H	3.68011417261104	-2.81954800257617	8.08704723300399
H	4.03885071235354	-3.52668866875549	9.68617942274078

H	4.17669334096087	-4.53279265553617	8.22268709616976
C	2.85652019478948	2.15618843145031	2.66759482817562
H	2.52975208543806	2.96494286371404	3.34150578776153
H	2.12107802264061	2.08476162200385	1.83893607760342
C	4.30971498865361	2.52231915917599	2.19005866806352
C	4.36459133606780	4.02791867997668	1.82768865988876
C	5.54778115788760	4.73650520962495	2.11186779612961
H	6.36294366064059	4.19741081916842	2.60252205961666
C	5.66413202328751	6.09526901723149	1.78805043833641
H	6.59434546252458	6.62854175688609	2.01576620540933
C	4.59530360552484	6.77530045789025	1.18073272013039
H	4.68615009264560	7.83728620697405	0.92804553599839
C	3.40856572384307	6.08167444511130	0.90208009309803
H	2.56301529560921	6.60055348431083	0.43614366728447
C	3.29587651710512	4.71848322086818	1.22175834313417
H	2.35629876302093	4.20116209979814	0.99416186797388
C	4.72392128079313	1.71261719830894	0.92454667603897
C	3.96848617313450	1.73328389726736	-0.26713040214194
C	4.37280940102285	0.99326741064069	-1.38831056561582
H	3.77147720335116	1.02354489834400	-2.30424256224506
C	5.54804589457451	0.22512669945351	-1.34184709043776
H	5.86659318138542	-0.34840275510768	-2.21913572645486
C	6.31319646218910	0.20828745506595	-0.16560967670335
H	7.23771335475530	-0.37770118875218	-0.11905707093822
C	5.90473173008911	0.94567204160187	0.95821033611271
H	6.49767238052869	0.94642799323859	1.87787195921641
N	5.50814041272250	2.42287432877285	7.24144548214043
H	6.07391734595418	1.93527791342664	6.53073955691977
N	3.67649000981902	1.70496713063753	5.98407080900975
N	2.86246276816666	0.90814054232887	3.46554014817570
N	4.17256062828850	-1.28923141152402	4.45073081013488
N	5.51976055084409	-2.06575011953385	6.18231482768425
H	6.01776309687543	-1.17550295807398	6.01940463273765
O	5.16866220432051	2.26335214745032	3.25266153339953
Cl	7.14751500586600	0.40622244810881	5.08347878004568
H	2.52820751130775	-4.81601528343841	4.03595537880749
H	4.27045495111190	-4.44123098797994	5.77351617427855
H	1.23570618513657	3.66806201927111	8.31662899341075
H	3.68220225742684	3.65830908124416	8.78958735430147
H	3.06205107025976	2.34569787887686	-0.33150792809957

Table S5. DFT optimized coordinates for **2**.

Fe	4.75096045465756	0.70746173432551	4.46128682825637
C	7.96091217071853	3.62305657005287	6.92398669813465
H	7.55173125171441	4.61517315962448	6.66053116695447
H	7.71017916813169	2.91885362589463	6.11210325619647

H	9.06188220147069	3.70646047130896	6.95641773189989
C	7.98199766795735	1.74460166853387	8.62798237206040
H	9.08549520391646	1.77342509510636	8.67719923845509
H	7.70612320973289	1.00021655240014	7.86183548855099
H	7.60762510822762	1.39393930800361	9.60748363108462
C	7.87330555480461	4.14339320600188	9.38779363280044
H	7.50507761741343	3.84206265451727	10.38603889940505
H	7.50315790042265	5.16445437756065	9.18174910292409
H	8.97583544784560	4.18969825165647	9.43648436756064
C	7.42717726817102	3.14624929381574	8.29367482470048
C	5.87873547518003	3.14259130295546	8.30879179513243
H	5.53802559049511	2.83360595286102	9.31897018368392
H	5.52372983424332	4.18362244810325	8.15219259509007
C	3.92280744619303	2.28818427148655	7.05972487359056
C	3.01181903712661	2.98427826387424	7.90904981711877
C	1.66452068262393	3.01373076819082	7.57439067393543
C	1.21894033802793	2.36616922106924	6.40738762037979
H	0.17029176100329	2.39757795008564	6.09958678121616
C	2.15861579459241	1.67475326315962	5.63958252669731
C	1.73242638745208	0.91786995946799	4.39362269850680
H	1.52896220347088	-0.13343990823556	4.66848785346848
H	0.78193511292941	1.33500748199324	3.99945454269666
C	2.77606794164407	-0.27896324964797	2.52112787206626
H	3.56945059608488	-0.15765165401845	1.76196198863465
H	1.81331065761325	-0.38935931324646	1.97447283885703
C	3.04111752652230	-1.51779360738841	3.35257436033552
C	2.38141752154190	-2.71460055902532	3.06926500815295
H	1.66458296840712	-2.76244322026983	2.24474357464606
C	2.67297853444835	-3.83910859416370	3.86159256328832
C	3.57378813604984	-3.71744324136662	4.91111225224224
C	4.19324860688609	-2.45792007267162	5.16645391117923
C	5.37032649432988	-3.38403370566190	7.13249305041409
H	5.90789633879590	-4.19448211081918	6.59168096889485
H	4.41917065708981	-3.81613852647439	7.50031955278392
C	6.21816656754802	-2.96399613113762	8.36068339420686
C	7.64797776111873	-2.56984842220859	7.92967388236215
H	8.14923306841633	-3.40808813920155	7.41098803100516
H	8.25673250873687	-2.30745192120316	8.81337458495326
H	7.65523512927142	-1.70122464425350	7.24798460539040
C	6.29383396512511	-4.19747503165078	9.28950887460261
H	5.29382308495606	-4.48770676698321	9.66093727228776
H	6.92849734090981	-3.98085642337410	10.16662493993957
H	6.73076778936748	-5.06990304241621	8.76966268471535
C	5.54208176590448	-1.79982967575763	9.11504773710120
H	5.49346195026372	-0.88473953407169	8.50101267981637
H	6.10738724626382	-1.55785613030766	10.03293498642550

H	4.51111303405305	-2.06394689256276	9.41223964132113
C	2.88388526309821	2.20055390551102	2.63991207610345
H	2.54727573040610	2.98783253491436	3.33395834811553
H	2.19457766715731	2.19617798762868	1.76987040513594
C	4.37397211663267	2.53343733714467	2.26653896977816
C	4.50514873481522	4.05106213159680	1.98221495412944
C	5.69817807146129	4.69613658434029	2.36055631158182
H	6.46492632923025	4.10137071879377	2.86462247560689
C	5.88416989020993	6.06277527518543	2.11063432656624
H	6.82153067880115	6.54518812116195	2.41045054611398
C	4.87588478522650	6.81437669350939	1.48461366876430
H	5.02097524593495	7.88261402266565	1.28955508793003
C	3.67954005498567	6.18416300629191	1.11224591746793
H	2.87998437776583	6.75932443830721	0.63131585548319
C	3.49765000810403	4.81288234527805	1.35722592236754
H	2.55200595426192	4.34656519049019	1.05741049718283
C	4.83665828150460	1.77091478728393	0.98858445670148
C	4.14974574942286	1.87006614843569	-0.23989890762372
C	4.59921866941569	1.17663374519676	-1.37347690950126
H	4.05132020462475	1.26830711136426	-2.31827948249246
C	5.75210660596101	0.37716899885627	-1.30197164852931
H	6.10612733954317	-0.15966343187902	-2.18872429860688
C	6.44892639608506	0.28150175790130	-0.08779494135441
H	7.35548857783885	-0.32995919774521	-0.02014284782845
C	5.99530767615322	0.97240947192028	1.04805063037126
H	6.53500798850487	0.91000884984318	1.99796674760053
N	5.26010567593392	2.27271784167273	7.30922862667635
H	5.84551256537264	1.81554482627186	6.59394613307138
N	3.47888185491610	1.60970863947115	5.95307948690579
N	2.79917879706459	0.91725170333480	3.37490751208874
N	3.93528743551173	-1.36515316811848	4.37046229152108
N	5.03763195321208	-2.28747001991584	6.22488052279112
H	5.70591437990013	-1.50388844716382	6.13432450663075
O	5.15666921767935	2.19345380556528	3.36514836348812
Br	7.09561699232420	0.11679202502481	5.11607290459982
H	2.19536796500730	-4.80311196481398	3.65818996817454
H	3.82335537725439	-4.58002629658878	5.53085457994119
H	0.95681454837855	3.55375749577014	8.21226802369579
H	3.37683097256530	3.49169423315359	8.80348080564053
H	3.26317278786378	2.50895445840811	-0.32370234241176

Table S6. DFT optimized coordinates for **3**.

Fe	6.88754495677967	12.76021691007227	4.32700089739328
Cl	8.79039223156907	12.26549291641061	2.96035363969664
O	5.92472791917811	11.21581224898221	3.72393034498958
H	6.49538188216198	10.49190231209836	3.43305357388292

C	4.58077114944614	8.66408469643328	6.30789586558758
H	5.42486069987048	9.35822000917382	6.22487671451054
H	4.41856258085149	8.21031757416273	5.32118881230963
H	4.87159206633113	7.86247599200367	6.99780133864809
C	2.15271795093296	8.36440596076221	6.90191494847957
H	2.39439081510301	7.56327576017975	7.61023540354079
H	1.94813556253941	7.89835197756542	5.92935894390177
H	1.22611155074605	8.84256253644579	7.24548685830141
C	3.57012019566417	9.99209594941273	8.19415672804861
H	4.36102929544746	10.74930893699329	8.15195023114723
H	3.88173544633714	9.21818827096299	8.90680710605125
H	2.66628012532438	10.46746112160365	8.59709574462318
C	3.31010188220254	9.37718079046408	6.80778172824740
C	2.88567835158662	10.47299028701983	5.78844223454367
H	2.62357862674011	9.97534990264481	4.84583603675244
H	1.97026539261157	10.96274157445384	6.13732769485627
C	4.00129656104719	12.72329857318852	5.97017108924847
C	3.07116449953602	13.26077576308958	6.89865368082457
H	2.23348862914650	12.66411455546390	7.23498796899977
C	3.26354271512766	14.53397897067281	7.39221686658866
H	2.56287148471947	14.94549018499695	8.11466097057302
C	4.37049397565444	15.28038566476395	6.97801626933838
H	4.56717328017826	16.27065100767014	7.37317943608959
C	5.23187140579534	14.70714867207931	6.05155590956503
C	6.38208464384481	15.55188086011672	5.53447501529482
H	5.97088307326517	16.21404765504636	4.76315009849450
H	6.74471393768938	16.19843718833684	6.34292086141387
C	7.94926802614353	15.49325710737932	3.68457621948602
H	8.87363106921283	15.01401469721960	3.34738596504443
H	8.15756140734424	16.55952100957357	3.85758660867599
C	6.90729877690142	15.32261419222608	2.60119987178346
C	6.71597189061717	16.30463176331735	1.64043604175420
H	7.26181322230069	17.24061819615777	1.69221023446595
C	5.82158009357376	16.02971213989145	0.59777842966526
H	5.65073752685156	16.76290632021257	-0.18679180924391
C	5.16012829645620	14.81967508346802	0.56012605293493
H	4.48470863280955	14.58989975204734	-0.25342404171259
C	5.37860865208105	13.86854502443054	1.59648325674055
C	3.90716846407179	12.21812185583057	0.51382430125392
H	4.52030733605985	12.08041116913393	-0.39248686584099
H	3.17016710188367	12.99920921303715	0.28420094777033
C	3.13052527929662	10.91076854300909	0.79410779848970
C	2.32016172033144	10.58885691852765	-0.47827785964931
H	1.73781289858946	9.67040849379582	-0.33943422450456
H	2.97765910131720	10.43893058419160	-1.34400741835850
H	1.61712002306936	11.39546025928041	-0.72256353622414
C	2.16397700272720	11.11106050686702	1.97646019156614
H	2.69748275290584	11.39638517647298	2.88839137231522
H	1.60756521881655	10.18696378541326	2.17898567711487
H	1.43280848188269	11.89913486425062	1.75627602602365
C	4.09262939638082	9.74080473497722	1.08187369118320

H	4.65429735872851	9.89145864181249	2.00923958277674
H	4.81259796829652	9.60841433289625	0.26416457313870
H	3.52892534001239	8.80503731879338	1.18460044965952
C	8.66187531206854	14.55340215539545	5.84291271207153
H	8.93152478565807	15.45809742287535	6.40276769058526
H	9.50714214178174	14.29350424005088	5.20344660093251
C	8.40441242061829	13.30607811040047	6.75289593386173
C	7.60992254911909	13.60707893313731	8.04452234158683
C	6.84441165804895	12.57249312758019	8.60318487646063
H	6.79564632476561	11.62649976307463	8.07433408304373
C	6.16421792450320	12.75111128725286	9.80670906521035
H	5.58169478175647	11.93141391979338	10.22093991368380
C	6.23220942563626	13.97260590435794	10.48317865007569
H	5.70462125863507	14.11083538486879	11.42325937524835
C	6.99247563374850	15.00858459489681	9.94272546522527
H	7.06204989990653	15.96327731759371	10.45944587332298
C	7.67683245206910	14.82477155215918	8.73640791166384
H	8.27272668613669	15.64816870003496	8.35155793843373
C	9.79683724494645	12.73827202616534	7.14158339107457
C	10.58226480171808	13.31652219634840	8.14874852368340
H	10.19982312553127	14.15172877941808	8.72805936129460
C	11.85256566664384	12.81481907495712	8.44013517024323
H	12.44357897582085	13.27487721940765	9.22884032467243
C	12.35546770616612	11.72201442306170	7.73213184025761
H	13.34166763420539	11.32692622294579	7.96237797767469
C	11.57887250743276	11.14117159442800	6.72772438093236
H	11.95951829855198	10.29074607224401	6.16725898543514
C	10.31135523510379	11.64580734680775	6.43140399636299
H	9.71284029672669	11.20432689069697	5.64333354705386
N	3.89517319287453	11.46875791923969	5.47201864997754
H	4.63462234962517	11.19017328205403	4.80583516944274
N	5.05854847837235	13.47629416163924	5.53645052011058
N	7.51756310267570	14.81674087260844	4.92658938634135
N	6.24724236543878	14.14700141062869	2.60835726313597
N	4.73976100666890	12.67515065442680	1.61924272189356
H	5.08918979387384	11.99630151431698	2.31220964746201
O	7.71138903708166	12.37827941764994	5.97021616329377

Table S7. DFT optimized coordinates for **4**.

Fe	6.87771314640161	12.76692493506602	4.32502144048586
Br	8.89100848469648	12.20443383760142	2.84792898757110
O	5.91277275223139	11.22363261824588	3.72650652551907
H	6.48304372079389	10.49630742586072	3.44361376624901

C	4.55351761725205	8.67091118188737	6.30203812012957
H	5.40075490721628	9.36132905002443	6.22029399018878
H	4.38755678303099	8.22179200199315	5.31385465511890
H	4.84166314903296	7.86526131647254	6.98836496231073
C	2.12586925793288	8.38021304830149	6.90124099898811
H	2.36582219513219	7.57639848356432	7.60711348002427
H	1.91697398408234	7.91728612070587	5.92810887297559
H	1.20204736684025	8.86138602211180	7.24811133313134
C	3.55344621613447	9.99808550090934	8.19436061481763
H	4.34638957598152	10.75318541116371	8.15257696865296
H	3.86486303982293	9.22092926544872	8.90358796946211
H	2.65222279709740	10.47467468901249	8.60166235217569
C	3.28732515849445	9.38828609665737	6.80685328899983
C	2.86469833060204	10.48811004220194	5.79097903282633
H	2.59857242487772	9.99337902713744	4.84806907252890
H	1.95176224704713	10.98036507788855	6.14299650542997
C	3.99097696846377	12.73174203617845	5.98104120089370
C	3.06864414007544	13.26555852667951	6.91945452046401
H	2.23024194842005	12.67015286109469	7.25617152408658
C	3.26990490916534	14.53354189081706	7.42288096778617
H	2.57545710565314	14.94163736781607	8.15325568249087
C	4.37752573281726	15.27887807418996	7.00841819979029
H	4.58092987404182	16.26492225118248	7.41052693669329
C	5.22990540837921	14.70980556632150	6.07115043027546
C	6.37726915472133	15.55537851731412	5.54977407623536
H	5.96050477948842	16.21980277096092	4.78342340467910
H	6.74528404001064	16.19933967400167	6.35783126774488
C	7.93073738418835	15.50998697524925	3.69103654625495
H	8.85513879013077	15.03695995819900	3.34441224518096
H	8.13436792060846	16.57636540403212	3.86880386505082
C	6.88364115479926	15.33890602203079	2.61330007660393
C	6.67983263999029	16.32595235106090	1.66063470028263
H	7.21806644999056	17.26600378227233	1.71719607479238
C	5.78331675306566	16.05102690111746	0.61972049066517
H	5.60236504793899	16.78853718741188	-0.15850731069741
C	5.13303252072998	14.83535056191413	0.57587982566217
H	4.45534053698881	14.60574497586219	-0.23583601147723
C	5.36458603721603	13.87794283848397	1.60366157362905
C	3.90945788100894	12.22202240725921	0.50802277684205
H	4.52328302917412	12.10605648610840	-0.40077228415312
H	3.15907955765694	12.99365515376071	0.28942005400415
C	3.15681256948003	10.89766203736453	0.77288133616059
C	2.35271760978680	10.57576887631128	-0.50345313706437
H	1.78416446996398	9.64735496424500	-0.37396300454715
H	3.01314362003354	10.44394638117254	-1.36993008886445
H	1.63774360006617	11.37391859006699	-0.74078054820162
C	2.18665430307664	11.06578602205171	1.95702885590866
H	2.71416244912069	11.35347167250232	2.87168499080654
H	1.65028566966594	10.12807298583133	2.15077617271679
H	1.43851897281219	11.84004972501213	1.74491312475496
C	4.14061554560385	9.74268296866433	1.04739080874891

H	4.69538116242357	9.89121977833884	1.97923452069766
H	4.86653642137146	9.63677925379824	0.23104749421873
H	3.59542368102485	8.79452117057504	1.13458030154261
C	8.66006651939147	14.55885203490846	5.83866505058982
H	8.93016400593444	15.46158779535702	6.40140811585804
H	9.50212701976157	14.30323682974140	5.19330034666049
C	8.40882971025384	13.30766588490879	6.74326752871287
C	7.62166530979628	13.59944518393148	8.04226597593907
C	6.86464416168532	12.55862429005025	8.60096462721609
H	6.81512324644752	11.61514944187298	8.06768347450284
C	6.19351821853571	12.72761340138840	9.81098298249835
H	5.61750767328904	11.90314432001203	10.22491481513337
C	6.26244484551116	13.94524427566356	10.49413777830278
H	5.74199639384066	14.07588985884663	11.43923995083151
C	7.01434431182406	14.98723401508570	9.95348344726025
H	7.08423527617695	15.93929785364669	10.47500551825938
C	7.68947469647394	14.81333945061280	8.74067588869937
H	8.27699080058669	15.64249115299335	8.35533462885095
C	9.80088038994254	12.74082748177247	7.13175430948244
C	10.63042576077355	13.39080262283481	8.05702921324392
H	10.28535747306756	14.28608788802799	8.56578798905332
C	11.89740652491384	12.88695571154994	8.35673812107352
H	12.52458703308868	13.40452005247538	9.07915496683148
C	12.35233091909934	11.71927391501904	7.74098134958180
H	13.33659600868381	11.32326427348770	7.97775614225136
C	11.53087839770067	11.06585156156996	6.82098975351604
H	11.87396540551764	10.15698266925619	6.33310558872445
C	10.26625634422568	11.57334410793116	6.51515186386260
H	9.63160826642519	11.07729003627540	5.79047610176546
N	3.87620931463921	11.48168063218868	5.47335593973199
H	4.61265030594027	11.20336403386849	4.80416395714488
N	5.04805759607416	13.48432033835393	5.54668808147090
N	7.50976347431676	14.82372482568638	4.93076643236796
N	6.23505220418459	14.15631597501290	2.61478125899638
N	4.73755792437404	12.67858554551088	1.61717021869733
H	5.08987937033500	11.99900937999381	2.30790456290761
O	7.71443210333452	12.38284704065770	5.95949942173752

Table S8. DFT optimized coordinates for **5**.

Fe	3.56294190214156	0.66339315666692	5.65040185552056
C	7.72847252982326	3.29578800805572	8.01868365539914
H	8.04744585220266	4.07810311889531	7.31811590895767
H	7.33641112817835	2.45569970734976	7.43728547776699

H	8.61943391719767	2.93854802600120	8.54926339975260
C	6.24264894203079	2.73049758003613	9.99164359105106
H	7.10159528422882	2.35773937226451	10.56254359140445
H	5.80186732517806	1.87554188075912	9.47028786467552
H	5.50253625421798	3.10875977906493	10.70876685690533
C	7.33959188167912	4.98364178884947	9.83736354391005
H	6.63505317112658	5.40724264787610	10.56490368401400
H	7.68642269653336	5.79707722559973	9.18742269316202
H	8.20674632337468	4.61026569202140	10.39404236149971
C	6.69489341966408	3.84259616166637	9.02353266560095
C	5.48242935453282	4.45718972431499	8.28724833012897
H	4.79922396548115	4.87814909685988	9.04068864482158
H	5.83635515784430	5.29677362003707	7.66864499301906
C	3.59837258237525	3.83554924517493	6.80939351961110
C	3.08042420378532	5.15975644668593	6.87659077158199
C	1.91008212258885	5.46667818734931	6.21772832821540
C	1.24534968404615	4.47234952805134	5.49079768326580
H	0.32350402229982	4.67748867863813	4.95773660662581
C	1.79603435196786	3.19946801464328	5.47369955928195
C	1.06624653671438	2.08237488877719	4.76686645071673
H	0.49280990154553	1.52248218642989	5.51176754992396
H	0.36342784574153	2.49668791513736	4.02934108169529
C	1.33013588809240	-0.13251542013127	3.79320632641438
H	0.75191607941190	-0.03105415855634	2.86332168322690
H	0.62642474072682	-0.34260696414689	4.60583539155555
C	2.26355903007310	-1.31669091256178	3.69714096634377
C	1.93992049926099	-2.35810485327095	2.84024583297440
H	1.07865469865455	-2.28068980766702	2.18553515118260
C	2.74333788852296	-3.50284905150215	2.86492335686144
C	3.82988891440373	-3.55296230408710	3.71091257044397
C	4.12586923146255	-2.43684625860314	4.54108480616706
C	6.14035930376682	-3.57262117898413	5.41788884467789
H	6.52386499657408	-3.77679440056394	4.40669422803768
H	5.60549137882156	-4.47704824270223	5.74846503338372
C	7.34350881503610	-3.34290346504607	6.36020473947089
C	8.17629796406783	-2.12954851822531	5.89933146520576
H	8.52540339409729	-2.26165458384043	4.86694444117793
H	9.05992944751652	-2.01441212637750	6.53814454049827
H	7.61030908487931	-1.19376566350570	5.95118508416552
C	8.21805916660665	-4.61123942162626	6.27788507310633
H	7.66681291170468	-5.50167974351999	6.60578800713303
H	9.09854360809201	-4.50941138814716	6.92253390215599
H	8.57217087839001	-4.78990789472288	5.25472455551918
C	6.87311275569344	-3.15187014569384	7.81634448503933
H	6.25579293484312	-2.25654326767882	7.94116437658681
H	7.73915261051309	-3.04836654705325	8.48107262700462

H	6.28967786106045	-4.01648631746984	8.15818088984499
C	2.69577861182901	1.78833119698552	2.96968989262049
H	2.54345425291424	2.86314667686418	3.07635037132286
H	2.20630479587243	1.48482202804809	2.03862175027392
C	4.25256317038115	1.54257515204755	2.95228078275250
C	4.93102270507193	2.85708478932545	2.48523649570198
C	5.81295399558319	3.52795815223889	3.33893280895282
H	6.01895566125470	3.10155116114475	4.31384690254320
C	6.41457308662682	4.72399218835348	2.93856095734467
H	7.10205749936908	5.22995163787670	3.61288443354905
C	6.13814770874414	5.27054036023331	1.68480335608746
H	6.60466877546226	6.20243432050677	1.37606869802587
C	5.25738215488354	4.60667418288944	0.82724909469321
H	5.03633516968905	5.01767714212724	-0.15475825000180
C	4.66361129696977	3.40797639934038	1.22345536302288
H	3.99861538288310	2.89371909097892	0.53425219474674
C	4.71691159246188	0.41468333740229	1.99664651009199
C	4.07134866850868	0.09202558246394	0.79620622071507
C	4.59417023036717	-0.87819055142298	-0.06447496115842
H	4.07136151802153	-1.11166881032625	-0.98890107625694
C	5.77681413641357	-1.54098395079791	0.25887014600478
H	6.18509203245043	-2.29374431340546	-0.41111047065772
C	6.43127378687367	-1.22506920345163	1.45249050885142
H	7.35746412912456	-1.73005881187104	1.71626216689847
C	5.90733431290439	-0.25877899414531	2.30979152400695
H	6.41145388994401	-0.01587790845430	3.23898737607504
N	4.75004327731087	3.51809454690561	7.44427752434340
H	5.05078655116628	2.54826035441018	7.41611374612314
N	2.94638706514327	2.87012575889364	6.10135342760528
N	2.00798292798921	1.13695589229845	4.12495058943950
N	3.32452953788070	-1.33384141230040	4.53152742657720
N	5.20876761753610	-2.45343478077954	5.35139731099589
H	5.35906547969560	-1.65384433063324	5.95852105159479
O	4.64628339716134	1.25353216856556	4.25345067685741
Cl	5.36557393079633	0.31894368607651	7.12043853167555
H	2.51789128609392	-4.34897101719797	2.22091939106665
H	4.46168473557599	-4.43066394618485	3.74303378094277
H	1.51268048025042	6.47750907344613	6.25981327772591
H	3.61229929683866	5.91866473311088	7.43477317806927
H	3.15080708825989	0.59183075144114	0.50657753032754
Cl	1.89069432492516	-0.06972137452609	7.12757071376347

Table S9. Crystallographic data for **1**.

Crystal data	
Chemical formula	$C_{36}H_{46}ClFeN_5O$
M_r	656.08
Crystal system, space group	Orthorhombic, $P2_12_12_1$
Temperature (K)	110
a, b, c (Å)	8.77732 (19), 17.1427 (3), 22.6633 (5)
V (Å^3)	3410.08 (12)
Z	4
Radiation type	Mo $K\alpha$
μ (mm^{-1})	0.56
Crystal size (mm)	0.39 × 0.18 × 0.14
Data collection	
Diffractometer	SuperNova, Dual, Cu at zero, Atlas
Absorption correction	Gaussian *CrysAlis PRO* 1.171.39.29c (Rigaku Oxford Diffraction, 2017) Numerical absorption correction based on gaussian integration over a multifaceted crystal model Empirical absorption correction using spherical harmonics, implemented in SCALE3 ABSPACK scaling algorithm.
T_{min}, T_{max}	0.524, 1.000
No. of measured, independent and observed [$I > 2\sigma(I)$] reflections	40871, 7799, 7456
R_{int}	0.030
$(\sin \theta/\lambda)_{max}$ (Å^{-1})	0.650
Refinement	
$R[F^2 > 2\sigma(F^2)]$, $wR(F^2)$, S	0.024, 0.055, 1.06
No. of reflections	7799
No. of parameters	409
No. of restraints	2
H-atom treatment	H atoms treated by a mixture of independent and constrained refinement
$\Delta\rho_{max}$, $\Delta\rho_{min}$ (e Å^{-3})	0.19, -0.18
Absolute structure	Flack x determined using 3149 quotients [(I+)-(I-)]/[(I+)+(I-)] (Parsons,

	Flack and Wagner, Acta Cryst. B69 (2013) 249-259).
Absolute structure parameter	-0.014 (4)

Table S10. Crystallographic data for **2**.

Crystal data	
Chemical formula	$C_{36}H_{46}BrFeN_5O$
M_r	700.54
Crystal system, space group	Orthorhombic, $P2_12_12_1$
Temperature (K)	110
a, b, c (Å)	8.9286 (2), 16.9996 (4), 22.4884 (5)
V (Å^3)	3413.35 (13)
Z	4
Radiation type	Mo $K\alpha$
μ (mm^{-1})	1.65
Crystal size (mm)	0.43 × 0.28 × 0.06
Data collection	
Diffractometer	SuperNova, Dual, Cu at zero, Atlas
Absorption correction	Gaussian *CrysAlis PRO* 1.171.39.29c (Rigaku Oxford Diffraction, 2017) Numerical absorption correction based on gaussian integration over a multifaceted crystal model Empirical absorption correction using spherical harmonics, implemented in SCALE3 ABSPACK scaling algorithm.
T_{min}, T_{max}	-0.291, 1.000
No. of measured, independent and observed [$I > 2\sigma(I)$] reflections	52117, 7837, 7522
R_{int}	0.039
$(\sin \theta/\lambda)_{max}$ (Å^{-1})	0.650
Refinement	
$R[F^2 > 2\sigma(F^2)]$, $wR(F^2)$, S	0.022, 0.050, 1.07
No. of reflections	7837
No. of parameters	409
No. of restraints	2
H-atom treatment	H atoms treated by a mixture of independent and constrained refinement
$\Delta\rho_{max}$, $\Delta\rho_{min}$ (e Å^{-3})	0.24, -0.22
Absolute structure	Flack x determined using 3191 quotients [(I+)-(I-)]/[(I+)+(I-)] (Parsons,

	Flack and Wagner, Acta Cryst. B69 (2013) 249-259).
Absolute structure parameter	-0.008 (2)

Table S11. Crystallographic data for **3**.

Crystal data	
Chemical formula	$C_{36}H_{47}Cl_{1.06}FeN_5O_{1.94}$
M_r	674.20
Crystal system, space group	Monoclinic, $P2_1/n$
Temperature (K)	110
a, b, c (Å)	12.6925 (3), 13.0034 (3), 21.3161 (5)
β (°)	102.247 (2)
V (Å^3)	3438.06 (14)
Z	4
Radiation type	Mo $K\alpha$
μ (mm^{-1})	0.56
Crystal size (mm)	0.34 × 0.20 × 0.09
Data collection	
Diffractometer	SuperNova, Dual, Cu at zero, Atlas
Absorption correction	Gaussian *CrysAlis PRO* 1.171.39.29c (Rigaku Oxford Diffraction, 2017) Numerical absorption correction based on gaussian integration over a multifaceted crystal model Empirical absorption correction using spherical harmonics, implemented in SCALE3 ABSPACK scaling algorithm.
T_{min}, T_{max}	0.530, 1.000
No. of measured, independent and observed [$I > 2\sigma(I)$] reflections	54628, 7900, 6650
R_{int}	0.040
$(\sin\theta/\lambda)_{max}$ (Å^{-1})	0.650
Refinement	
$R[F^2 > 2\sigma(F^2)]$, $wR(F^2)$, S	0.042, 0.110, 1.05
No. of reflections	7900
No. of parameters	467
No. of restraints	123
H-atom treatment	H atoms treated by a mixture of independent and constrained refinement
$\Delta\rho_{max}$, $\Delta\rho_{min}$ (e Å^{-3})	0.78, -0.50

Table S12. Crystallographic data for **4**.

Crystal data	
Chemical formula	$C_{36}H_{46.99}Br_{1.01}FeN_5O_{1.99}$
M_r	718.33
Crystal system, space group	Monoclinic, $P2_1/n$
Temperature (K)	110
a, b, c (Å)	12.6479 (4), 13.0462 (4), 21.3658 (7)
β (°)	101.978 (3)
V (Å^3)	3448.75 (19)
Z	4
Radiation type	Mo $K\alpha$
μ (mm^{-1})	1.65
Crystal size (mm)	0.42 × 0.20 × 0.04
Data collection	
Diffractometer	SuperNova, Dual, Cu at zero, Atlas
Absorption correction	Gaussian *CrysAlis PRO* 1.171.39.29c (Rigaku Oxford Diffraction, 2017) Numerical absorption correction based on gaussian integration over a multifaceted crystal model Empirical absorption correction using spherical harmonics, implemented in SCALE3 ABSPACK scaling algorithm.
T_{min}, T_{max}	0.446, 1.000
No. of measured, independent and observed [$I > 2\sigma(I)$] reflections	51445, 7906, 6298
R_{int}	0.064
$(\sin\theta/\lambda)_{max}$ (Å^{-1})	0.650
Refinement	
$R[F^2 > 2\sigma(F^2)]$, $wR(F^2)$, S	0.039, 0.089, 1.03
No. of reflections	7906
No. of parameters	425
No. of restraints	3
H-atom treatment	H atoms treated by a mixture of independent and constrained refinement
$\Delta\rho_{max}$, $\Delta\rho_{min}$ (e Å^{-3})	0.51, -0.49

Table S13. Crystallographic data for **5**.

Crystal data	
Chemical formula	$C_{36}H_{46}Cl_2FeN_5O \cdot 2(C_4H_8O)$
M_r	835.73
Crystal system, space group	Monoclinic, *C*2/*c*
Temperature (K)	110
a, *b*, *c* (Å)	32.8869 (9), 11.1130 (3), 23.5812 (5)
β (°)	90.019 (2)
V (Å^3)	8618.3 (4)
Z	8
Radiation type	Mo *K*α
μ (mm^{-1})	0.52
Crystal size (mm)	0.51 × 0.45 × 0.06
Data collection	
Diffractometer	SuperNova, Dual, Cu at zero, Atlas
Absorption correction	Gaussian *CrysAlis PRO* 1.171.39.29c (Rigaku Oxford Diffraction, 2017) Numerical absorption correction based on gaussian integration over a multifaceted crystal model Empirical absorption correction using spherical harmonics, implemented in SCALE3 ABSPACK scaling algorithm.
T_{min}, T_{max}	0.196, 1.000
No. of measured, independent and observed [$I > 2\sigma(I)$] reflections	66787, 9900, 9178
R_{int}	0.049
$(\sin \theta/\lambda)_{max}$ (Å^{-1})	0.650
Refinement	
$R[F^2 > 2\sigma(F^2)]$, $wR(F^2)$, *S*	0.032, 0.079, 1.05
No. of reflections	9900
No. of parameters	546
No. of restraints	162
H-atom treatment	H atoms treated by a mixture of independent and constrained refinement
$\Delta\rho_{max}$, $\Delta\rho_{min}$ (e Å^{-3})	0.46, -0.28

E. Supporting Figures.

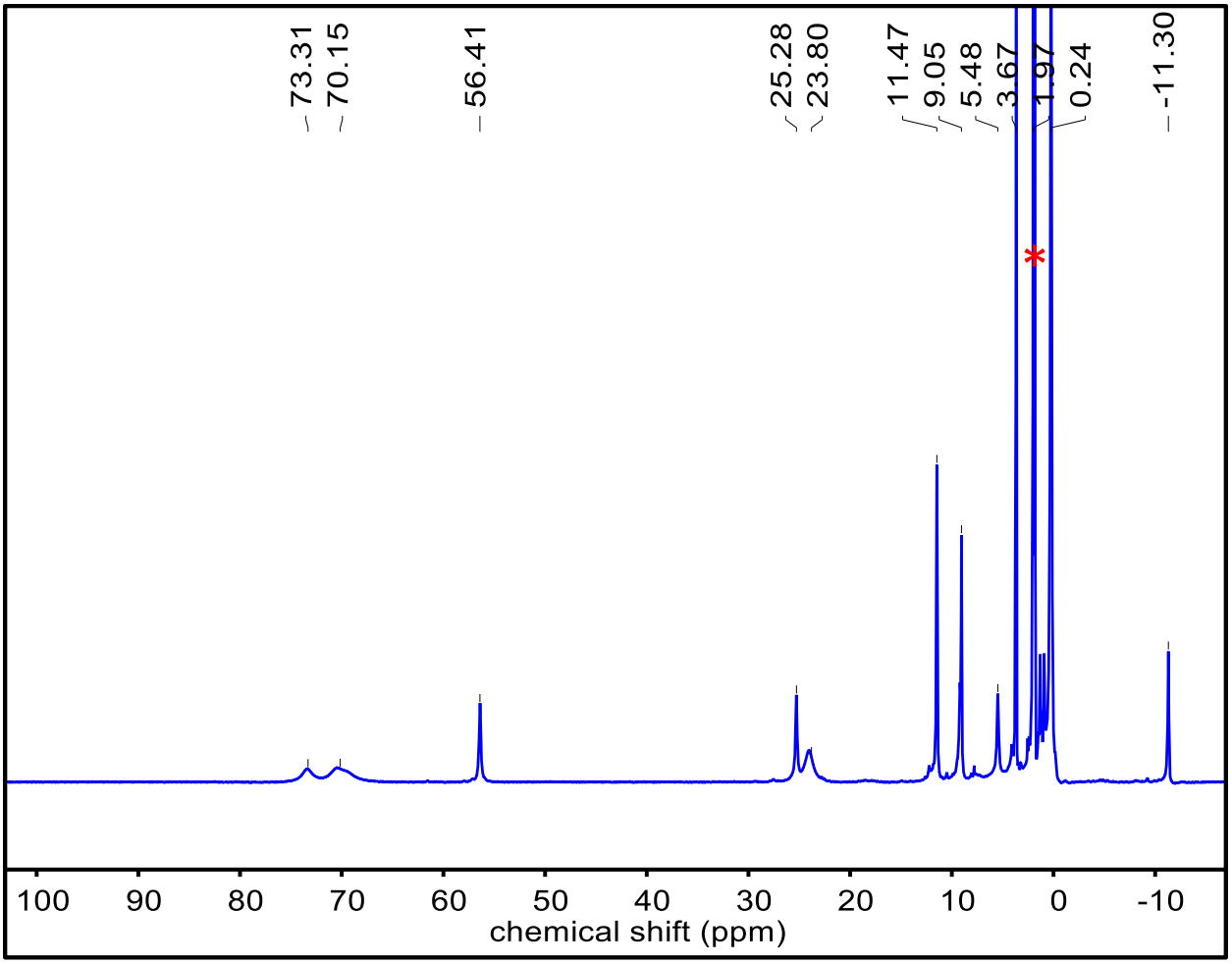

Figure S1. ^{1}H NMR spectrum of $Fe^{II}(BNPA^{Ph2}O)(Cl)$ (**1**) in CD_3CN at 23 ^{o}C. Residual solvent peak for CD_3CN peak is marked with a red asterisk (*).

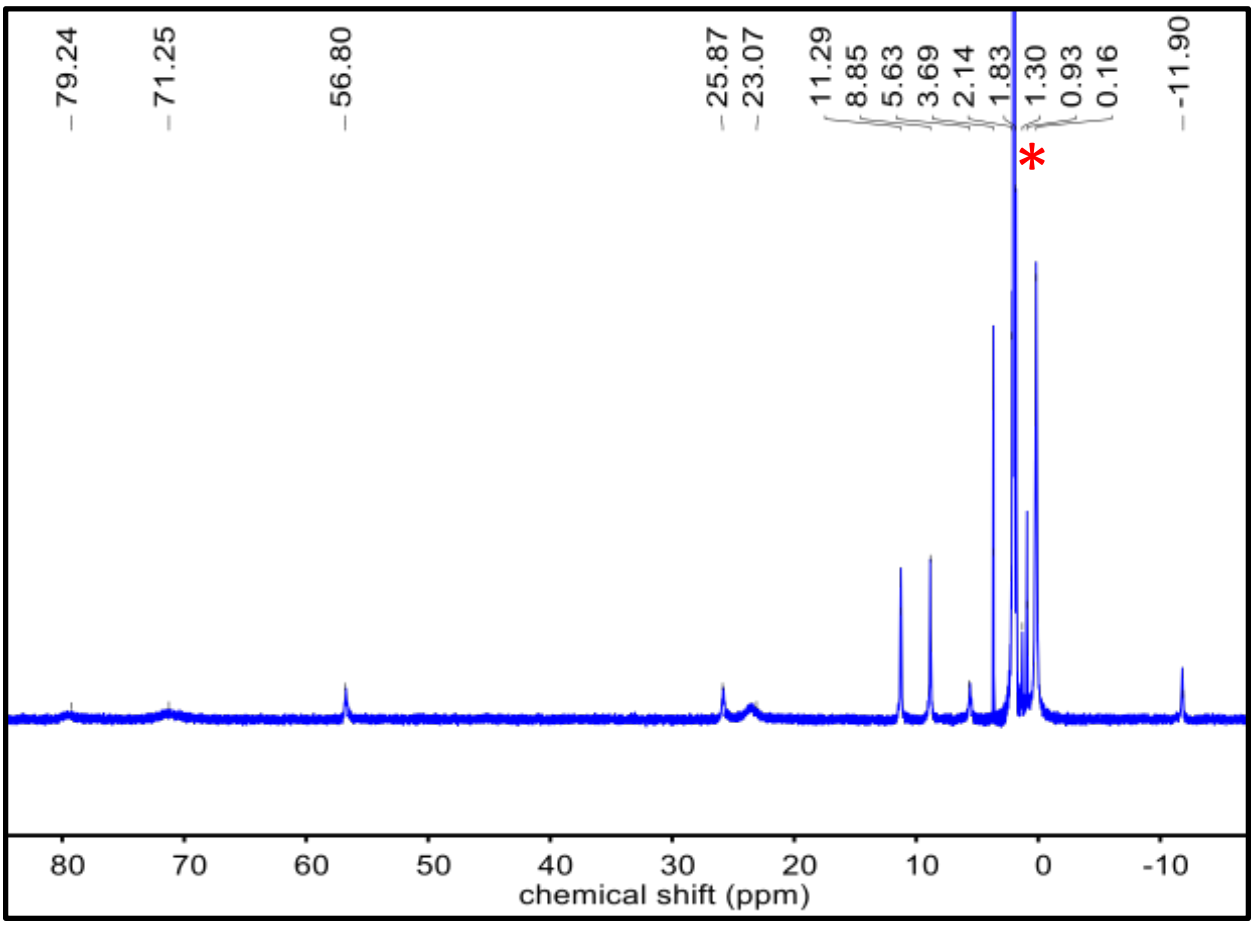

Figure S2. ^{1}H NMR spectrum of $Fe^{II}(BNPA^{Ph2}O)(Br)$ (**2**) in CD_3CN at 23 ^{o}C. Residual solvent peak for CD_3CN peak is marked with a red asterisk (*).

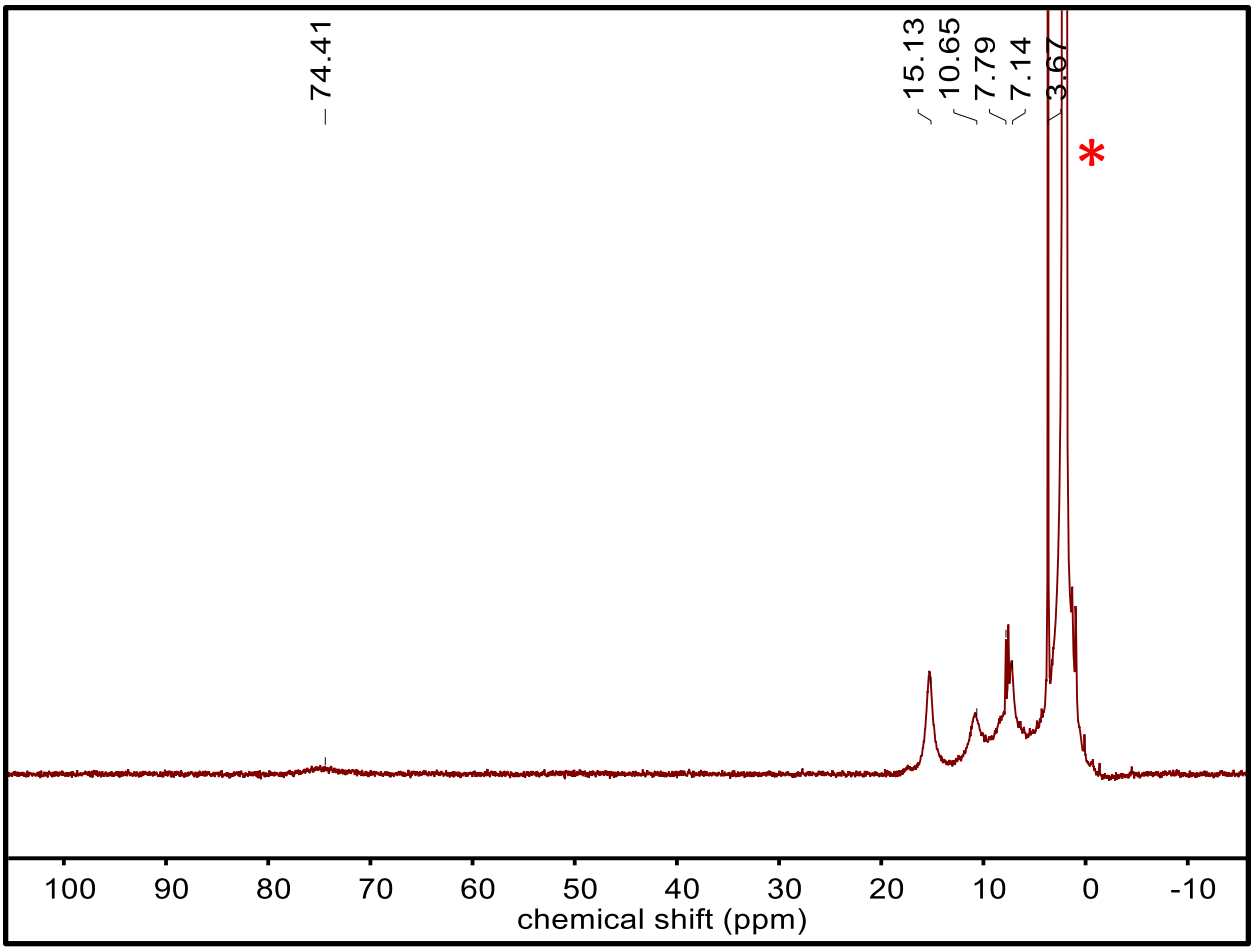

Figure S3. ^{1}H NMR spectrum of $Fe^{III}(BNPA^{Ph2}O)(OH)(Cl)$ (**3**) in CD_3CN at 23 ^{o}C. Residual solvent peak for CD_3CN is marked with a red asterisk (*).

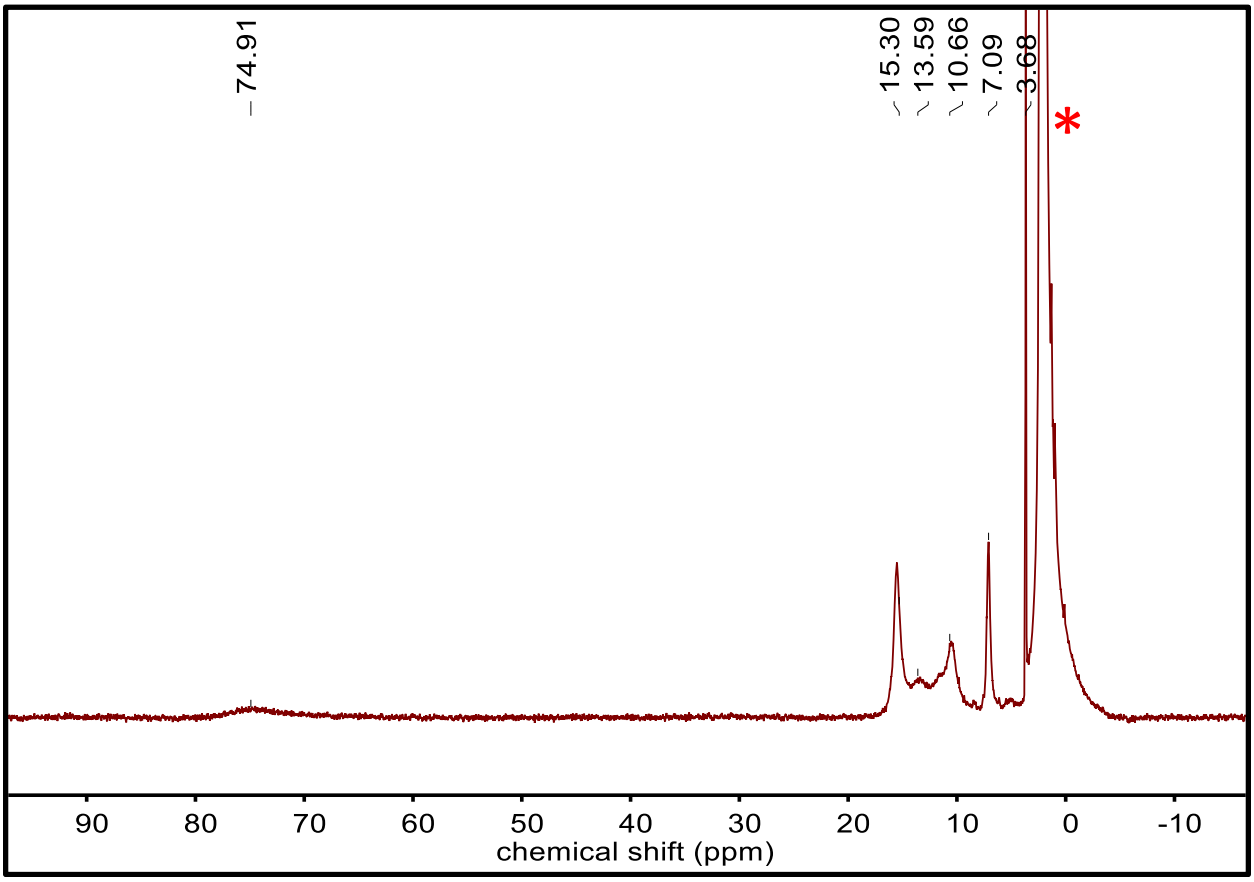

Figure S4. ^{1}H NMR spectrum of $Fe^{III}(BNPA^{Ph2}O)(OH)(Br)$ (**4**) in CD_3CN at 23°C. Residual solvent peak for CD_3CN is marked with a red asterisk (*).

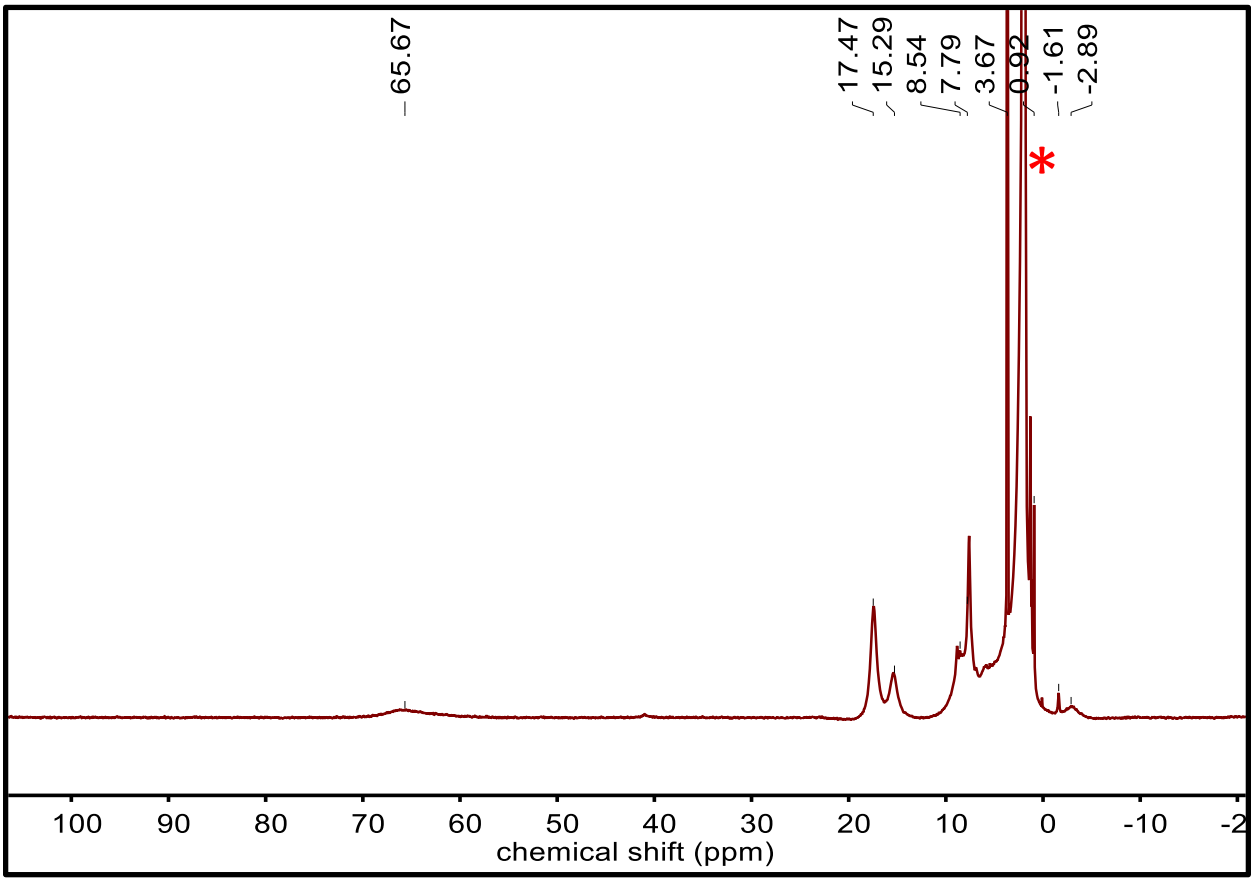

Figure S5. ^{1}H NMR spectrum of $Fe^{III}(BNPA^{Ph2}O)(Cl)_2$ (**5**) in CD_3CN at 23 °C. Residual solvent peak for CD_3CN is marked with a red asterisk (*).

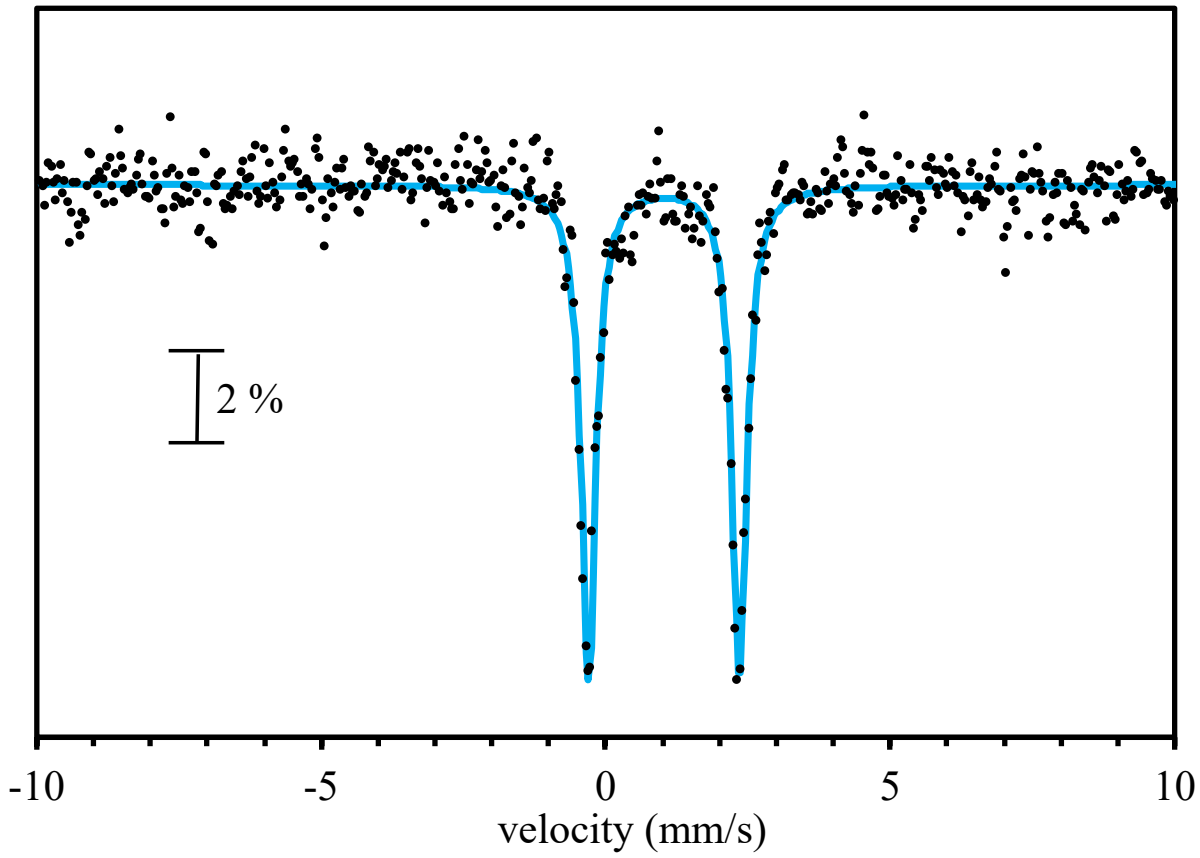

Figure S6. Zero field ^{57}Fe Mössbauer spectrum of $Fe^{II}(BNPA^{Ph2}O)(Cl)$ (**1**) in frozen 2-MeTHF at 80 K. Experimental data = black circles, best fit = blue line, with parameters δ = 1.02 mm s^{-1} and $|\Delta E_Q|$ = 2.65 mm s^{-1}, $\Gamma_R = \Gamma_L$ = 0.32.

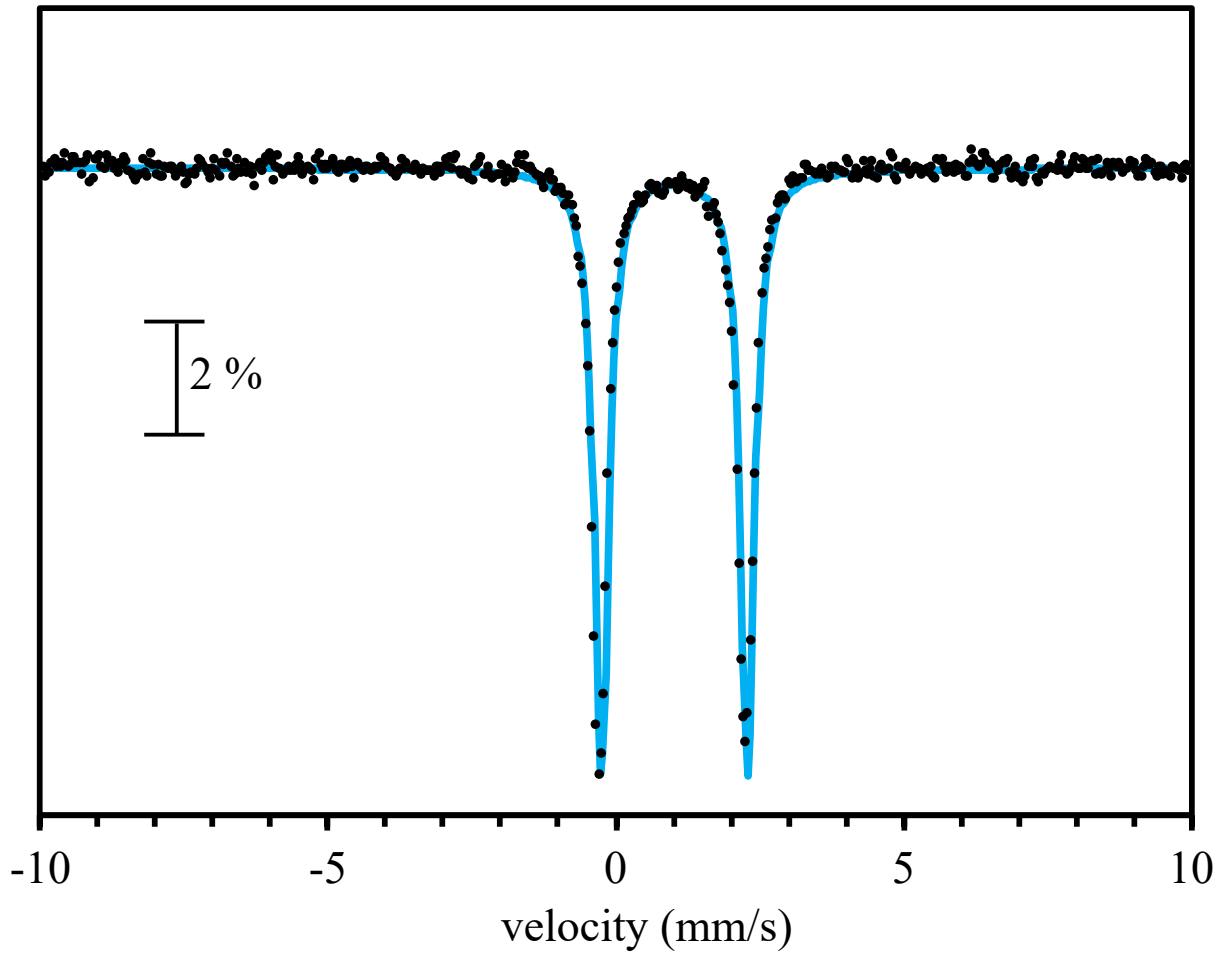

Figure S7. Zero field ^{57}Fe Mössbauer spectrum of $Fe^{II}(BNPA^{Ph2}O)(Br)$ (**2**) in frozen 2-MeTHF at 80 K. Experimental data = black circles, best fit = blue line, with parameters δ = 1.03 mm s^{-1} and $|\Delta E_Q|$ = 2.55 mm s^{-1}, $\Gamma_R = \Gamma_L$ = 0.29.

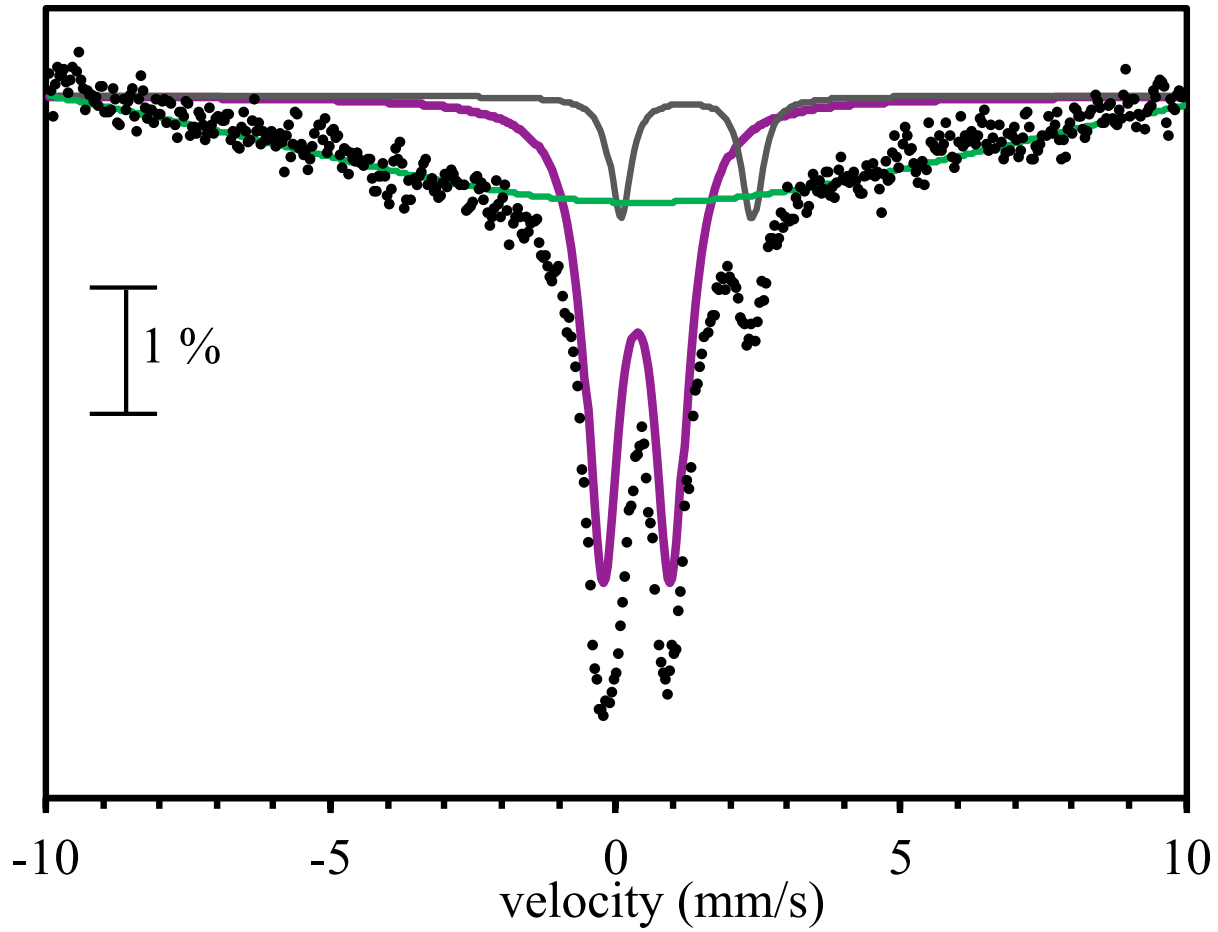

Figure S8. Zero field ^{57}Fe Mössbauer spectrum of $Fe^{III}(BNPA^{Ph2}O)(OH)(Cl)$ (**3**) as a solid film at 80 K. Experimental data = black circles, best fits = solid lines, with parameters: subsite 1 (purple line) $\delta = 0.42$ mm s^{-1} and $|\Delta E_Q| = 1.01$ mm s^{-1}, $\Gamma_R = \Gamma_L = 0.72$, % I = 92; subsite 2 (gray line) $\delta = 0.99$ mm s^{-1} and $|\Delta E_Q| = 2.83$ mm s^{-1}, $\Gamma_R = \Gamma_L = 0.42$, % I = 08; subsite 3 (green line) $\delta = 0.22$ mm s^{-1} and $|\Delta E_Q| = 0.56$ mm s^{-1}, $\Gamma_R = \Gamma_L = 16.7$. The third component was added to represent the intermediate relaxation of the doublet at 80 K.

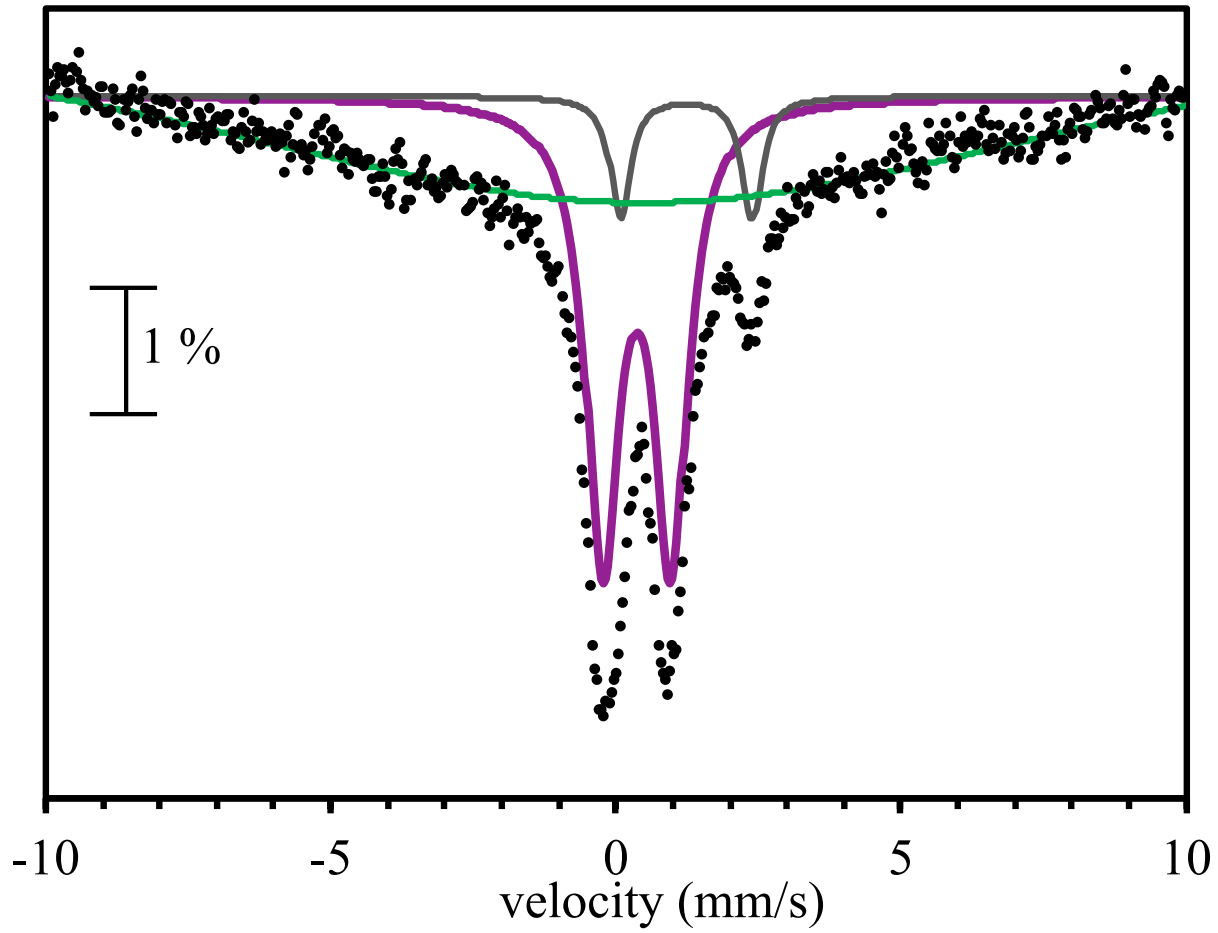

Figure S9. Zero field ^{57}Fe Mössbauer spectrum of $Fe^{III}(BNPA^{Ph2}O)(OH)(Br)$ (**4**) as a solid film at 80 K. Experimental data = black circles, best fits = solid lines, with parameters: subsite 1 (purple line) $\delta = 0.41$ mm s^{-1} and $|\Delta E_Q| = 1.10$ mm s^{-1}, $\Gamma_R = \Gamma_L = 0.71$, % area = 91; subsite 2 (gray line) $\delta = 1.23$ mm s^{-1} and $|\Delta E_Q| = 2.30$ mm s^{-1}, $\Gamma_R = \Gamma_L = 0.42$, % area = 09; subsite 3 (green line) $\delta = 0.24$ mm s^{-1} and $|\Delta E_Q| = 0.47$ mm s^{-1}, $\Gamma_R = \Gamma_L = 17.4$. The third component was added to represent the intermediate relaxation of the doublet at 80 K.

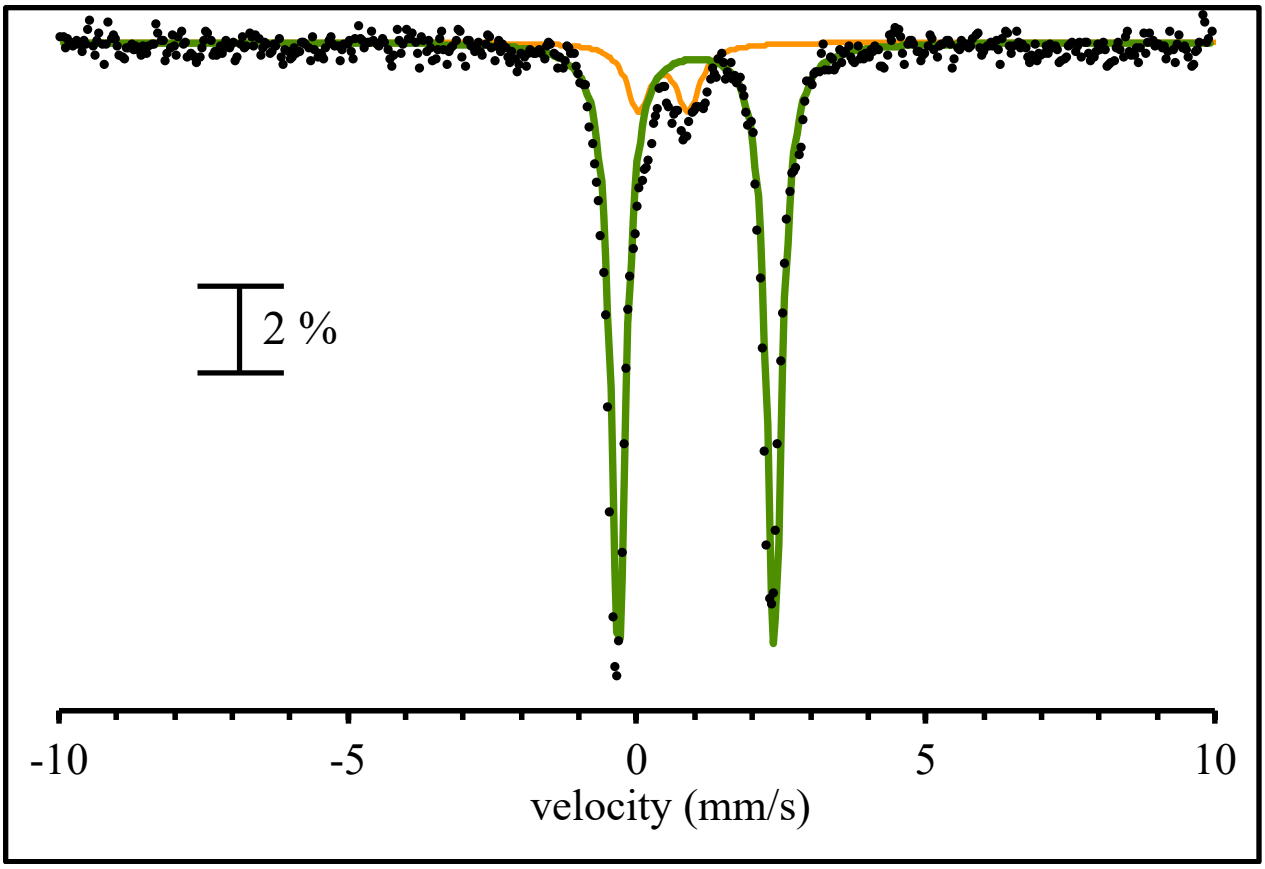

Figure S10. Zero field ^{57}Fe Mössbauer spectrum of the reaction $^{57}Fe^{III}(BNPA^{Ph2}O)(OH)(Cl)$ (**3**) with (p-OMe-$C_6H_4)_3C$• (1 equiv) in 2-MeTHF at 80 K. Experimental data = black circles, best fits = solid lines, with parameters: subsite 1 (green line) δ = 1.02 mm s^{-1} and $|\Delta E_Q|$ = 2.69 mm s^{-1}, $\Gamma_R = \Gamma_L$ = 0.32, % area = 94; subsite 2 (orange line) δ = 0.45 mm s^{-1} and $|\Delta E_Q|$ = 0.86 mm s^{-1}, $\Gamma_R = \Gamma_L$ = 0.49, % area = 06.

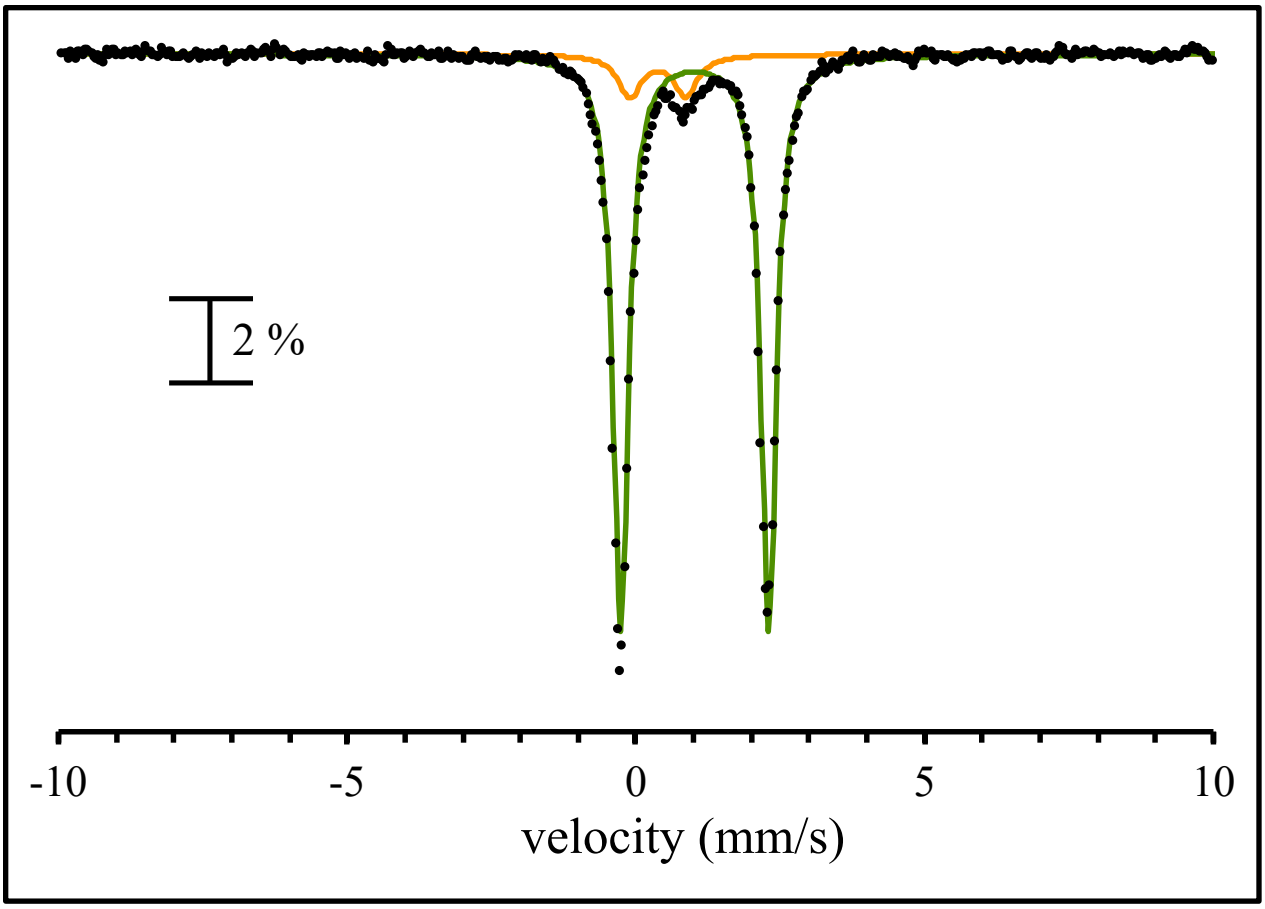

Figure S11. Zero field ^{57}Fe Mössbauer spectrum of the reaction $^{57}Fe^{III}(BNPA^{Ph2}O)(OH)(Br)$ (**4**) with (p-OMe-$C_6H_4)_3C$• (1 equiv) in 2-MeTHF at 80 K. Experimental data = black circles, best fits = solid lines, with parameters: subsite 1 (green line) δ = 1.03 mm s^{-1} and $|\Delta E_Q|$ = 2.55 mm s^{-1}, $\Gamma_R = \Gamma_L$ = 0.30, % area = 95; subsite 2 (orange line) δ = 0.43 mms^{-1} and $|\Delta E_Q|$ = 0.91 mms^{-1}, $\Gamma_R = \Gamma_L$ = 0.47, % area = 05.

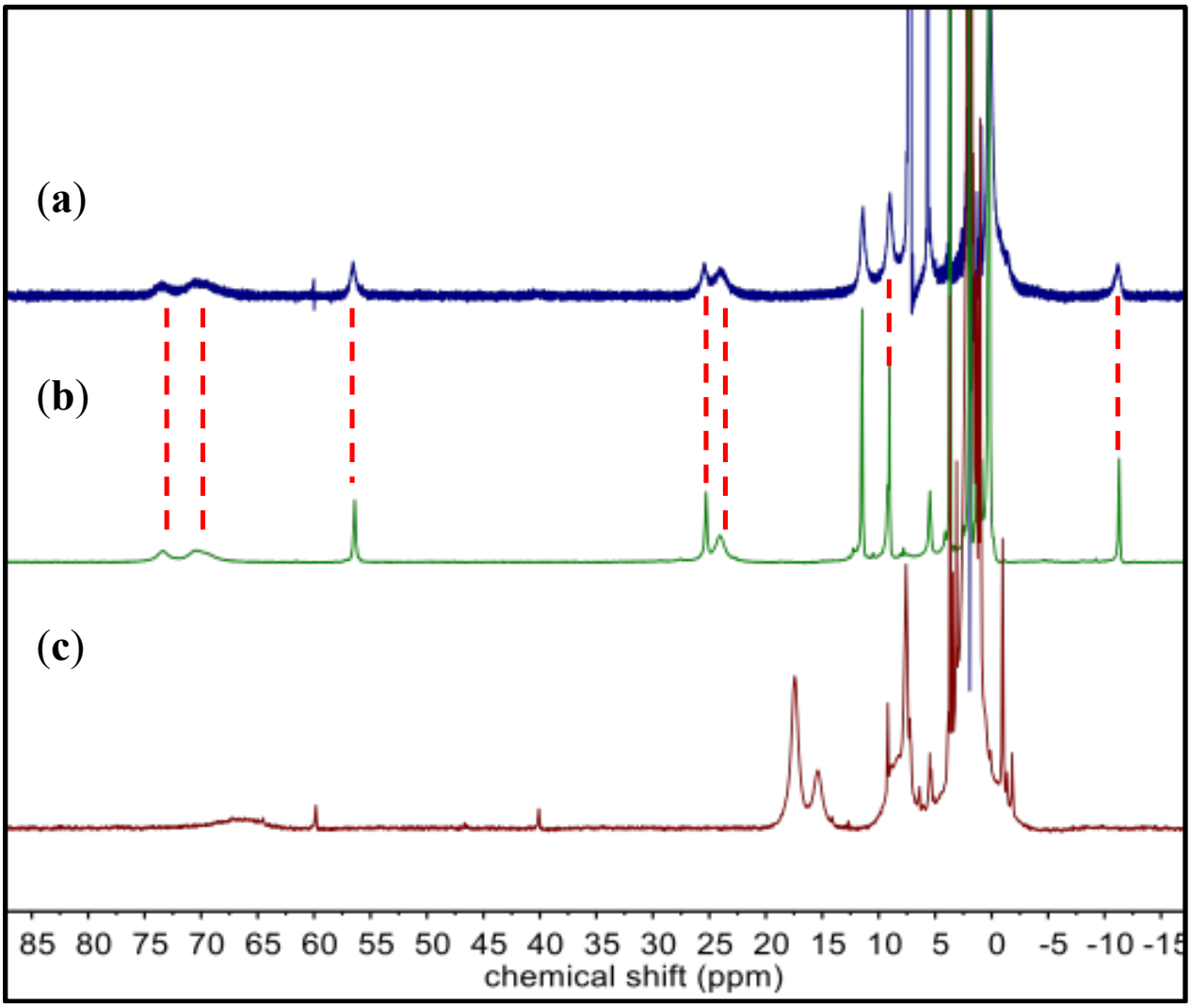

Figure S12. ^{1}H NMR spectra of (a) reaction mixture of $Fe^{III}(BNPA^{Ph2}O)(Cl)_2$ (**5**) with (p-OMe-$C_6H_4)_3C$•, (b) $Fe^{II}(BNPA^{Ph2}O)(Cl)$ (**3**) and (c) $Fe^{III}(BNPA^{Ph2}O)(Cl)_2$ in CD_3CN at 23 °C.

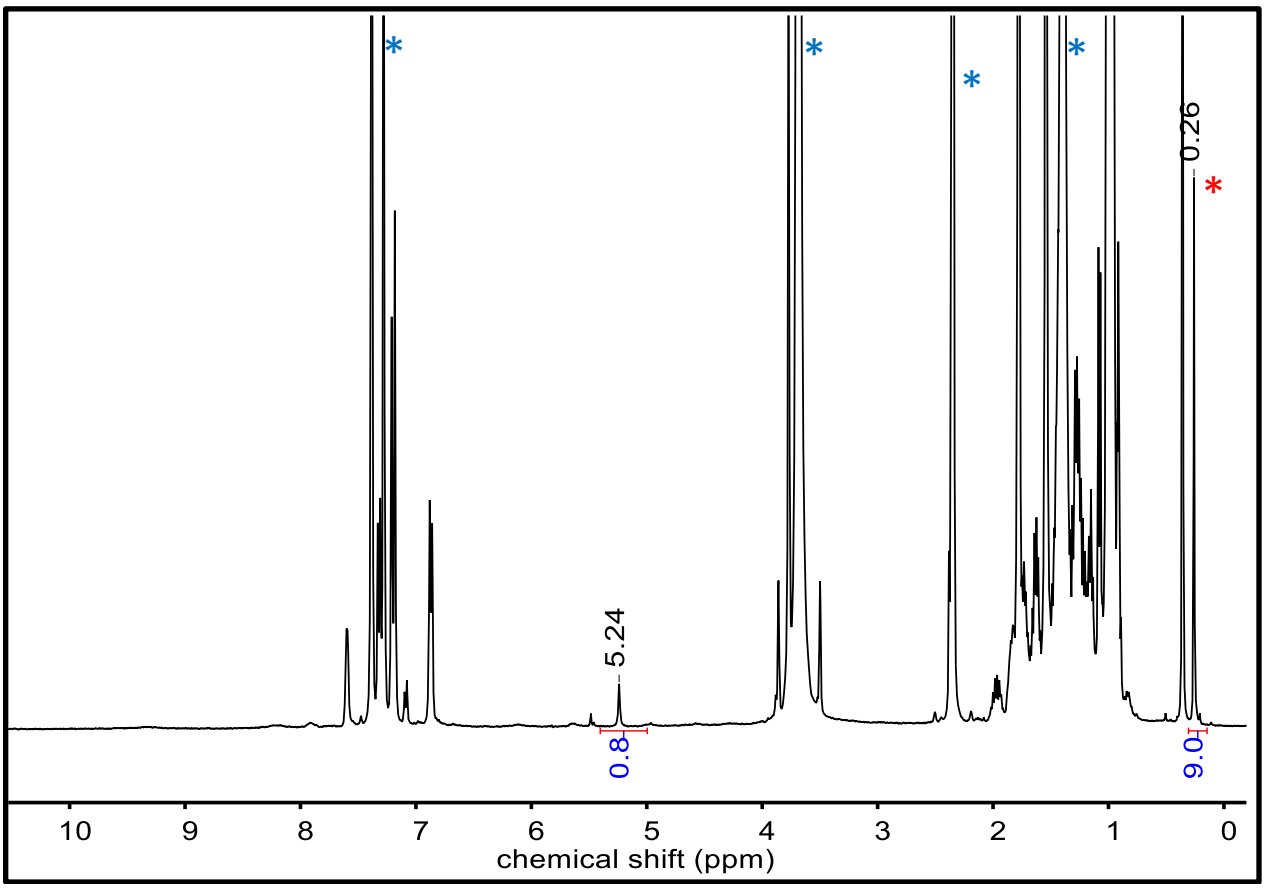

Figure S13. Quantification by ^{1}H NMR spectroscopy of (*p*-OMe-C_6H_4)$_3$COH in the reaction of **3** and (*p*-OMe-C_6H_4)$_3$C• in THF-d_8/toluene-d_8 (5/1 v/v) at 23 °C. The peak for the internal standard trimethylphenylsilane is marked with a red asterisk (*). The peak at δ 5.24 ppm corresponds to the -OH peak of (*p*-OMe-C_6H_4)$_3$COH. Residual solvent peaks for THF-d_8 and toluene-d_8 are marked with a blue asterisk (*).

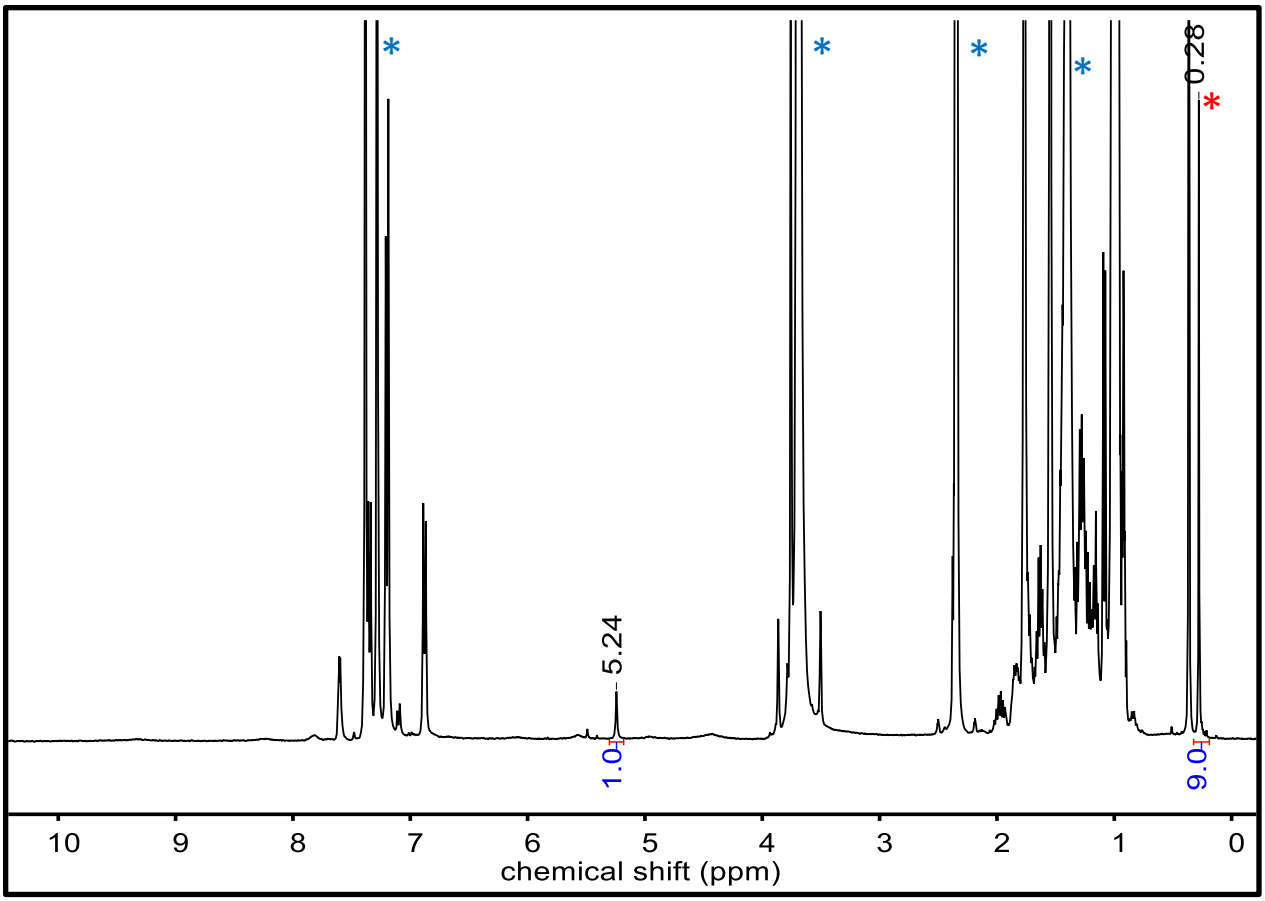

Figure S14. Quantification by ^{1}H NMR spectroscopy of (p-OMe-C_6H_4)$_3$COH in the reaction of **4** and (p-OMe-C_6H_4)$_3$C• in THF-d_8 /toluene-d_8 (5/1 v/v) at 23 °C. The peak for the internal standard trimethylphenylsilane is marked with a red asterisk (*). The peak at δ 5.24 ppm corresponds to the -OH peak of (p-OMe-C_6H_4)$_3$COH. Residual solvent peaks for THF-d_8 and toluene-d_8 are marked with a blue asterisk (*).

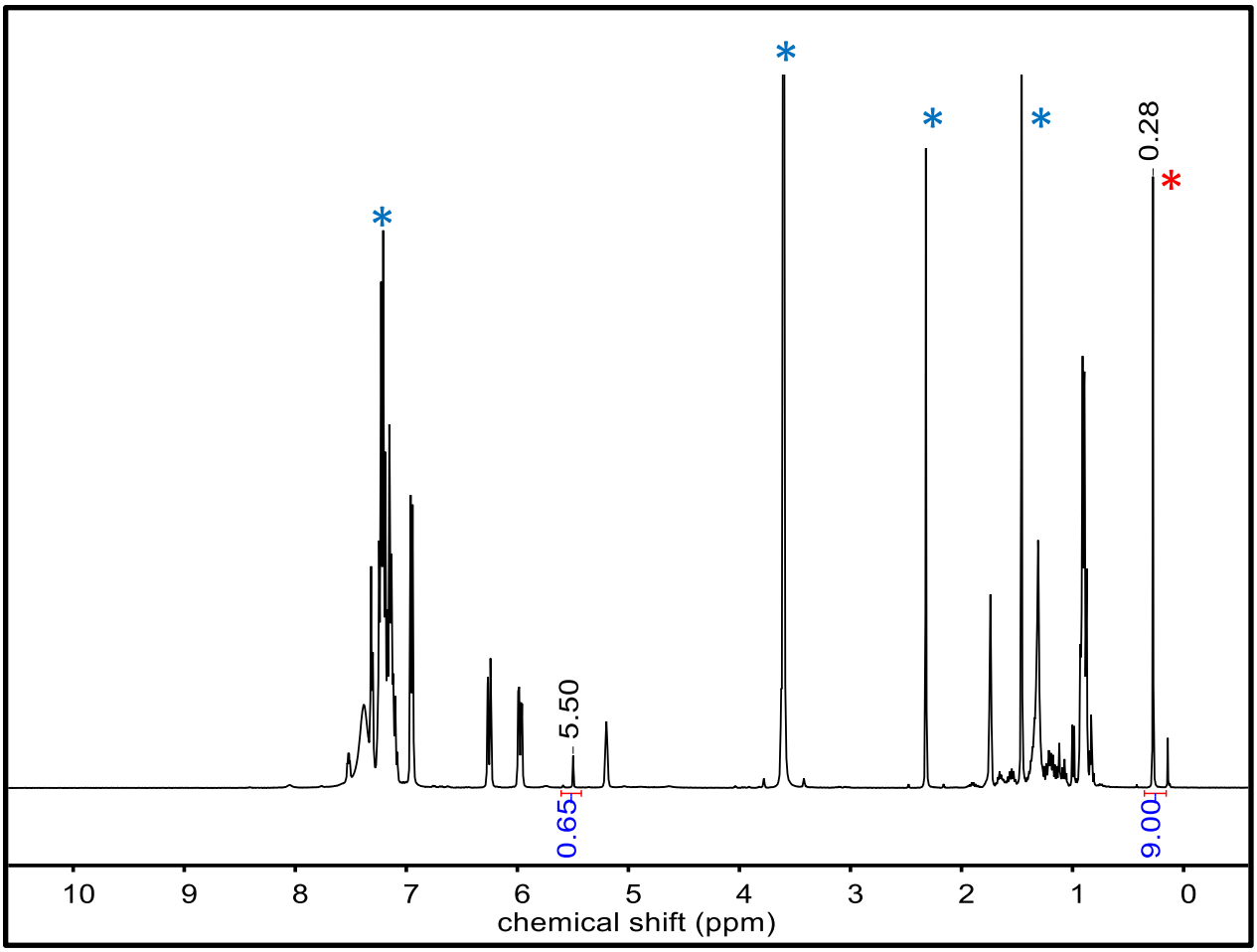

Figure S15. Quantification by ^{1}H NMR spectroscopy of Ph_3COH in the reaction of **3** and Ph_3C• in THF-d_8 /toluene-d_8 (4/1 v/v) at 23 °C. The peak for the internal standard trimethylphenylsilane is marked with a red asterisk (*). The peak at δ 5.50 ppm corresponds to the -OH peak of Ph_3COH. Residual solvent peaks for THF-d_8 and toluene-d_8 are marked with a blue asterisk (*).

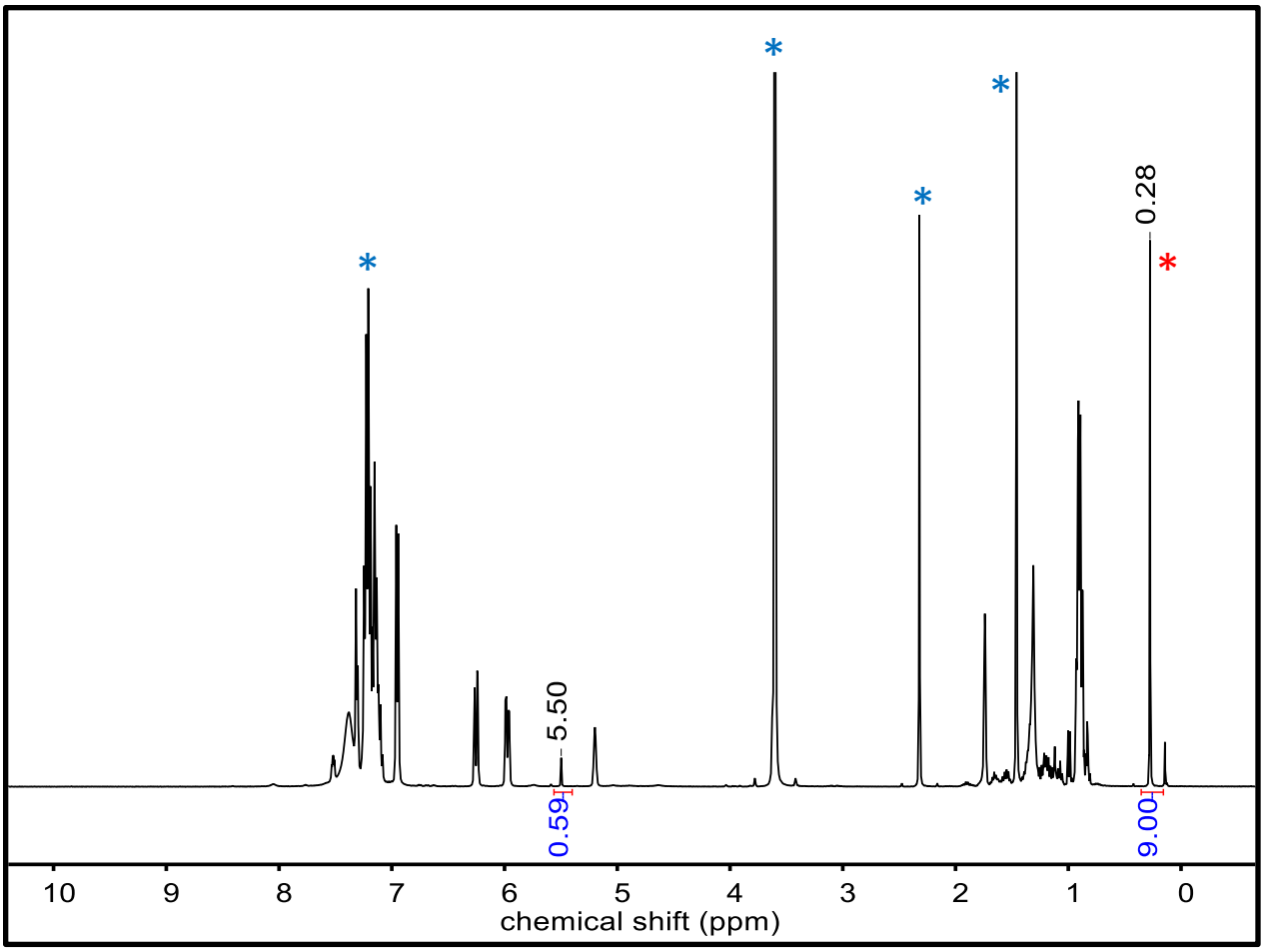

Figure S16. Quantification by ^{1}H NMR spectroscopy of Ph_3COH in the reaction of **4** and Ph_3C• in THF-d_8 /toluene-d_8 (4/1 v/v) at 23 °C. The peak for the internal standard trimethylphenylsilane is marked with a red asterisk (*). The peak at δ 5.50 ppm corresponds to the -OH peak of Ph_3COH. Residual solvent peaks for THF-d_8 and toluene-d_8 are marked with a blue asterisk (*).

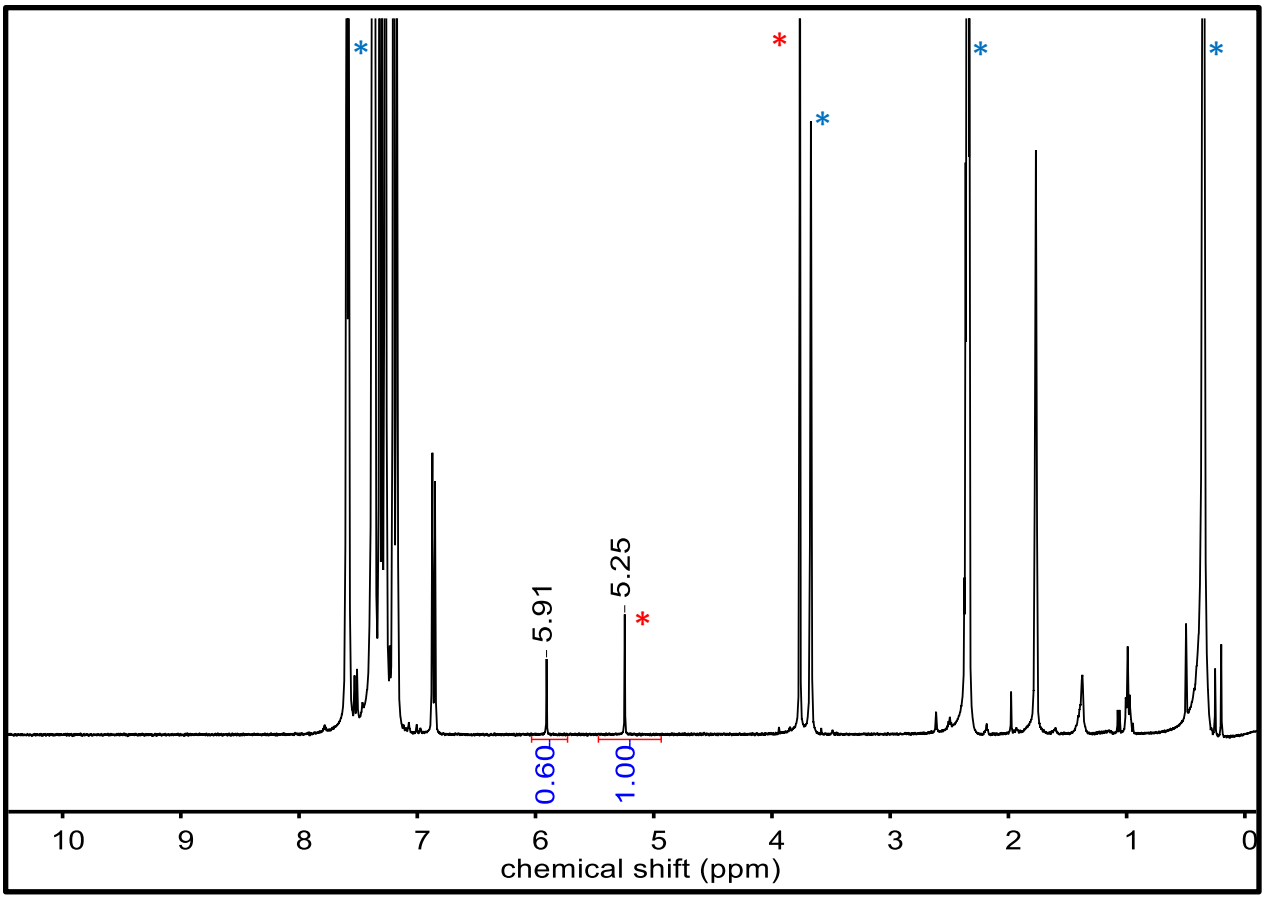

Figure S17. Quantification by ^{1}H NMR spectroscopy of (p-Cl-C_6H_4)$_3$COH in the reaction of **3** and (p-Cl-C_6H_4)$_3$C• in THF-d_8 /toluene-d_8 (4/2 v/v) at 23 °C. The peaks for the internal standard (p-OMe-C_6H_4)$_3$COH are marked with a red asterisk (*). The peak at δ 5.91 ppm corresponds to the -OH peak of (p-Cl-C_6H_4)$_3$COH and the peak at δ 5.25 ppm corresponds to the -OH peak for the internal standard. Residual solvent peaks for THF-d_8 and toluene-d_8 are marked with a blue asterisk (*).

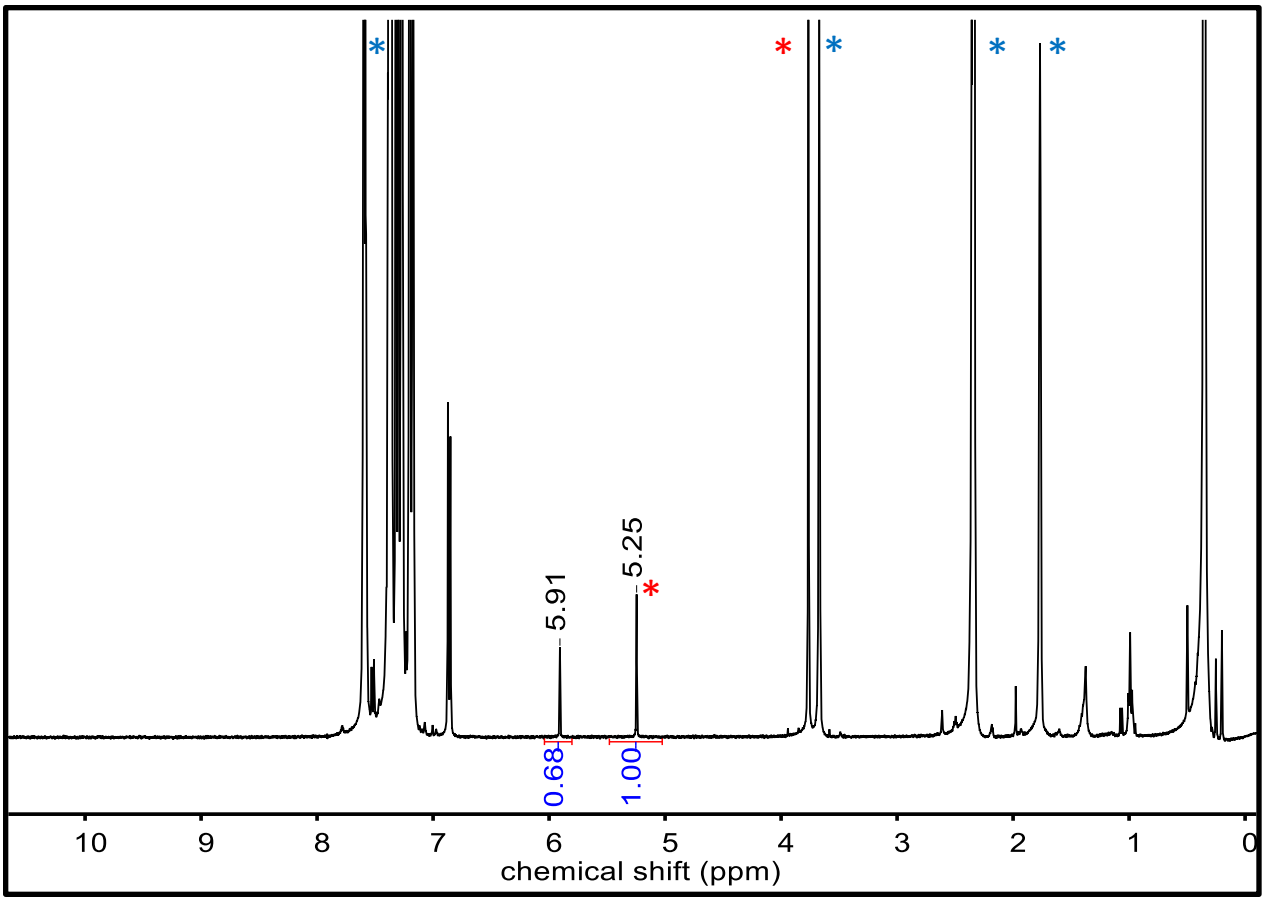

Figure S18. Quantification by ^{1}H NMR spectroscopy of (p-Cl-C_6H_4)$_3$COH in the reaction of **4** and (p-Cl-C_6H_4)$_3$C• in THF-d_8 /toluene-d_8 (4/2 v/v) at 23 °C. The peaks for the internal standard (p-OMe-C_6H_4)$_3$COH are marked with a red asterisk (*). The peak at δ 5.91 ppm corresponds to the -OH peak of (p-Cl-C_6H_4)$_3$COH and the peak at δ 5.25 ppm corresponds to the -OH peak for the internal standard. Residual solvent peaks for THF-d_8 and toluene-d_8 are marked with a blue asterisk (*).

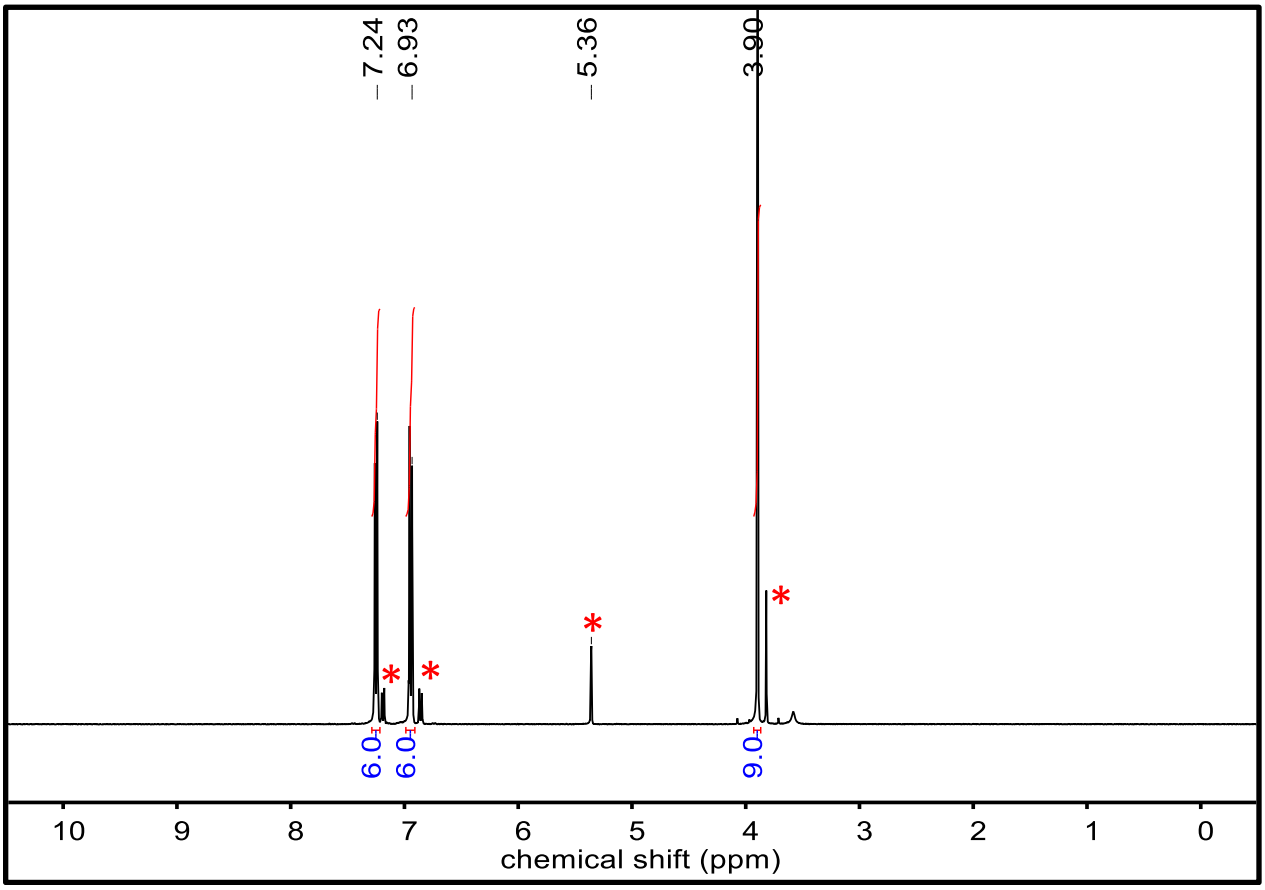

Figure S19. ^{1}H NMR spectrum of (p-OMe-C_6H_4)$_3$CCl isolated from the reaction of **5** and (p-OMe-C_6H_4)$_3$C• in CD_2Cl_2 at 23 °C. Peaks from residual solvent and a minor impurity of (p-OMe-C_6H_4)$_3$COH are marked with an asterisk.

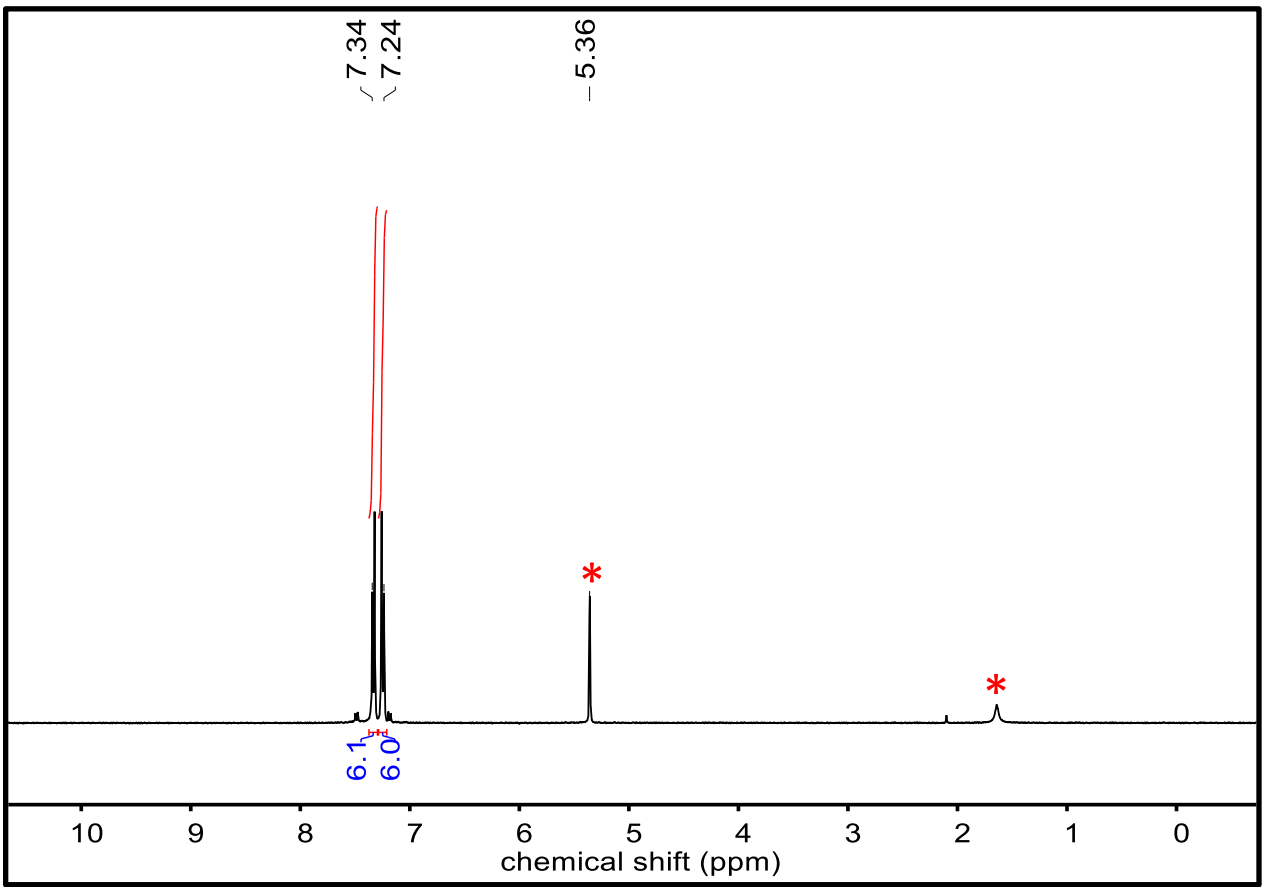

Figure S20. ^{1}H NMR spectrum of (p-Cl-C_6H_4)$_3$CCl isolated from the reaction of **5** and (p-Cl-C_6H_4)$_3$C• in CD_2Cl_2 at 23 °C. Residual solvent and water peaks are marked with an asterisk.

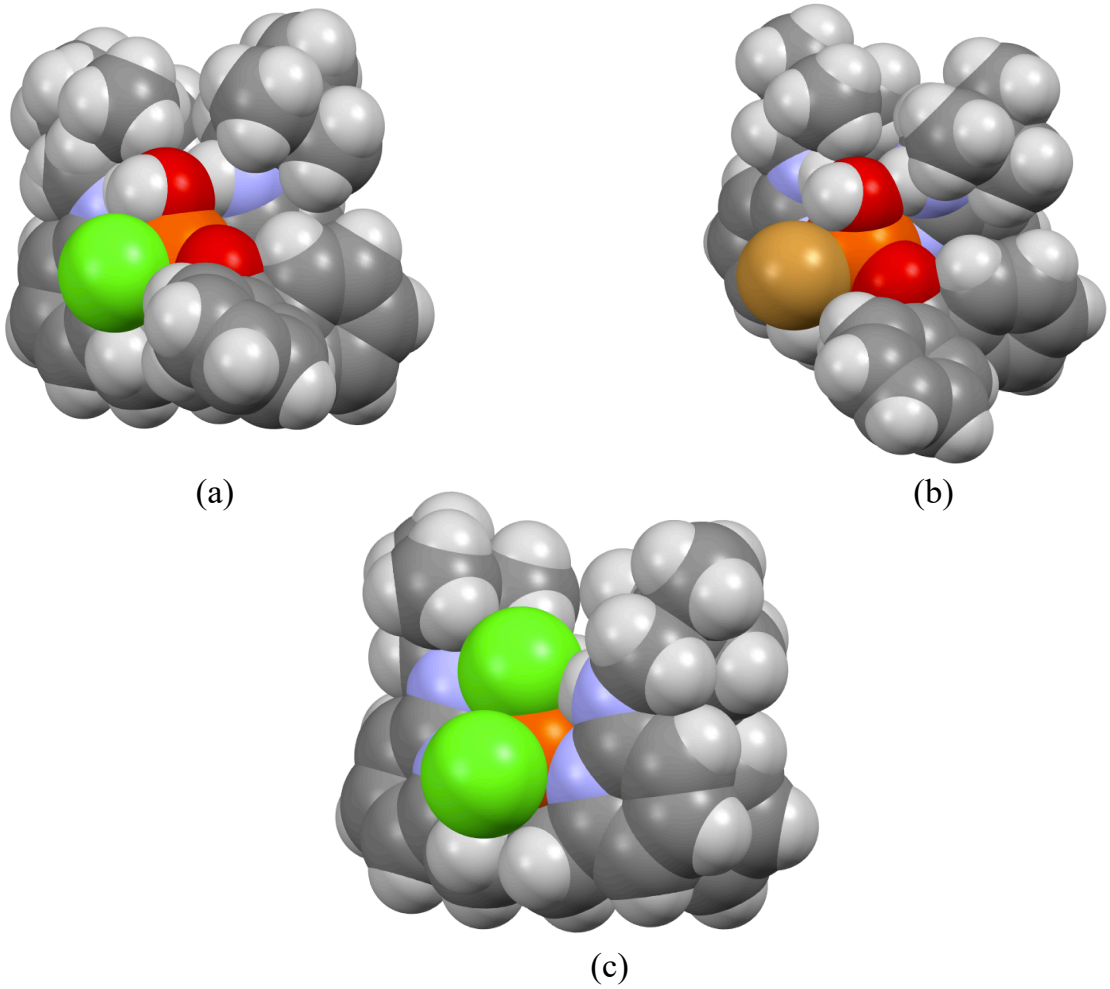

Figure S21. Space filling model of (a) **3**, (b) **4** and (c) **5**.

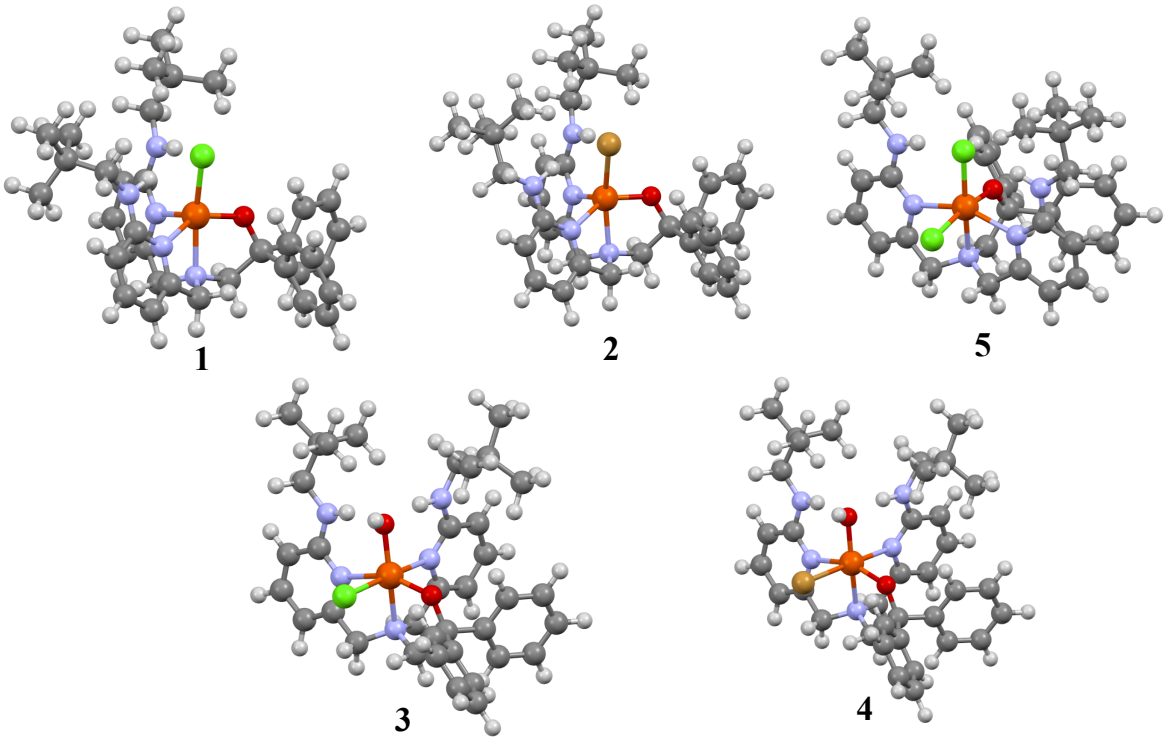

Figure S22. DFT optimized structure of **1** – **5** using B3LYP/6-311g* level of theory.

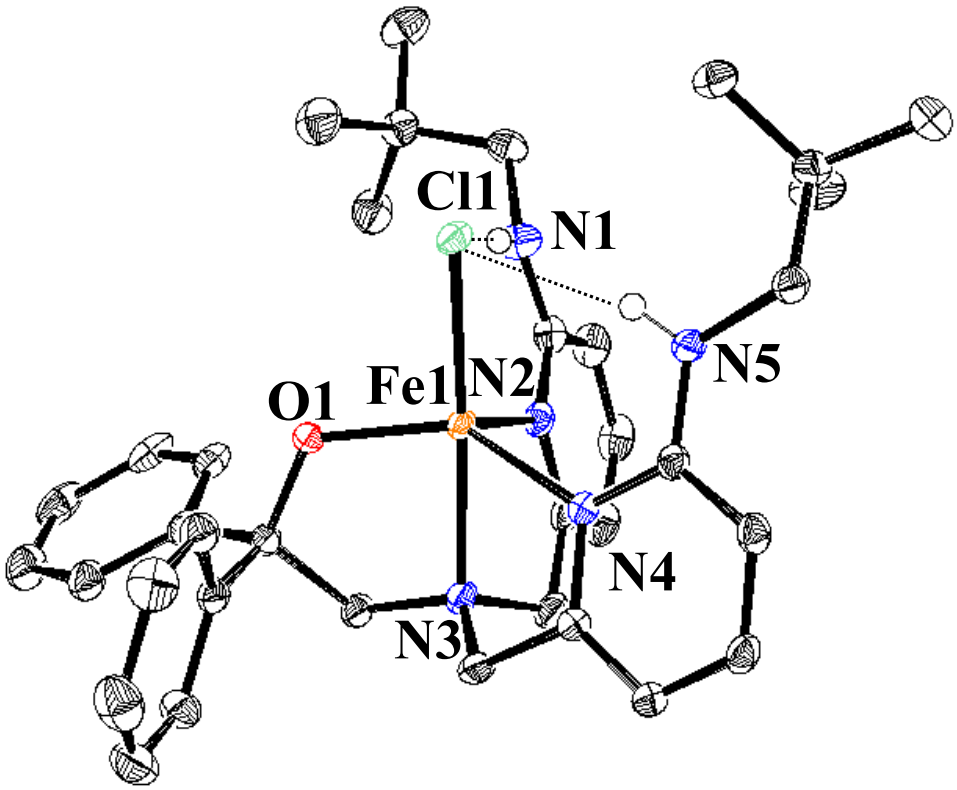

Figure S23. Displacement ellipsoid plot (50% probability) of $Fe^{II}(BNPA^{Ph2}O)(Cl)$ (**1**) at 110(2) K. H-atoms except those attached to N1 and N5 are removed for clarity.

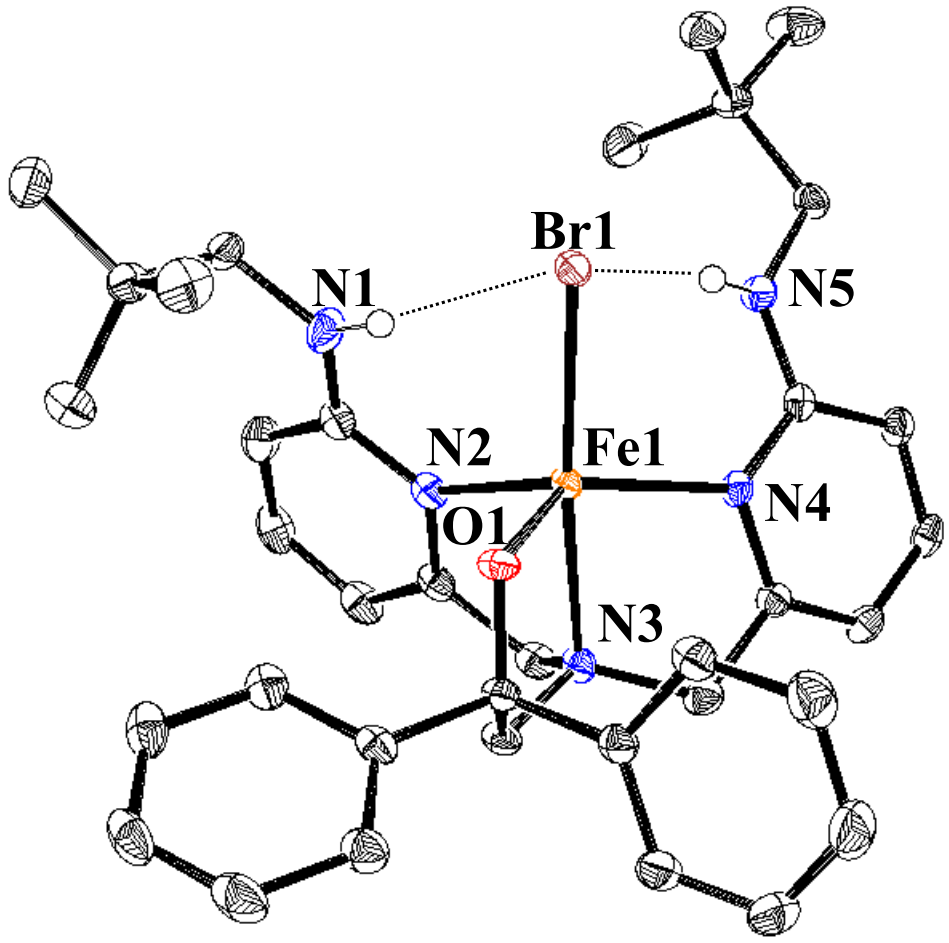

Figure S24. Displacement ellipsoid plot (50% probability) of $Fe^{II}(BNPA^{Ph2}O)(Br)$ (**2**) at 110(2) K. H-atoms except those attached to N1 and N5 are removed for clarity.

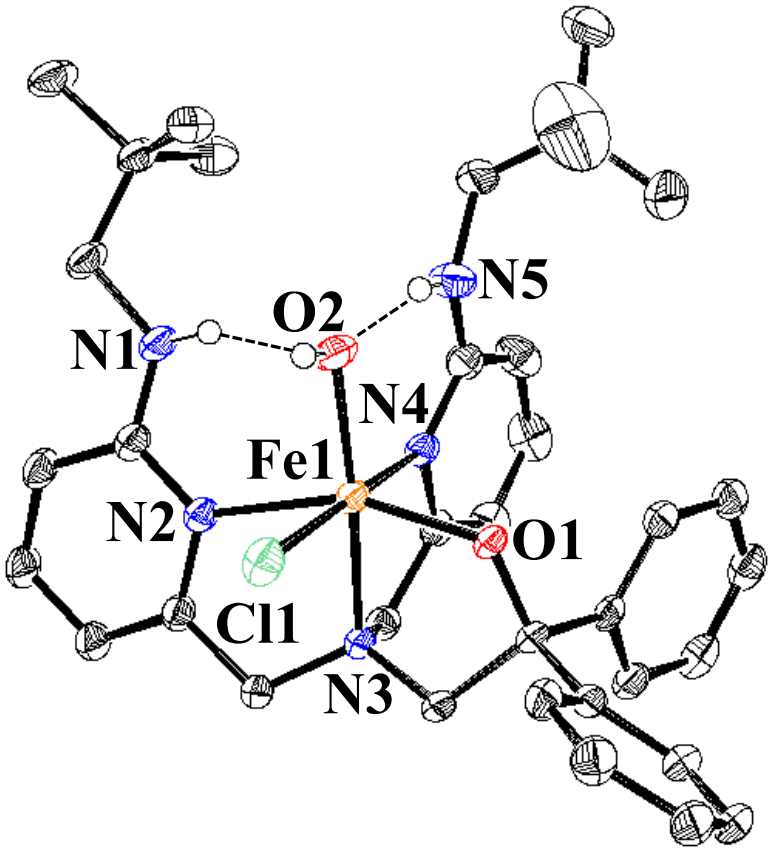

Figure S25. Displacement ellipsoid plot (50% probability) of $Fe^{III}(BNPA^{Ph2}O)(OH)(Cl)$ (**3**) at 110(2) K. H-atoms except those attached to N1, N5 and O2 are removed for clarity.

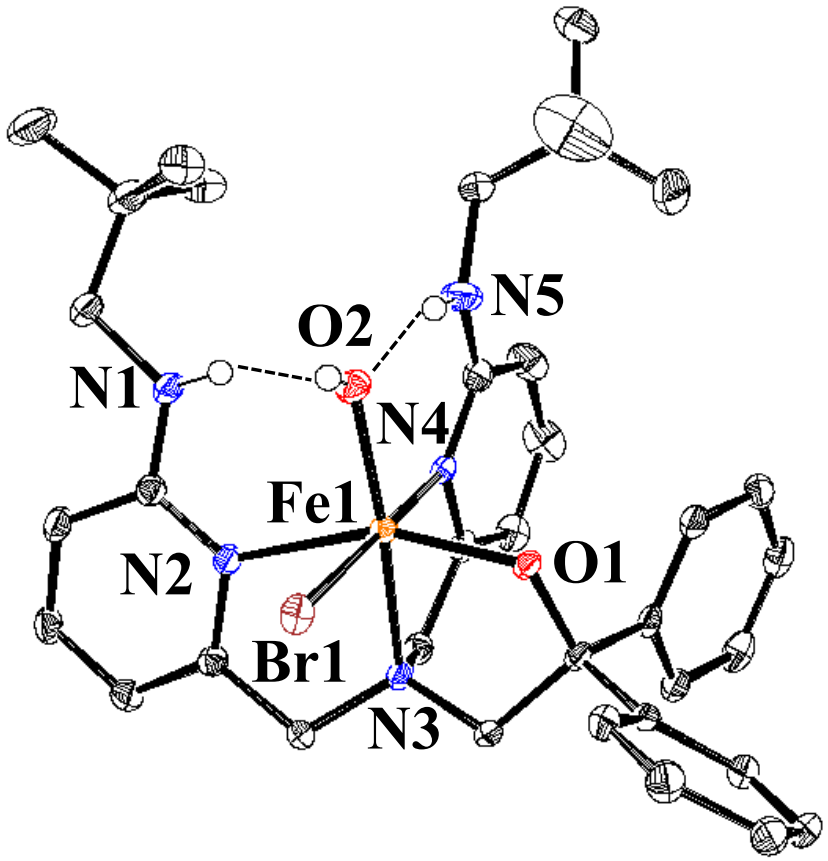

Figure S26. Displacement ellipsoid plot (50% probability) of $Fe^{III}(BNPA^{Ph2}O)(OH)(Br)$ (**4**) at 110(2) K. H-atoms except those attached to N1, N5 and O2 are removed for clarity.

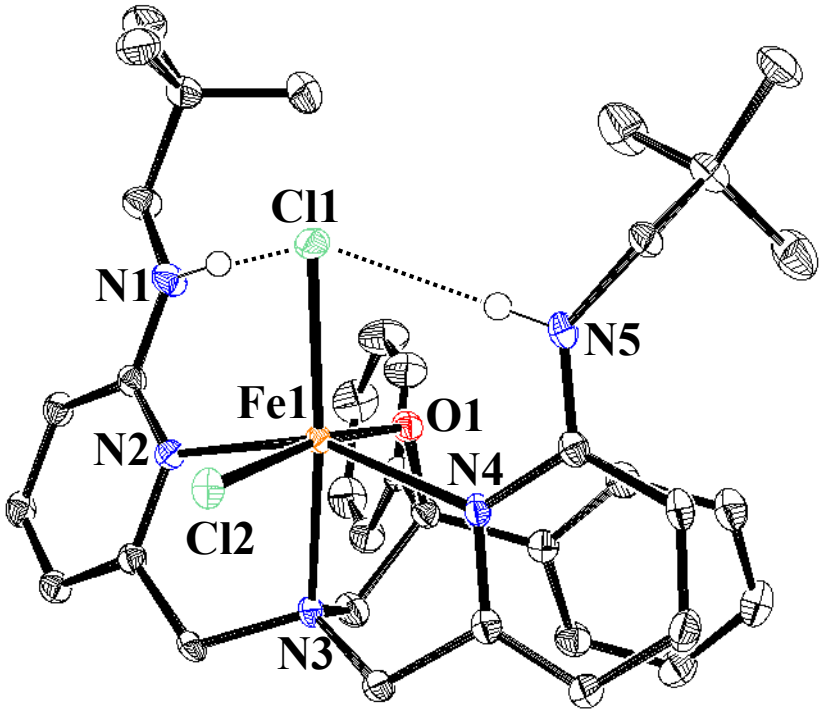

Figure S27. Displacement ellipsoid plot (50% probability) of $Fe^{III}(BNPA^{Ph2}O)(Cl)_2$ (**5**) at 110(2) K. H-atoms except those attached to N1, N5 and O2 are removed for clarity.

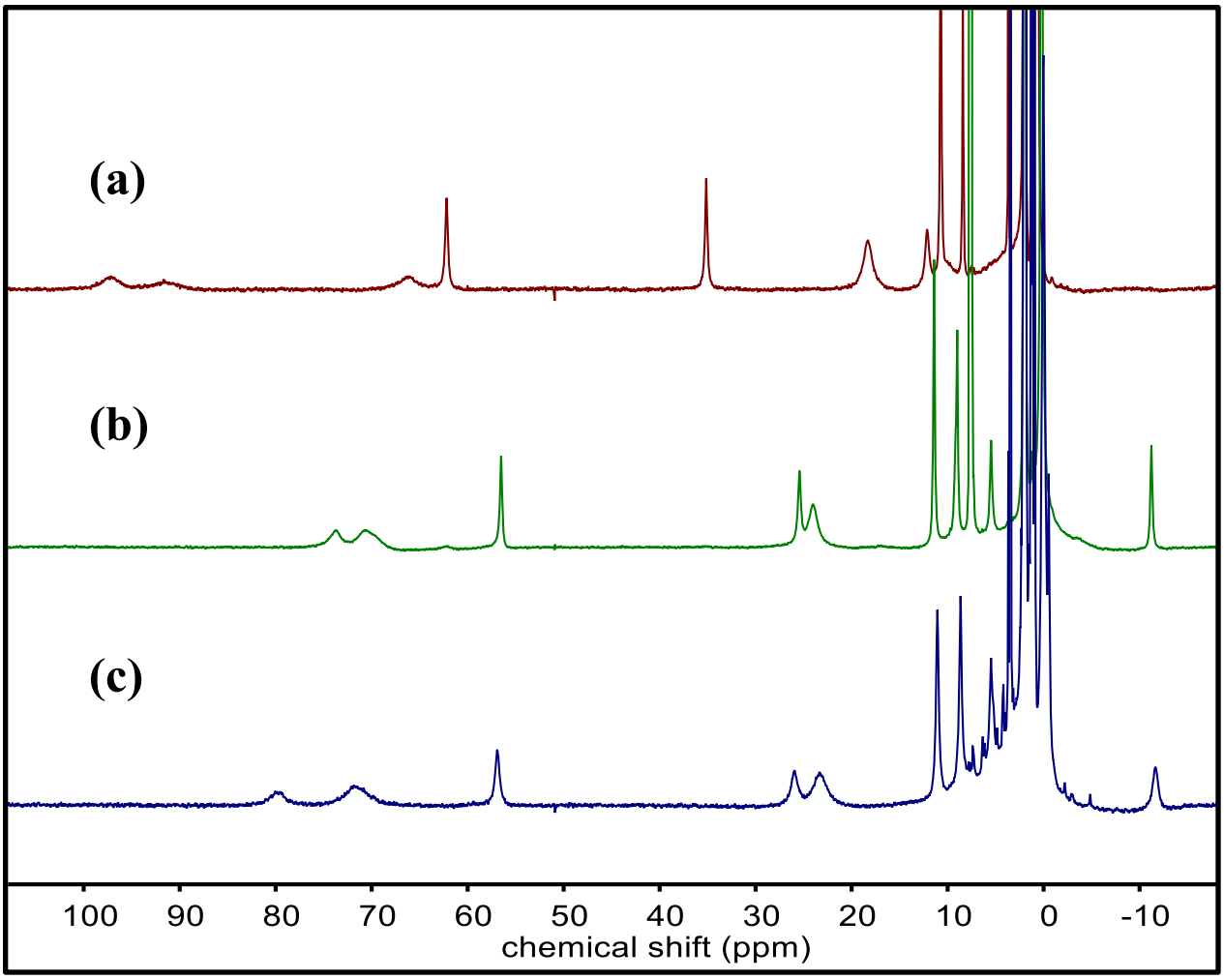

Figure S28. ^{1}H NMR spectra of (a) $^{57}Fe^{II}(BNPA^{Ph2}O)(OTf)$, (b) $^{57}Fe^{II}(BNPA^{Ph2}O)(OTf)$ + Bu_4NCl (1 equiv) and (c) $^{57}Fe^{II}(BNPA^{Ph2}O)(OTf)$ + Bu_4NBr (1 equiv) in CD_3CN.

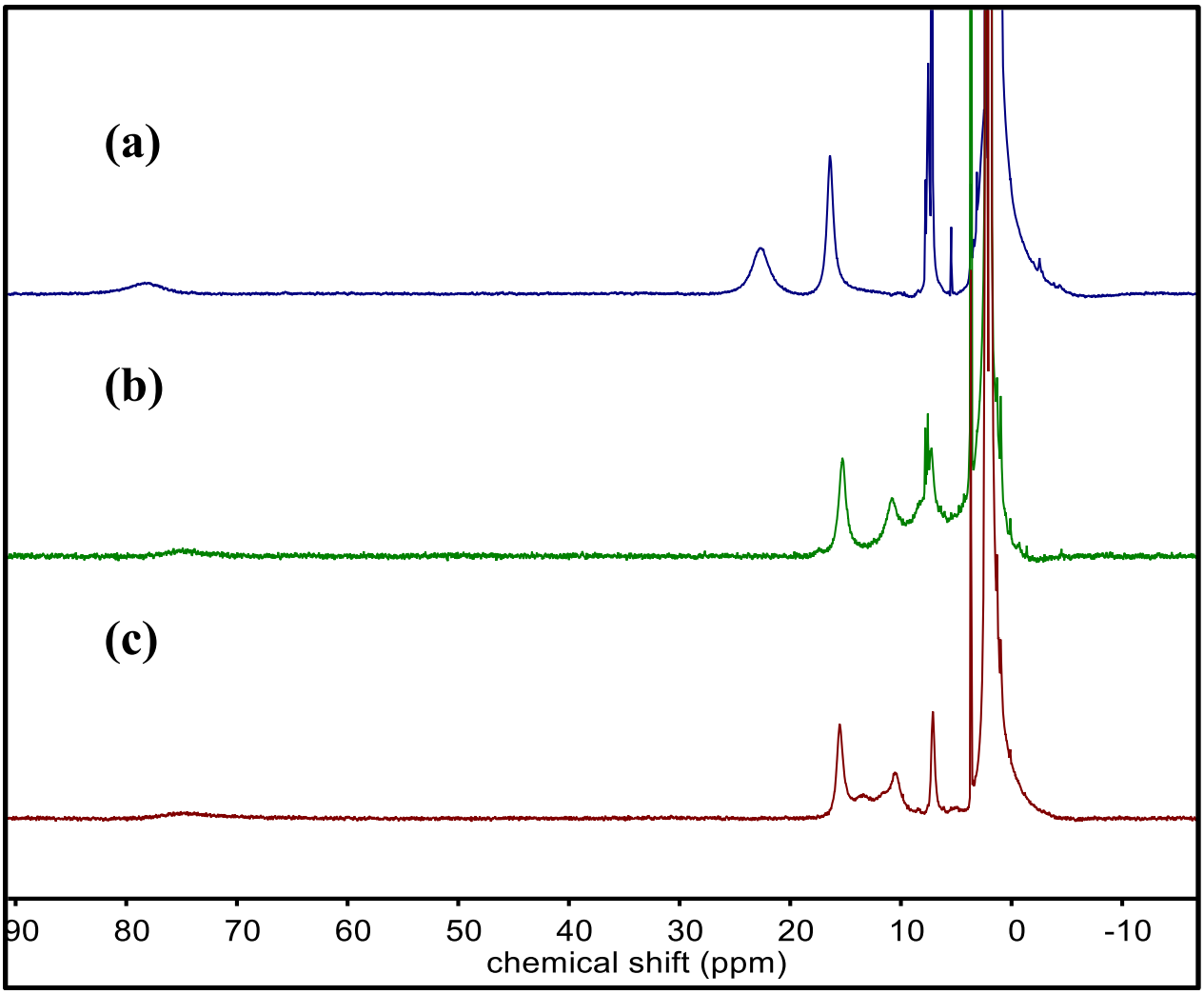

Figure S29. ^{1}H NMR spectra of (a) $^{57}Fe^{III}(BNPA^{Ph2}O)(OH)(OTf)$, (b) $^{57}Fe^{III}(BNPA^{Ph2}O)(OH)(OTf)$ + Bu_4NCl (1 equiv) and (c) $^{57}Fe^{III}(BNPA^{Ph2}O)(OH)(OTf)$ + Bu_4NBr (1 equiv) in CD_3CN.

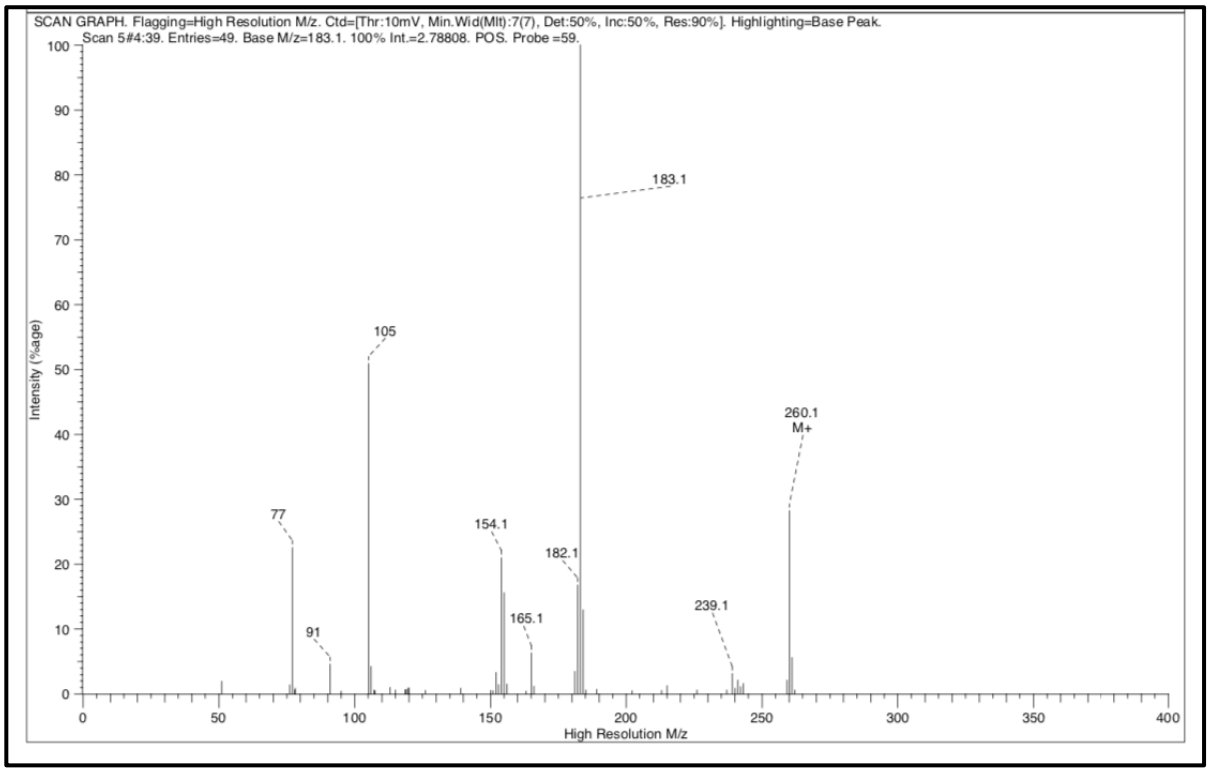

Figure S30. EI-MS spectrum of the reaction mixture of **3** and Ph_3C• in THF at 23 °C. EI-MS: *m/z* = 260.1 (M^+); 260.2 calculated for Ph_3COH.

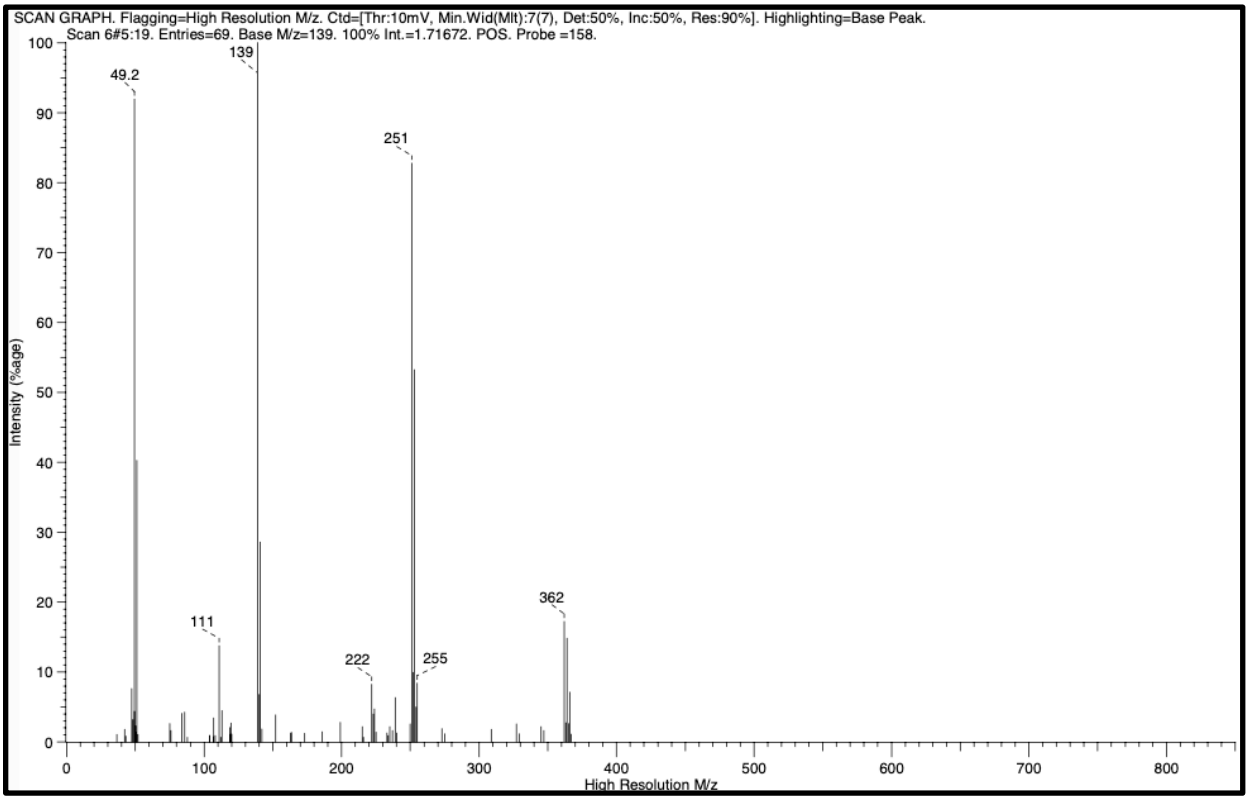

Figure S31. EI-MS spectrum of the reaction mixture of **4** and (p-Cl-C_6H_4)$_3$C• in THF at 23 °C. EI-MS: m/z = 362 (M^+); 362.2 calculated for (p-Cl-C_6H_4)$_3$COH.

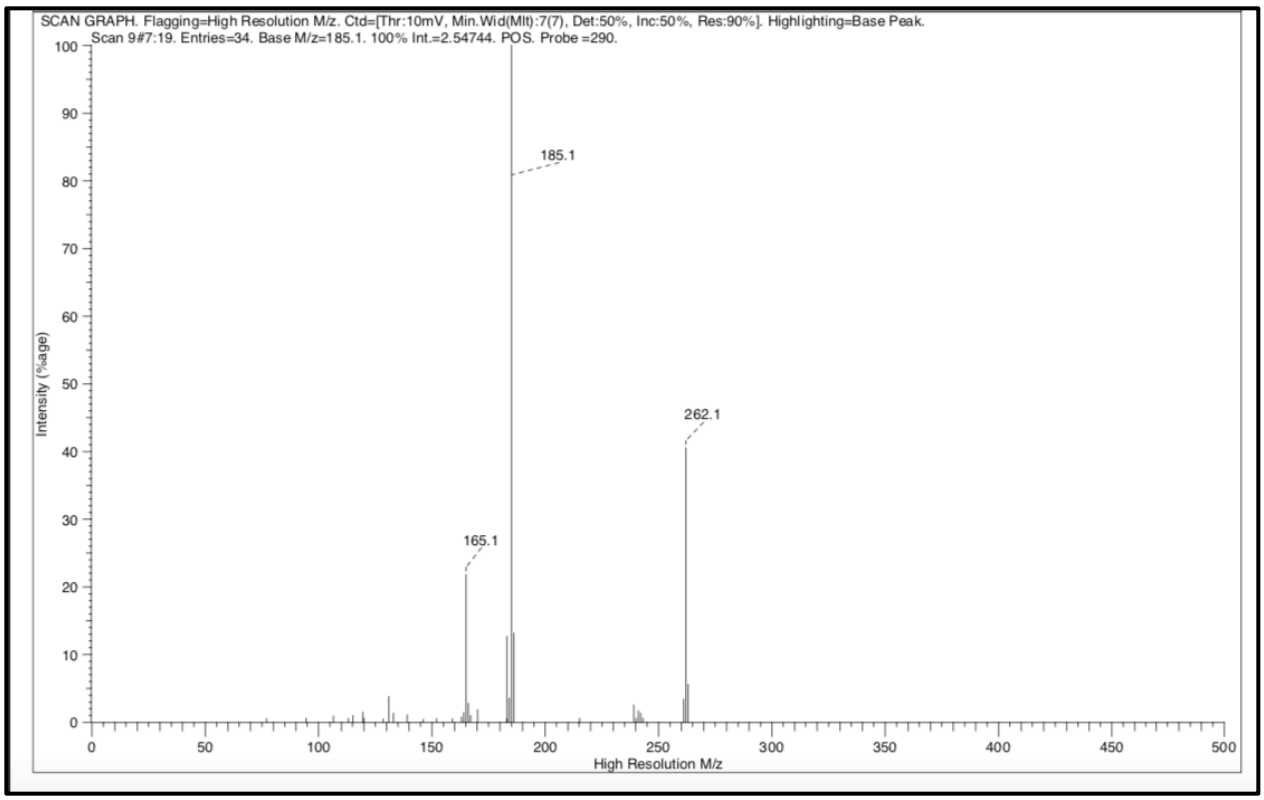

Figure S32. EI-MS spectrum of the reaction mixture of ^{18}O labeled **3** and $Ph_3C\bullet$ in THF at 23 °C. EI-MS: *m/z* = 262.1(M^+); 262.2 calculated for $Ph_3C^{18}OH$.

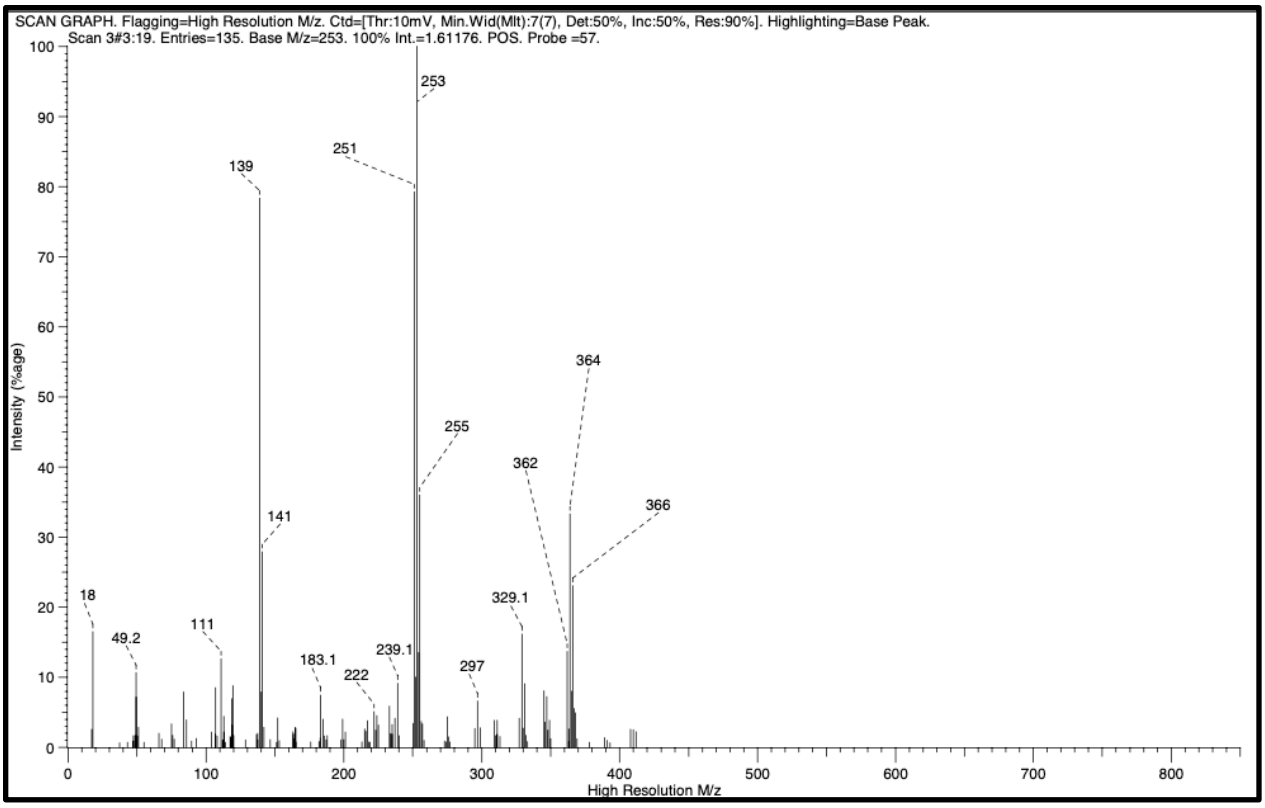

Figure S33. EI-MS spectrum of the reaction mixture of ^{18}O labeled **4** and (p-Cl-C_6H_4)$_3$C• in THF at 23 °C. EI-MS *m/z* = 364 (M^+); 364.2 calculated for (p-Cl-C_6H_4)$_3$C^{18}OH.

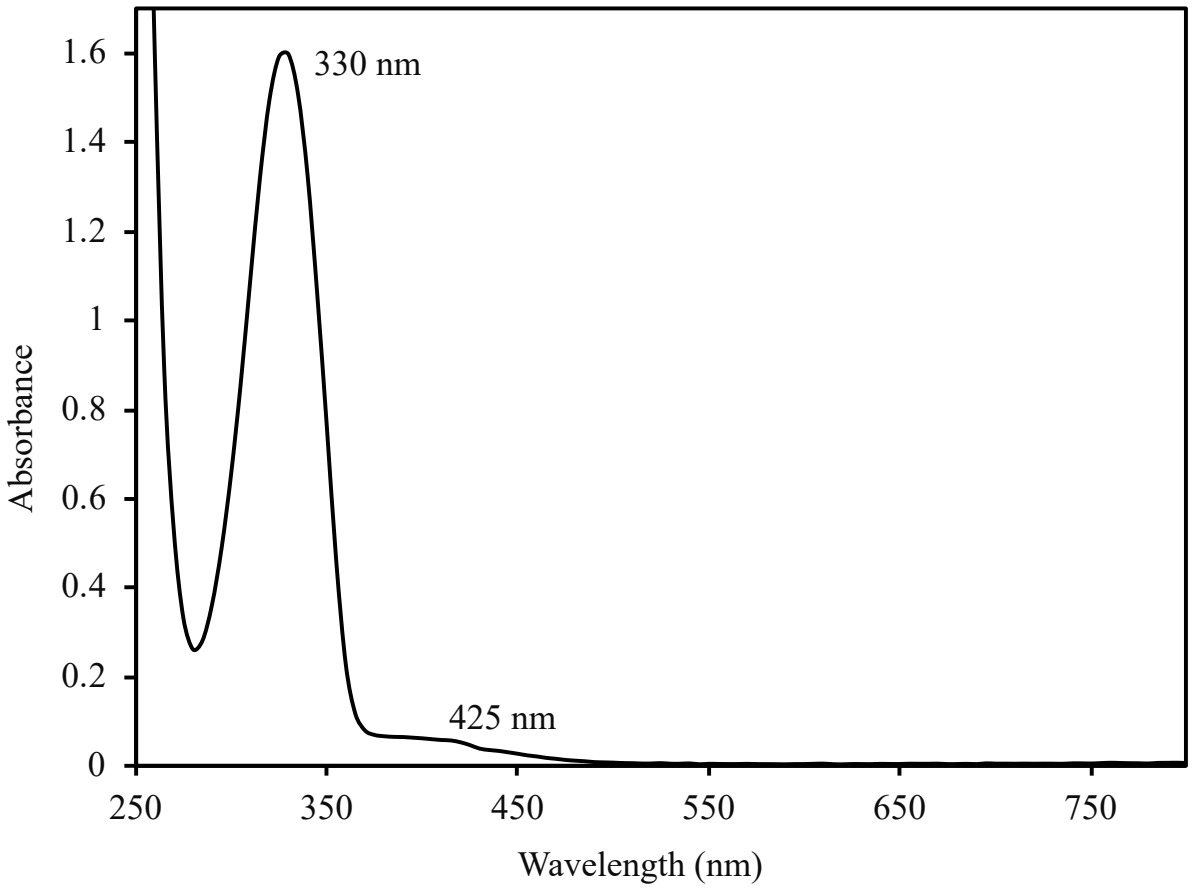

Figure S34. UV-vis spectrum of **1** in THF (145 μM) at 23 °C.

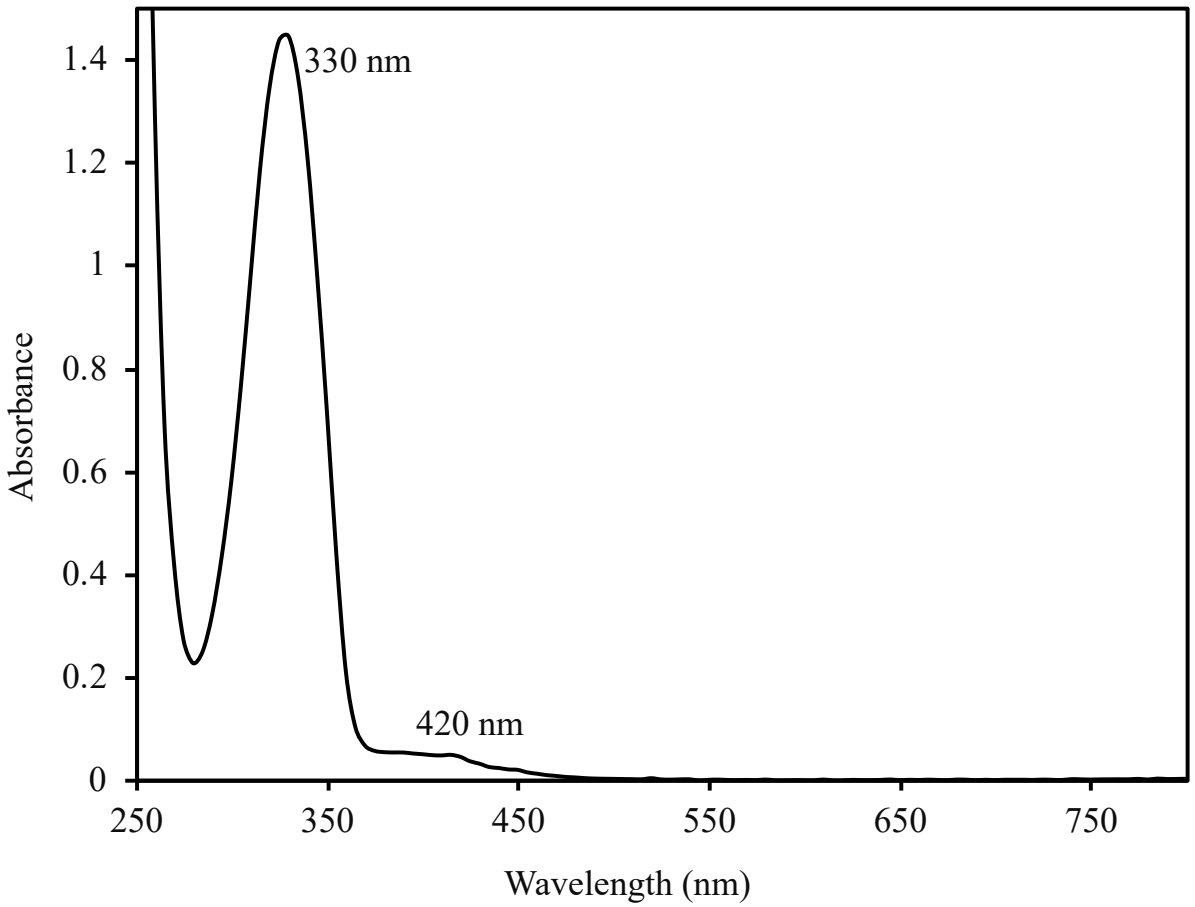

Figure S35. UV-vis spectrum of **2** in THF (125 μM) at 23 °C.

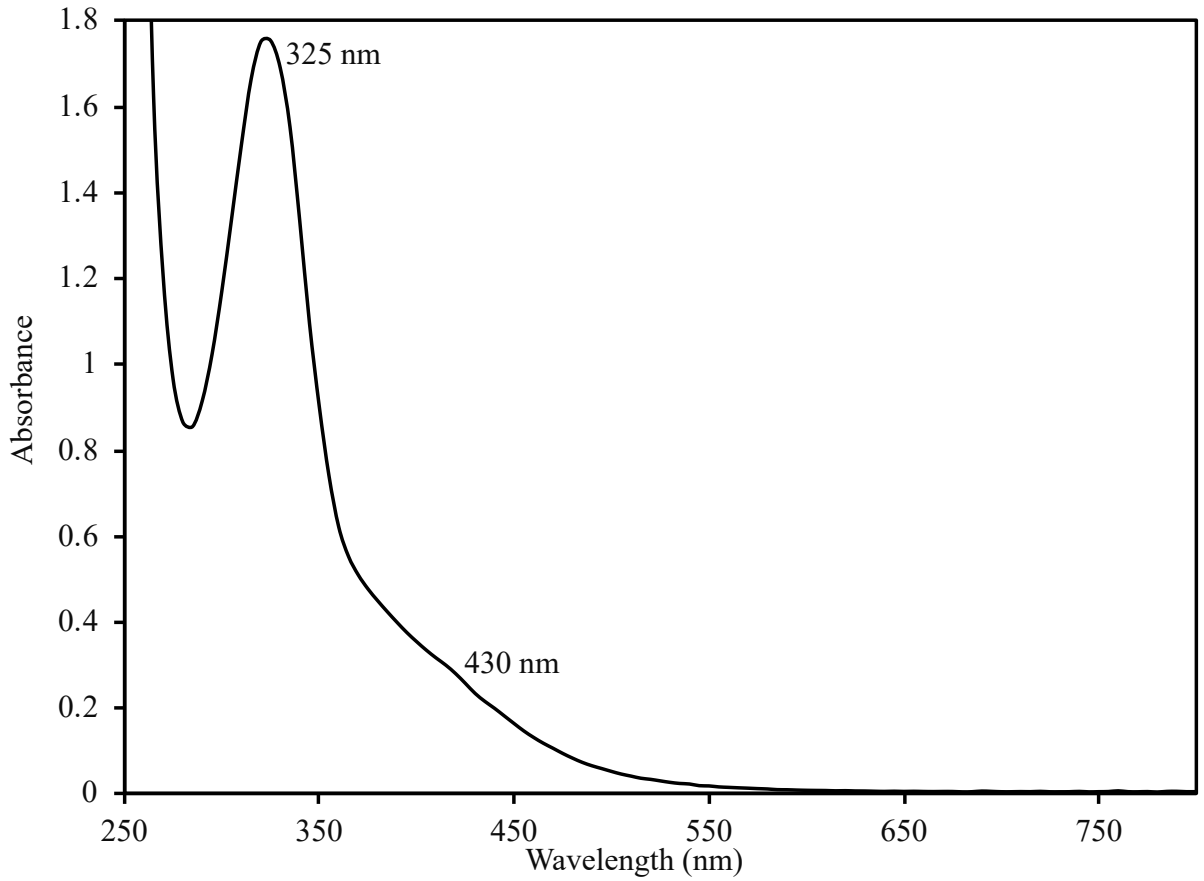

Figure S36. UV-vis spectrum of **3** in THF (125 μM) at 23 °C.

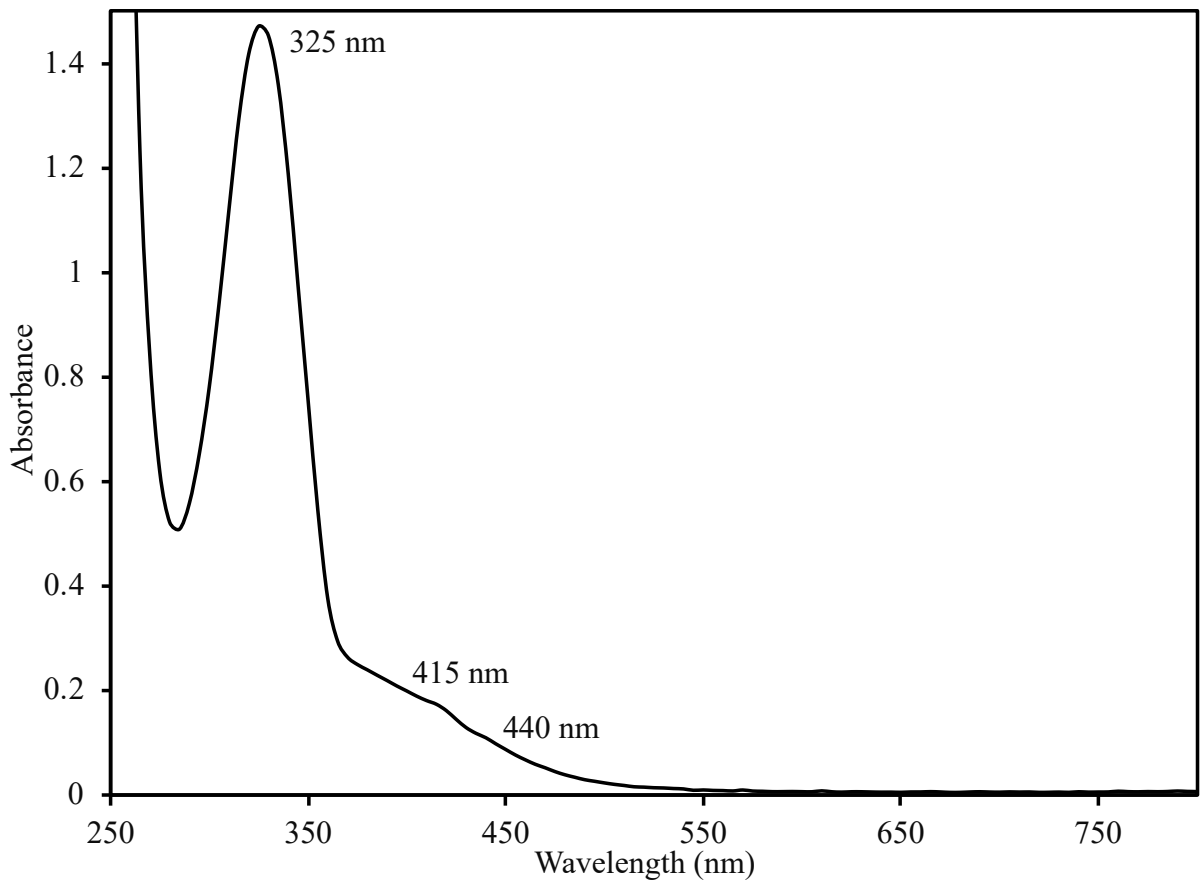

Figure S37. UV-vis spectrum of **4** in THF (125 μM) at 23 °C.

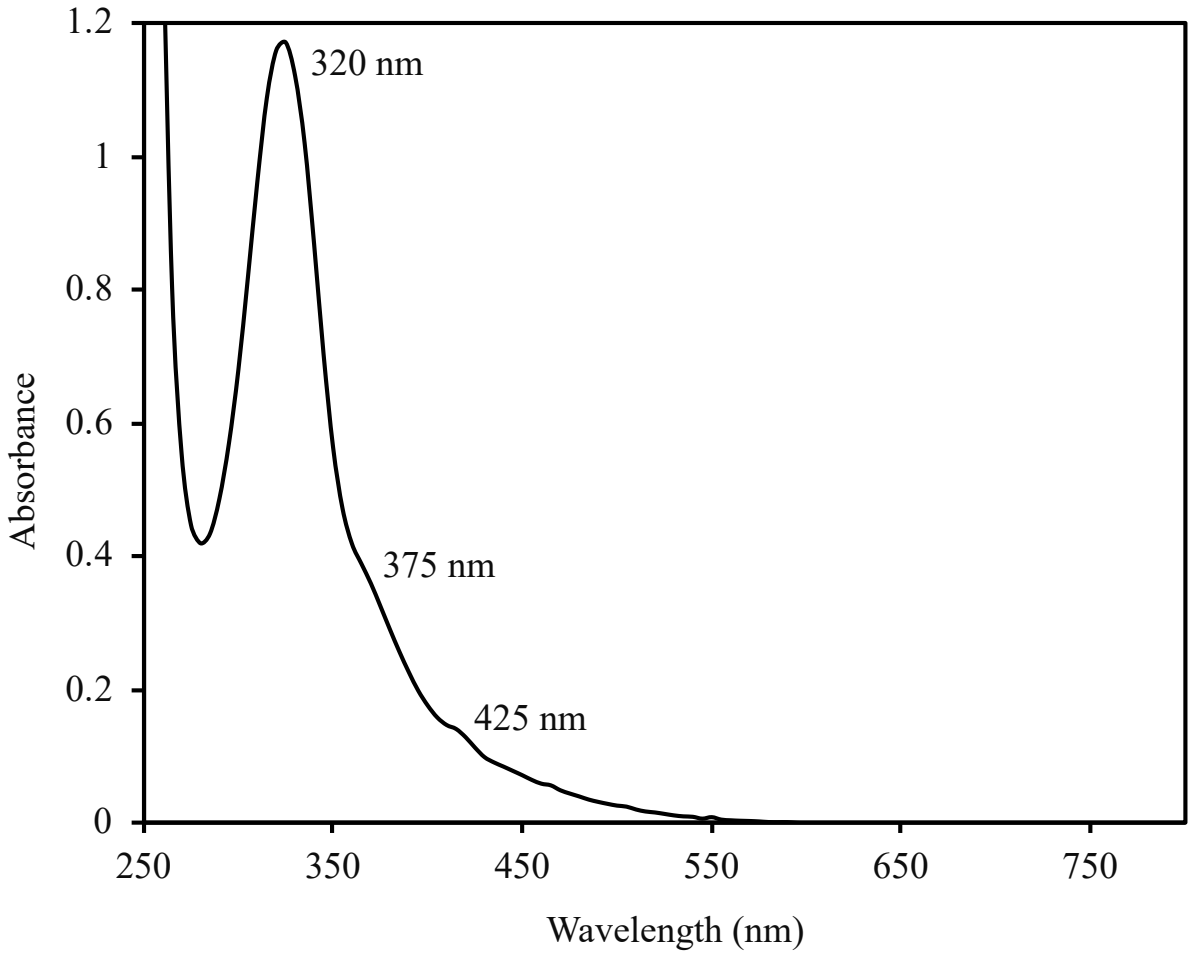

Figure S38. UV-vis spectrum of **5** in THF (115 μM) at 23 °C.

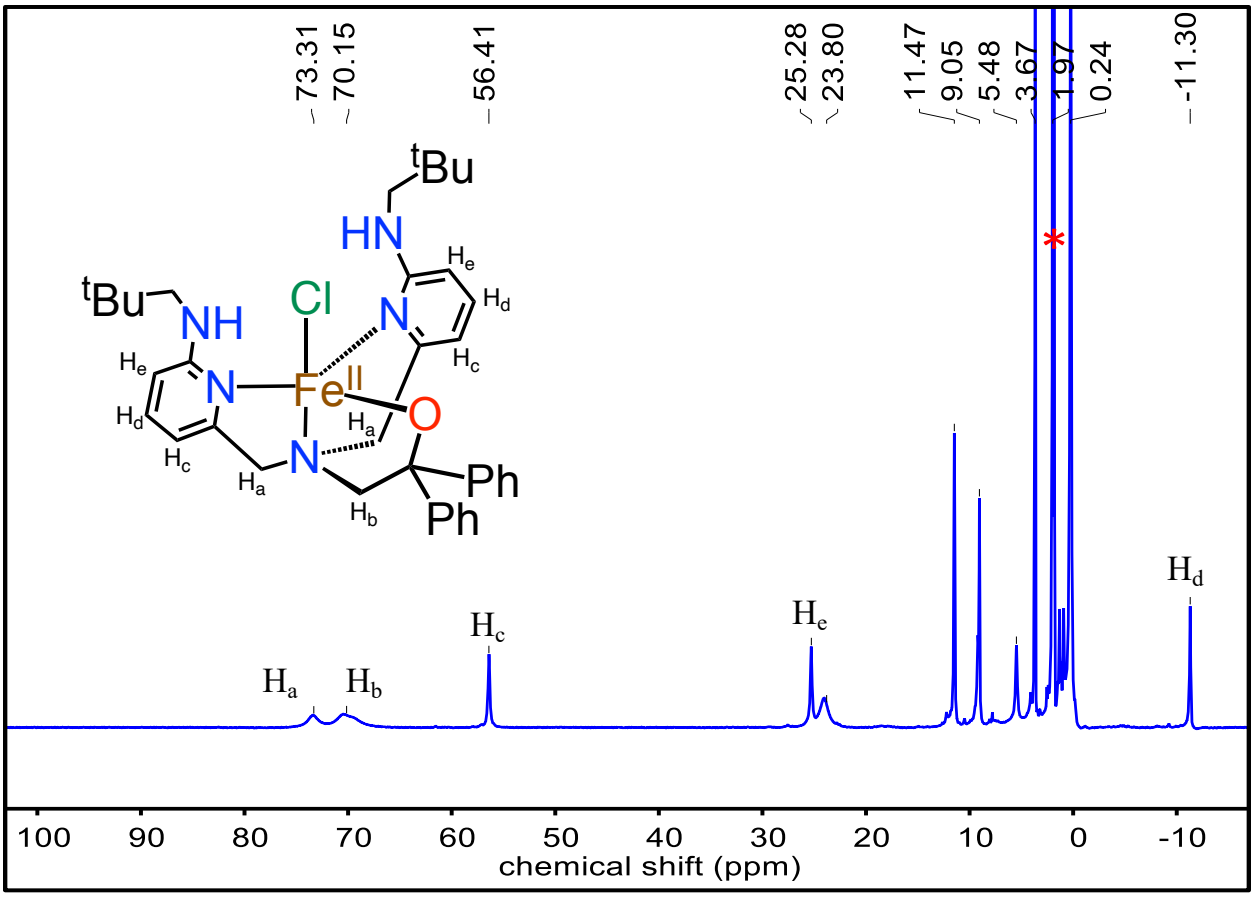

Figure S39. The ^{1}H NMR spectrum of **1** in CD_3CN at 23 °C. The residual solvent peak for CD_3CN peak is marked with a red asterisk (*).

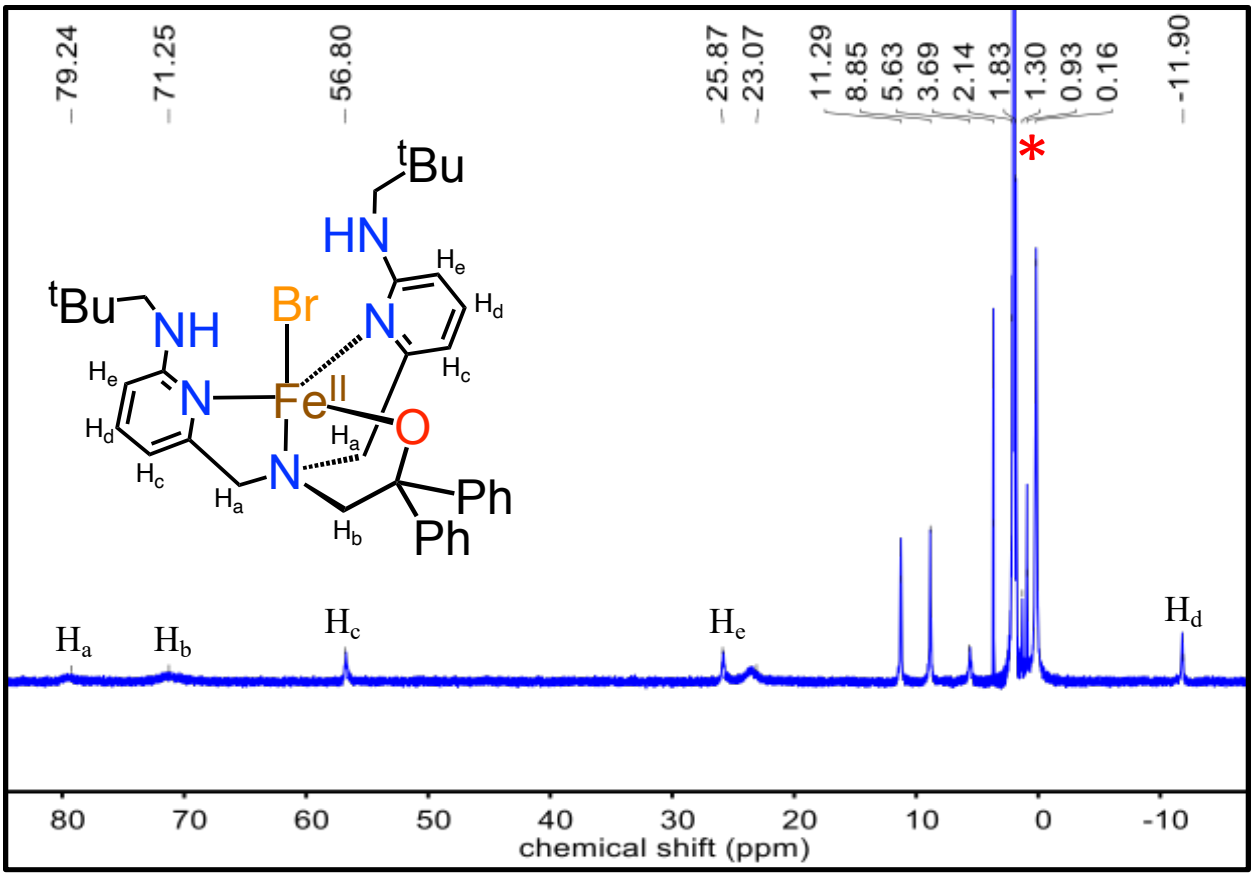

Figure S40. The ^{1}H NMR spectrum of **2** in CD_3CN at 23 °C. The residual solvent peak for CD_3CN peak is marked with a red asterisk (*).

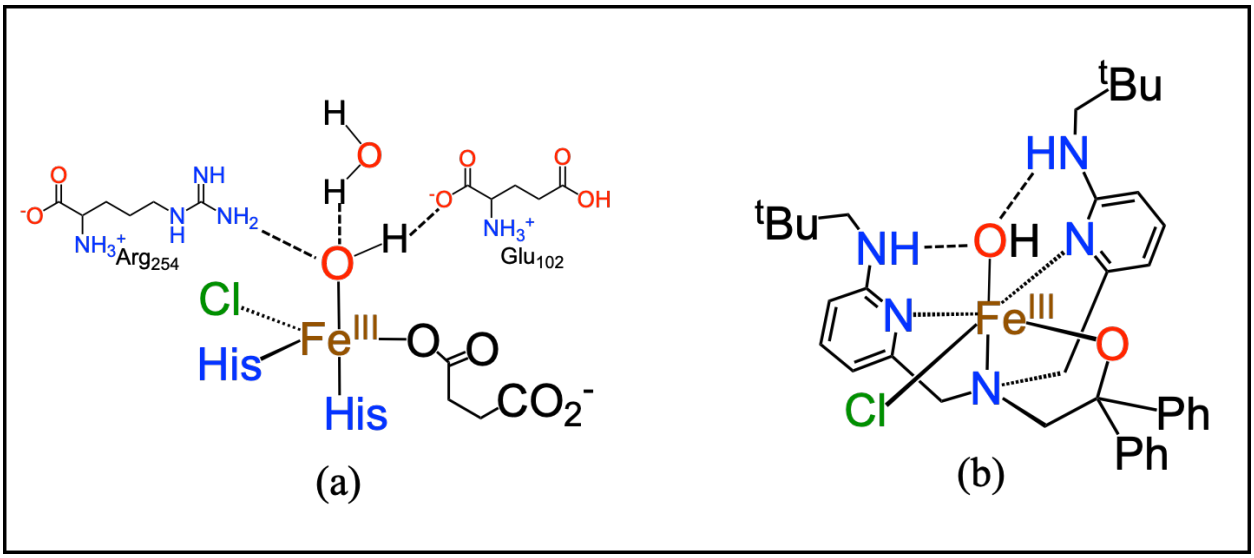

Figure S41. The H-bonding interactions in (a) the calculated structure of the $Fe^{III}(OH)(Cl)$ intermediate in the SyrB2 enzyme[7, 8] and (b) complex **3**.

F. References:

1. Albano, S.; Olivo, G.; Mandolini, L.; Massera, C.; Ugozzoli, F.; Di Stefano, S., Formation of Imidazo[1,5-a]pyridine Derivatives Due to the Action of Fe^{2+} on Dynamic Libraries of Imines. *J. Org. Chem.* **2017,** *82*, 3820.
2. Yadav, V.; Gordon, J. B.; Siegler, M. A.; Goldberg, D. P., Dioxygen-Derived Nonheme Mononuclear Fe^{III}(OH) Complex and Its Reactivity with Carbon Radicals. *J. Am. Chem. Soc.* **2019,** *141*, 10148.
3. Zaragoza, J. P. T.; Yosca, T. H.; Siegler, M. A.; Moënne-Loccoz, P.; Green, M. T.; Goldberg, D. P., Direct Observation of Oxygen Rebound with an Iron-Hydroxide Complex. *J. Am. Chem. Soc.* **2017,** *139*, 13640.
4. Jang, E. S.; McMullin, C. L.; Käß, M.; Meyer, K.; Cundari, T. R.; Warren, T. H., Copper(II) Anilides in sp^3 C-H Amination. *J. Am. Chem. Soc.* **2014,** *136*, 10930.
5. Fulmer, G. R.; Miller, A. J. M.; Sherden, N. H.; Gottlieb, H. E.; Nudelman, A.; Stoltz, B. M.; Bercaw, J. E.; Goldberg, K. I., NMR Chemical Shifts of Trace Impurities: Common Laboratory Solvents, Organics, and Gases in Deuterated Solvents Relevant to the Organometallic Chemist. *Organometallics* **2010,** *29*, 2176.
6. Neese, F., Software update: the ORCA program system, version 4.0. *WIREs Comput. Mol. Sci.* **2018,** *8*, e1327.
7. Huang, J.; Li, C.; Wang, B.; Sharon, D. A.; Wu, W.; Shaik, S., Selective Chlorination of Substrates by the Halogenase SyrB2 Is Controlled by the Protein According to a Combined Quantum Mechanics/Molecular Mechanics and Molecular Dynamics Study. *ACS Catal.* **2016,** *6*, 2694.
8. Srnec, M.; Solomon, E. I., Frontier Molecular Orbital Contributions to Chlorination versus Hydroxylation Selectivity in the Non-Heme Iron Halogenase SyrB2. *J. Am. Chem. Soc.* **2017,** *139*, 2396.